

Spring 1-1-2016

# Characterization of *Streptomyces coelicolor* ParH in development-associated chromosome segregation

Metis Hasipek

Follow this and additional works at: <https://dsc.duq.edu/etd>

---

## Recommended Citation

Hasipek, M. (2016). Characterization of *Streptomyces coelicolor* ParH in development-associated chromosome segregation (Doctoral dissertation, Duquesne University). Retrieved from <https://dsc.duq.edu/etd/1502>

This One-year Embargo is brought to you for free and open access by Duquesne Scholarship Collection. It has been accepted for inclusion in Electronic Theses and Dissertations by an authorized administrator of Duquesne Scholarship Collection.

CHARACTERIZATION OF *STREPTOMYCES COELICOLOR* PARH  
IN DEVELOPMENT-ASSOCIATED CHROMOSOME SEGREGATION

A Dissertation

Submitted to Bayer School of Natural and Environmental Sciences

Duquesne University

In partial fulfillment of the requirements for  
the degree of Doctor of Philosophy

By

Metis Hasipek

May 2016

Copyright by

Metis Hasipek

2016

CHARACTERIZATION OF *STREPTOMYCES COELICOLOR* PARH  
IN DEVELOPMENT-ASSOCIATED CHROMOSOME SEGREGATION

By

Metis Hasipek

Approved March 21, 2016

---

Joseph McCormick, Ph.D.  
Associate Professor of Biological  
Sciences  
(Committee Chair)

---

Jana Patton-Vogt, Ph.D.  
Professor of Biological Sciences  
(Committee Member)

---

Michael I. Seaman, Ph.D.  
Associate Professor of Biological  
Sciences  
(Committee Member)

---

Valerie Oke, Ph.D.  
Director of Undergraduate programs  
University of Pittsburgh  
(Committee Member)

---

Philip Reeder, Ph.D.  
Dean, Bayer School of Natural and  
Environmental Sciences  
Professor of Biological Sciences

---

Joseph McCormick, Ph.D.  
Chair, Department of Biological Sciences  
Associate Professor of Biological  
Sciences

## ABSTRACT

### CHARACTERIZATION OF *STREPTOMYCES COELICOLOR* PARH IN DEVELOPMENT-ASSOCIATED CHROMOSOME SEGREGATION

By

Metis Hasipek

May 2016

Dissertation supervised by Joseph R. McCormick

*S. coelicolor* uses an active chromosome partitioning system for developmentally-regulated genome segregation, which is associated with spore formation. There are four known *trans*-acting segregation proteins (ParA, ParB, ParJ and Scy) and *cis*-acting centromere-like sites (*parS*). *parA* encodes a Walker-type ATPase that is required for efficient DNA segregation and proper placement of the ParB-*parS* nucleoprotein complexes. A paralogue of ParA is encoded by the *S. coelicolor* genome, SCO1772 (named ParH), that has 45% identical residues to ParA. In *S. coelicolor* aerial hyphae, a  $\Delta parH$  mutant produces 5% of anucleate spores. In this study, ParH was identified as a novel interaction partner of *S. coelicolor* ParB. However, a Walker A motif K99E substitution in ParH and removal an N-terminal extension in ParH impaired interaction between ParH and ParB, as judged by bacterial two-hybrid analyses. ParH-

EGFP localization resembles the evenly-spaced localization pattern of ParH-EGFP in aerial hyphae, which might suggest that ParH colocalizes with ParB. A *parH*-null mutant appears to be unable to properly organize the *oriC* regions within a subset of prespores, as judged by ParB-EGFP foci. In this study, through a random chromosomal library screening, a novel protein that interacts with ParA and ParH was also identified. HaaA (ParH and ParA Associated protein A) is required for proper chromosome segregation and is one of the 24 signature proteins of the Actinomycetes that are not found in other bacterial lineages. A bacterial two-hybrid analysis showed that HaaA interacts with itself and interaction between ParH and ParA was through the C-terminal unstructured region. Interaction between HaaA and ParA and ParA-like proteins was conserved in other Actinomycetes, such as *S. venezuelae*, *C. glutamicum* and *M. smegmatis*. There was no evidence for interaction with other tested segregation proteins. In addition, a *haaA* insertion-deletion mutant strain revealed that loss of HaaA affected chromosome segregation (6% anucleate spores) and HaaA-EGFP localizes within spores of the mature spore chains. Together these data revealed new information to further understand chromosome segregation in *S. coelicolor*.

## DEDICATION

This dissertation is dedicated to my parents Seniha and Mehmet Emin Hasipek who instilled in me the virtues of perseverance and raised me to be the person I am today. Words cannot describe how grateful I am to be your daughter. Your unconditional love, guidance, and support encouraged me to go on every adventure, especially this one. Without you, my success would not be possible.

## ATTRIBUTIONS

Rebekah Dedrick constructed the strains RMD29 ( $\Delta parH::acc(3)IV parB-egfp$ ) and RMD30 ( $parH-egfp acc(3)IV$ ) and was first to observe the disrupted ParB-EGFP foci in a *parH*-null mutant that were used in Chapter 2.

Rachel Monaghan, pre-doctoral rotation student, did the site-directed mutagenesis use to express the ParH(K99E) variant.



## TABLE OF CONTENTS

	Page
Abstract.....	iv
Dedication.....	vi
Attributions .....	vii
List of Tables .....	xii
List of Figures. ....	xiii
Chapter 1: Literature Review.....	1
Bacterial Chromosome and Low-Copy-Number Plasmid Segregation and Partitioning Proteins.....	1
Segregation systems in plasmids.....	2
Type I <i>par</i> segregation system.....	3
Type II <i>par</i> segregation system.....	4
Type III (Tubulin-like) partition system.....	5
Bacterial Chromosome Segregation.....	6
Chromosome segregation in <i>Escherichia coli</i> .....	6
Chromosome segregation in <i>Bacillus subtilis</i> .....	12
Chromosome segregation in <i>Caulobacter crescentus</i> .....	15
Chromosome segregation in <i>Corynebacterium glutamicum</i> .....	19
Chromosome segregation in <i>Streptomyces coelicolor</i> .....	21
References.....	26
CHAPTER 2: Characterization of <i>Streptomyces coelicolor</i> ParH in Developmental- Associated Chromosome Segregation.....	58

Abstract .....	58
Introduction.....	60
Materials and Methods.....	64
Bacterial strains, media, and growth conditions.....	64
Plasmids and general DNA techniques.....	64
Isolation of <i>parH</i> -null strains.....	65
Creation of the ParH-EGFP expressing strain.....	65
Creation of the ParB-mCherry and ParH-EGFP strain.....	66
Creation of <i>parH</i> genes expressing K99E, R273E, and $\Delta$ 20-80 variants of ParH.....	66
Analysis of <i>in vivo</i> DNA binding ability of ParH by GFP-ParH localization in <i>E. coli</i> .....	67
Creation of plasmids expressing fusions to ParH, ParH-variants, SMC, ScpA and ScpB for use in a bacterial two-hybrid assay.....	69
Fluorescence Microscopy.....	70
Results.....	72
<i>S. coelicolor</i> possesses a gene to express a second ParA-like ATPase.....	72
Deletion of ParH affects chromosome segregation.....	74
Localization of ParB-EGFP is slightly disrupted in <i>parH</i> deletion mutant....	74
ParH-EGFP localizes at evenly spaced intervals within aerial filaments.....	77
ParH does binds to nucleoid in a heterologous <i>in vivo</i> assay.....	79
<i>S. coelicolor</i> ParA-like protein ParH interacts with centromere-binding protein ParB in a bacterial two-hybrid assay.....	81

ParH forms homodimers as do homologs of this type of Walker ATPases...	83
ParH does not appear to interact with proteins that make up the bacterial condensin SMC, ScpA, and ScpB complexes.....	83
Small leucine zipper ( <i>slzA</i> ) interacts with ScpB and ParH.....	84
Discussion.....	86
References.....	93
CHAPTER 3: <i>Streptomyces coelicolor</i> HaaA interacts with ParA and ParH and is a novel segregation component	
Abstract.....	126
Introduction.....	128
Materials and Methods.....	130
Bacterial strains, media, and growth conditions.....	130
Plasmids and general DNA techniques.....	130
Creating plasmids containing <i>haaA</i> , <i>parA</i> , <i>parB</i> , and <i>parH</i> for use in a bacterial two-hybrid assay.....	131
Constructing a genomic library of M145.....	132
Isolation of <i>haaA</i> -null strain .....	133
Creation of a <i>haaA</i> in-frame deletion expressing a $\Delta$ 338-345 variant of HaaA.....	133
Creation of the HaaA-EGFP expressing strain.....	134
Construction of a <i>haaA</i> genetic complementation plasmid .....	134
Fluorescence Microscopy.....	135
Results.....	136

ParH and ParA interacts with a highly conserved signature protein for <i>Actinomycetes</i> .....	136
HaaA interactions with ParA and ParA-like proteins are also conserved in other <i>Actinomycetes</i> .....	139
Deletion of <i>haaA</i> affects the formation of aerial hyphae formation and chromosome segregation into spores.....	140
HaaA-EGFP is located notably in spore chains, but not in vegetative hyphae.....	141
Discussion.....	142
References.....	145
CHAPTER 4: Summary and Future Directions.....	170
Characterization of a new partitioning protein.....	170
Identification of a novel ParA and ParH interacting protein.....	175
References.....	178

## LIST OF TABLES

	Page
Table 1.1. Elements that are found in Type I, II, and III plasmid partition systems.....	48
Table 1.2. Elements that are found in bacterial chromosome segregation.....	49
Table 2.1: <i>E. coli</i> strains used in this study.....	99
Table 2.2: <i>S. coelicolor</i> A3(2) strains used in this study.....	100
Table 2.3: Cosmids and plasmids used in this study.....	101
Table 2.4: Oligonucleotides used in this study.....	106
Table 2.5. Analysis of ParB-EGFP localization in wild type and <i>parH</i> null mutant strains.....	119
Table 3.1: <i>E. coli</i> strains used in this study.....	148
Table 3.2: <i>S. coelicolor</i> strains used in this study.....	149
Table 3.3: Cosmids and plasmids used in this study.....	150
Table 3.4: Oligonucleotides used in this study.....	155

## LIST OF FIGURES

	Page
Figure 1.1. Partitioning systems in plasmids.....	52
Figure 1.2. Chromosome segregation models for <i>E. coli</i> , <i>C. crescentus</i> , and <i>C. glutamicum</i> .....	55
Figure 1.3. Chromosome segregation model for <i>S. coelicolor</i> .....	57
Figure 2.1. Sequence alignment of ParA and ParH for <i>S. coelicolor</i> .....	108
Figure 2.2. Multiple sequence alignment of ParH homologs among different <i>Streptomyces</i> species.....	109
Figure 2.3. Multiple sequence alignment of ParA homologs among different <i>Streptomyces</i> species.....	111
Figure 2.4. Diagram of the gene organization at the <i>parH</i> region of <i>S. coelicolor</i> chromosome.....	113
Figure 2.5. Phylogenetic analysis of ParA and ParA-like protein sequences. ....	114
Figure 2.6. Developmental segregation phenotypes of a WT, <i>parA</i> , <i>parH</i> , or <i>parA parH</i> mutants.....	116
Figure 2.7. ParH-EGFP localization in predivisinal aerial filaments.....	117
Figure 2.8. Localization of ParB-EGFP foci in $\Delta parH::acc(3)IV parB-egfp$ strain.....	118
Figure 2.9. Localization of ParB-mCherry and ParH-EGFP fusion proteins in aerial hyphae.. ..	120
Figure 2.10 Scanning laser confocal microscope images of the same <i>E. coli</i> strains expressing fusion proteins.....	121
Figure 2.11. SDS-PAGE analysis of GFP-Soj and GFP-ParH fusion expression in	

<i>E. coli</i> .....	122
Figure 2.12 Bacterial two-hybrid analysis of interaction between ParH and known segregation proteins. ....	123
Figure 2. 13 Bacterial two-hybrid analysis of ParH and ParH variants with ParB. ....	124
Figure 2.14 Summary of bacterial two hybrid protein-protein interactions identified for <i>S. coelicolor</i> genome segregation proteins. ....	125
Figure 3.1. Representation of genomic library screening for ParH interacting proteins.....	157
Figure 3.2 Alignment of HaaA homologs from several divergent <i>Actinomycetes</i> species. ....	159
Figure 3.3 Multiple sequence alignment of HaaA among different <i>Streptomyces</i> species. ....	160
Figure 3.4 Diagram of the gene organization at the <i>haaA</i> region of <i>S. coelicolor</i> chromosome and structure of HaaA. ....	162
Figure 3.5 Quantification of beta-galactosidase activity for selected positive interactions for plasmids expressing <i>S. coelicolor</i> fusion proteins. ....	164
Figure 3.6 Quantification of beta-galactosidase activity for HaaA, ParA, ParB, and ParH interactions in other <i>Actinomycetes</i> . ....	166
Figure 3.7 Macroscopic phenotype of <i>haaA</i> . ....	167
Figure 3.8 Developmental segregation phenotype of the <i>haaA</i> null mutant. ....	168
Figure 3.9 Localization of HaaA-EGFP fusion protein in aerial hyphae. ....	169
Figure 4.1. Putative model for segregation proteins during development-associated genome segregation of aerial hyphae in <i>S. coelicolor</i> .....	180

## **CHAPTER 1: LITERATURE REVIEW**

### **Bacterial Chromosome and Low-Copy-Number Plasmid Segregation and Partitioning Proteins**

The proper distribution of chromosomes into daughter cells during cell division is an important part of the bacterial cell cycle. Chromosome organization and segregation after DNA replication and before cell division is mediated by an active partitioning mechanism, which is still quite elusive. This literature review mainly focuses on what is known about partitioning proteins in low-copy-number plasmids and the chromosome of model organisms, such as *Escherichia coli*, *Bacillus subtilis*, *Caulobacter crescentus*, *Corynebacterium glutamicum*, and *Streptomyces coelicolor*.

The first model for chromosome partitioning, the ‘replicon model’, was proposed for *E. coli* by Jacob and Brenner (1963). According to this model, both chromosomes attach to specific positions in the cell membrane and the chromosomes passively separate with cell growth from insertion of new cell envelope material between these attachment points.

Studies on low-copy-number plasmid partitioning brought insight into alternative mechanisms to this topic. While high copy number plasmids randomly distribute into daughter cells, low-copy-number plasmids must need active partitioning in a dividing cell to secure their presence in daughter cells (Bignell and Thomas, 2001). Studies in *E. coli* on plasmid F and prophage P1 led to the discovery of active partitioning proteins, ParA/SopA and ParB/SopB (Abeles *et al.*, 1986; Mori *et al.*, 1986). This literature review mainly concentrates on the homologs of these partitioning proteins and their partners in low-copy-number plasmids and the chromosome of model bacterial species. Also, it



includes discussion of additional proteins that are implicated in chromosome segregation, such as FtsK and SMC in these model organisms. Table 1.1 and Table 1.2 summarize the main systems and proteins in plasmid and bacterial chromosome segregation, which are discussed in this chapter.

### **Segregation systems in plasmids**

Plasmid-encoded partition loci have been a useful model to study the mechanism of bacterial chromosome segregation. There are three major classes of segregation systems in low-copy-number plasmids (Gerdes *et al.*, 2010). Each system has three common components that include a putative nucleotide-driven motor protein, centromere-like *cis*-acting DNA region, and a small centromere DNA-binding adaptor. There are three important steps in plasmid partitioning: formation of a partition complex by binding of multiple centromere binding proteins (CBPs) to the centromere repeats, recruitment of the nucleotide triphosphatase (NTPase) to these partition complexes, and separation of plasmids toward opposite bacterial poles mediated by polymers of the NTPase (Gerdes *et al.*, 2000). These three classes of segregation systems are defined by the type of nucleotide-driven motor protein (Figure 1.1) (Salje *et al.*, 2010).

A Type I *par* system includes a ParA-like protein that is a deviant Walker A-type protein. Deviant Walker A proteins belong to the superfamily of ATPases, which are characterized by the A type motif (Walker box) that consists of a hydrophobic beta-strand and P loop. In a deviant Walker A box, the A motif is modified from glycine rich residues (GXXGXGK[ST]) to lysine rich residues (KGGXXK[ST]) (Walker *et al.*, 1982; Koonin, 1993). A Type II *par* system includes a ParM family protein that is an ATPase protein that assembles into dynamic actin-like filaments (Salje *et al.*, 2010). Finally, a

Type III *par* system contains a TubZ family protein that assembles into dynamic filaments and have a tubulin-like GTPase fold at the monomer level (Ni *et al.*, 2010).

Table 1.1 summarizes the main systems in plasmid partitioning discussed in this chapter.

### **Type I *par* segregation system**

Type I *par* is the most common type of plasmid segregation system that encodes ParA NTPases with deviant Walker-A box and ParB centromere binding proteins (Koonin, 1993; Schumacher 2012). Depending on the size and sequences of ATPase protein and the centromere binding protein (CPB), the Type I *par* system can be subdivided into Type Ia and Ib (Gerdes *et al.*, 2000).

Type Ia CBPs are different than Type Ib and consists of three domains: an NTPase binding domain, a helix-turn-helix (HTH) domain, and a dimer domain, which are required for interacting with the partition ATPase, binding to *par* sites, and for oligomerization with itself, respectively (Ah-Seng *et al.*, 2009; Delbruck *et al.*, 2002; Khare *et al.*, 2004; Radnedge *et al.*, 1998; Ravin *et al.*, 2003; Schumacher and Funnell, 2005; Schumacher *et al.*, 2010; Surtees and Funnell, 1999). The main-studied Type Ia CBPs are *E. coli* P1 ParB, *E. coli* RP4 KorB, *E. coli* F plasmid SopB, and *S. enterica* TP228 ParG (Abeles *et al.*, 1985; Delbruck *et al.*, 2002).

Even though sequence homology among various Type Ib CBPs is sparse, their structures show a ribbon-helix-helix (RHH) DNA binding motif (Golovanov *et al.*, 2003; Huang *et al.*, 2011; Murayama *et al.*, 2001). The N-terminal region of the Type Ib CBPs contains an arginine finger that functions in ParA binding and stimulates ATP hydrolysis by ParA (Barilla *et al.*, 2007).

The major difference between Type Ia and Ib segregation systems is that ParA is not only involved in segregation, but ParA also serves as a transcriptional repressor by binding to the *par* promoter and autoregulating *parAB* transcription. ParA switches its functional role by binding to different types of nucleotides. ADP binding promotes its transcription factor role and ParA binds to *par* promoter and ATP binding activates partitioning function to separate replicated plasmids (Davey and Funnell, 1994,1997; Davis *et al.*, 1992).

Type I *par* systems use a pulling mechanism by de-polymerization of the motor protein filament to separate plasmids to the quarter-cell positions before cell division (Figure 1.1, A) (Gerdes *et al.* 2010). First, a CBP complex pairs two sister plasmids together by binding to *par* sites and spreading on naked DNA surrounding *par* sites (Pillet *et al.*, 2011; Rodionov and Yarmolinsky, 2004). ParA binds and nucleates on CBP-DNA complexes, which also promotes ParA polymerization (Bouet *et al.*, 2007). ParA filament extension is followed by ATP hydrolysis of ParA, which is stimulated by CBP-DNA complexes (Ah-Seng *et al.*, 2009). ATP hydrolysis causes filaments to de-polymerize and de-polymerization pulls the plasmids apart in opposite directions.

### **Type II *par* segregation system**

*E. coli* plasmid R1 represents the characteristic model of the Type II *par* segregation family. R1 Type II partitioning contains a centromeric element (*parC*), a CBP (ParR) (Kunst *et al.*, 1997), and an actin-like ATPase (ParM) (Jensen and Gerdes, 1997; Jensen *et al.*, 1998). The region upstream of the *parRM* promoter is flanked by a 160 base pair *parC* site, which contains an array of ten 11 bp direct repeats (Dam and Gerdes, 1994). Even though the sequence similarity is low, ParM is structurally and

biochemically similar to actin in eukaryotes and represents one example of a prokaryotic cytoskeletal element (van den Ent *et al.*, 2002). ParR binds to *parC* sequences as a dimer and binding bends the DNA (Figure 1.1, B) (Popp *et al.*, 2008). ParM forms filaments in the ATP-bound state and its ATPase activity is stimulated by the oligomerization (Million-Weaver and Camps, 2014). ParM polymerization occurs in the presence of ATP (or GTP) and is dynamically unstable. Filaments are stable in the ATP-bound conformation and association between ParR bound to *parC* stabilizes the ends of ParM filaments (Galkin *et al.*, 2009; Moller-Jensen *et al.*, 2003). ParM filament extension occurs at both ends of this anti-parallel assembly and this bi-directional elongation pushes plasmids to opposite poles of the cell. ParM filaments disassemble by ATP hydrolysis with plasmids segregated to opposite sites. Therefore, the Type II plasmids are pushed to opposite poles of the cells instead of pulled as in the Type I *par* system (See Figure 1.1, B) (Million-Weaver and Camps, 2014).

### **Type III (Tubulin-like) partition system**

The first protein in this relatively newly identified partitioning system was discovered for the virulence plasmid pXO1 of *B. anthracis* (Tinsley and Khan, 2006). RepX is a tubulin-like GTPase protein, which is necessary for replication and segregation of pXO1 plasmid. A similar gene and function was also discovered for *B. thuringiensis* pBtoxis plasmid, which encodes an NTPase called TubZ and CBP called TubR (Larsen *et al.*, 2007). The partitioning process in Type III, called treadmilling, is different than either of the pushing or pulling mechanisms for Type I and II, respectively. TubR is a HTH protein, which autoregulates the expression of the *tubRZ* genes (Berry *et al.*, 2002; Larsen *et al.*, 2007). The crystal structure of TubR shows that dimerized TubR

oligomerizes on *tubC* centromeric DNA of pBtoxis (Aylett and Lowe, 2012; Ni *et al.*, 2010). TubR structure includes an intertwined dimer with a winged HTH motif and forms a protein/DNA complex by recognizing the major groove of *tubC* centromeric site by the N-terminal of HTH, which then recruits the TubZ polymer. TubZ is a GTPase that forms dynamic polarized protofilaments with plus and minus ends in the presence of GTP (Aylett and Lowe, 2012; Larsen *et al.*, 2007). GTP hydrolysis of TubZ polymer elongates at the plus end and disassembles from the minus end by a mechanism called treadmilling. Upon plasmids migrating to the cell poles, the TubZ filament encounters the cell pole, bends and releases the TubR-bound plasmid (See Figure 1.1, C) (Aylett and Lowe, 2012; Larsen *et al.*, 2007; Ni *et al.*, 2010).

### **Bacterial Chromosome Segregation**

DNA segregation mechanisms and proteins are typically conserved among the unicellular bacteria. Most of the unicellular bacteria that have been studied so far have homologs of known DNA segregation proteins. However, the function of these proteins may be diverse in different organisms.

#### **Chromosome segregation in *Escherichia coli***

*E. coli* is a Gram-negative gamma-proteobacterium model for the study of chromosome segregation. In newly born *E. coli* cells, the origin of replication (*ori*) and terminus (*ter*) region of the chromosome localize at the midcell (Nielsen *et al.*, 2006, Wang *et al.*, 2006). After replication, daughter *ori* regions segregate to the pre-divisional cell quarter positions, but the *ter* regions remain at the center until late in the cell cycle. The *ter* region contains a 50 kb segment that links the two replicated nucleoid edges (Liu *et al.*, 2010, Wiggins *et al.*, 2010). The final step of chromosome segregation includes

removal of catenation links by Topo IV topoisomerase and resolution of chromosome dimers by the XerCD/*dif* site-specific recombination system (Espeli *et al.*, 2004; Lesterlin *et al.*, 2004).

The *ter* region is also involved in chromosome segregation by interacting with the FtsK DNA translocase (Bigot *et al.*, 2007). FtsK plays an important role in actively segregating sister chromosomes (Stouf *et al.*, 2013). FtsK belongs to the family of FtsK/SpoIIIE/Tra ATPase DNA motor proteins. *E. coli* FtsK associates with the division septum through the N-terminal region of the protein (FtsK<sub>N</sub>), which includes membrane-spanning segments and is essential for growth and cell division (Yu *et al.*, 1998; Wang *et al.*, 1998). The central region of the linker domain of FtsK (FtsK<sub>L</sub>) is involved in interacting with other cell division proteins (Bigot *et al.*, 2004; Grenga *et al.*, 2008; Dubarry and Barre *et al.*, 2010; Dubarry *et al.*, 2010). The C-terminal domain of FtsK (FtsK<sub>C</sub>) includes a Walker-type ATPase motif and forms a hexameric motor, which is responsible for translocating dsDNA (Aussel *et al.*, 2002; Massey *et al.*, 2006), interacting with Topo IV, and activating Topo IV decatenation activity *in vitro* (Espeli *et al.*, 2003; Bigot *et al.*, 2010). Based on structure, sequence, and function, FtsK<sub>C</sub> has three subdomains  $\alpha$ ,  $\beta$ , and  $\gamma$  (Massey *et al.*, 2006; Sivanathan *et al.*, 2006). FtsK $\alpha$  and FtsK $\beta$  form the translocation motor and FtsK $\gamma$  is responsible for controlling the translocation activity (Yates *et al.*, 2003). FtsK $\gamma$  includes a winged-helix DNA-binding domain that recognizes FtsK orienting polar sequences (KOPS) within the DNA (Sivanathan *et al.*, 2006; Ptacin *et al.*, 2006; Lowe *et al.*, 2008; Graham *et al.*, 2010). FtsK $\gamma$  also interacts with XerD of the XerCD/*dif* recombination machinery to resolve circular chromosome dimers (Yates *et al.*, 2006; Nolivos *et al.*, 2010; Grainge *et al.*, 2011). Interacting with the

KOPS motif (GGGNAGGG) causes the assembly of the FtsK<sub>C</sub> hexameric motor (Graham *et al.*, 2010) and orients translocation along the entire chromosome towards the *dif* site (Bigot *et al.*, 2005).

In addition to the role of FtsK, MukBEF is another key player in chromosome segregation in *E. coli*. In *E. coli*, MukB is the structural analog of SMC (structural maintenance of chromosome) and MukEF are the structural analog of ScpAB (non-SMC segregation and condensation proteins A and B) protein complexes, which are present in all three domains of life and play various roles in chromosome organization, segregation and processing (Reyes-Lamothe *et al.*, 2012).

In bacteria, the quaternary structure of the SMC-ScpAB (MukBEF) complex includes 5 subunits: two SMC proteins, a single ScpA subunit and a dimer of ScpB protein. SMC has an ABC-type ATPase head domain and a hinge homodimerization domain, which are connected with a long antiparallel coiled-coil domain (Hirano *et al.*, 2001). ScpA belongs to the family of kleisin proteins, which interacts with the head and coiled-coil region of SMC through its C-terminal winged-helix domain and N-terminal helical domain, respectively, (Burmam *et al.*, 2013) and ScpB binds to the central region of ScpA as a dimer (Burmam *et al.*, 2013; Kamada *et al.*, 2013).

MukBEF is associated with *oriC* and the loss of *mukBEF* causes mispositioning of *ori* to the outer nucleoid edge from the midcell in *E. coli* cells, temperature sensitivity and defects in chromosome segregation (Niki *et al.*, 1991). Although MukBEF associates with *oriC*, the initiation of DNA replication is independent from MukBEF, but the condensin is required to generate and maintain wild-type chromosome positioning in *E. coli* cells (Petrushenko *et al.*, 2006; Badrinarayanan *et al.*, 2012; Yamazoe *et al.*,

1999). Even though the exact *in vivo* mechanism of MukBEF function remains elusive, biochemical studies revealed that MukB interacts with MukEF and binds to DNA and produces ATP-controlled macromolecular clamps that are required for efficient intramolecular DNA bridging (Cui *et al.*, 2008).

In addition to the roles of FtsK and MukBEF in chromosome segregation, ParAB/*parS* system is another key player contributing to chromosome partitioning. The Par systems described for plasmid segregation are involved in the partitioning of some low-copy-number plasmids and chromosomes for many bacteria (Gerdes *et al.*, 2010; Ringgaard *et al.* 2009). However, *E. coli* lacks a chromosomal Par segregation system. The deviant Walker A-type ATPase MinD is the closest homolog of ParA in *E. coli* and *migS* is the centromere-like element. However, there is no evidence that MinD interacts with *migS*. *migS* plays an undefined role in bipolar positioning (localization near the cell quarters) of *oriC*, but is not required for proper chromosome segregation in dividing cells (Yamaichi and Niki, 2004; Fekete and Chatteraj, 2005). *migS* consists of 25 bp long sequence, which is also located close to *oriC* region like *parS* sequences (Yamaichi and Niki, 2004).

Even though *E. coli* lacks a chromosomal Par segregation system, it has other systems that help coordinate chromosome segregation. Although no single system is necessary or sufficient for chromosome segregation, some systems are related to other cellular processes, such as the Min system in controlling cell division. The Min system includes three proteins: MinC, MinD, and MinE. ParA-like MinD inhibits cell division at sites away from the mid-cell (Lutkenhaus 2007, 2012). MinD-ATP binds to the cytoplasmic membrane and polymerizes by interacting with other membrane-associated



MinD-ATP molecules at the cell poles (Rothfield *et al.*, 2005). The Min and Par systems are very similar to each other, such as both MinD and ParA are deviant Walker A P loop ATPases that form dynamic patterns on the cell membrane and nucleoid, respectively (Ebersbach and Gerdes, 2001; Hu *et al.*, 2002; Raskin and de Boer, 1999; Shih *et al.*, 2003). The ATP-bound dimers of ParA and MinD form cytoskeletal-like filaments on DNA and membranes, respectively (Hu *et al.*, 2002; Leonard *et al.*, 2005). Even though there is no homology between MinE and ParB, they both stimulate the ATPase activity of MinD and ParA, respectively, (Leonard *et al.*, 2005; Ma *et al.*, 2004). At the same time, MinD also binds to DNA in a non-sequence specific manner. This MinD-DNA association creates a dynamic gradient of DNA binding sites near the membrane, which gradually moves from midcell to cell poles in the process of MinD oscillation (Di Ventura *et al.*, 2013). MinD recruits MinC and MinE to the cell poles. MinC is a cell division inhibitor that binds to FtsZ protofilaments and leads to disassembly of FtsZ polymers, thus preventing FtsZ ring formation from the cell poles and restricts formation at the mid-cell. MinD associates with MinC and oscillates in spiral-shaped structures between the poles of the cells. MinE is the topological regulator factor that stimulates the ATPase activity of MinD, thus oscillation of MinCD complex (de Boer *et al.*, 1989; Lutkenhaus, 2007). This MinCDE recruitment extends from the pole towards the midcell, where MinE molecules form the E-ring. MinE activates MinD ATPase, which causes MinD-ADP to release from the membrane due to its lower affinity for the bilayer, and polar zone disassembly. Release of MinC, MinD, and MinE molecules forms the zone of division inhibition. Upon MinD release from the membrane, MinD-ADP undergoes nucleotide exchange to be converted into MinD-ATP in the cytoplasm and its

concentration starts to increase at the other cell pole to repeat the process of forming the new polar zone inhibition (Figure 1.2, A) (Di Ventura *et al.*, 2013; Pinho *et al.*, 2013; Rothfield *et al.*, 2005).

In addition to the Min system, *E. coli* also evolved a nucleoid occlusion (NO) system to prevent inaccurate placement of the Z-ring, therefore avoiding cells lacking chromosomal DNA, or guillotined chromosomes (Hussain *et al.*, 1987; Mulder and Woldringh, 1989; Woldringh *et al.*, 1990; Wu and Errington, 2011). SlmA (synthetic lethal with a defective Min system) has been identified as a nucleoid occlusion effector protein (Bernhardt and de Boer, 2005). SlmA binds to specific DNA sequences containing a 12-bp palindromic site with the consensus, GTGAGTACTCAC, which are distributed over the chromosome with an exception of the *ter* region of the chromosome (Wu *et al.*, 2009; Cho *et al.*, 2011; Tonthat *et al.*, 2011). Before the initiation of DNA replication, mid-cell region of the cell is occupied by the *oriC* region of the chromosome, therefore it is protected by SlmA mediated NO system. As replication advances, *oriC* region migrates towards the cell quarters and away from the midcell, thus a SlmA/NO free zone is formed at the mid-cell, which allows FtsZ polymerization and cell division.

All the systems described above (FtsK, MukBEF, MinDEC, NO) have been implicated directly or indirectly in bacterial chromosome segregation. Unfortunately, no single system is necessary or sufficient for chromosome segregation. However, understanding the complexities and interplay of each system would help to understand the coordination with other cellular processes.

### **Chromosome segregation in *Bacillus subtilis***

The specific organization of the bacterial chromosome within the cell was first

discovered by the genetic studies in *B. subtilis* (Wu and Errington, 1994). *B. subtilis* is a low GC, Gram-positive, endospore forming bacterium. In newborn vegetative cells of *B. subtilis*, *oriC* region of the chromosome is localized to one pole and the *ter* region is located at the opposite cell pole (Webb *et al.*, 1997). However, in sporulating cells, *oriC* regions of sister chromosomes are anchored to each cell pole through RacA and DivIVA. RacA is a DNA-binding protein, which is conserved only in related spore-forming bacteria (such as *B. halodurans* and *Clostridium acetobutylicum*) (Wu and Errington, 2003). RacA is required for chromosome segregation during spore formation in *B. subtilis* (Wu and Errington, 2003; Ben-Yehuda *et al.*, 2003). RacA binds to sites in the *oriC* region of the chromosome and interacts with the curvature-sensitive membrane binding protein DivIVA (Wu and Errington, 2003; Ben-Yehuda *et al.*, 2003; Lenarcic *et al.*, 2009). Homologs of DivIVA are known to recruit proteins that are involved in chromosome segregation, cell division and cell wall synthesis to the poles in various bacteria (van Baarle *et al.*, 2013).

SpoIIIE, the FtsK homolog of *B. subtilis*, is another protein that is involved in chromosome segregation. During sporulation SpoIIIE travels to the asymmetrically positioned division septum and helps translocate one copy of the chromosome from the mother cell to the prespore compartment (Wu and Errington, 1997; Bath *et al.*, 2000; Chary and Piggot, 2003; Liu *et al.*, 2006). SpoIIIE is an essential protein for efficient *B. subtilis* sporulation (Wu and Errington, 1997). Similar to FtsK in *E. coli*, SpoIIIE utilizes SpoIIIE recognition sequences (SRS) [GAG(C/A)AGGG] and orients DNA translocation (Ptacin *et al.*, 2008).

The ParAB-like proteins of *B. subtilis* are among the most thoroughly studied

chromosomal partitioning proteins. *B. subtilis* has *soj* (*parA* homolog) and *spo0J* (*parB* homolog) genes that are located in an operon with close proximity to *oriC* region of the chromosome (Gerard *et al.*, 1998; Ogasawara and Yoshikawa, 1992). *soj* was first identified as a suppressor of the *spo0J* mutants in which the sporulation defect caused by *spo0J* was suppressed by a mutation in *soj* (which stands for suppressor of *spo0J*) (Ireton *et al.*, 1994). *Soj* is also a transcription initiation inhibitor that blocks transcription of some early sporulation genes (Cervin *et al.*, 1998; Quisel and Grossman, 2000).

A *soj* deletion mutant has no effect on vegetative chromosome segregation whereas *spo0J* deletion mutant produces 1-2% of anucleate cells (Ireton *et al.*, 1994). Even though a *soj spo0J* double mutant has no defect in origin movement, it has a bigger defect in partitioning during sporulation such that 70% of the prespores lose their DNA content (Sharpe and Errington, 1996).

*Spo0J* has specific DNA binding sites (*parS* sites) as its counterparts in plasmid partitioning systems (Lin and Grossman, 1998). *B. subtilis* genome has 10 *parS* sites that consist of 16 bp consensus sequences (Kunst *et al.*, 1997). *Spo0J* binds to these multiple *parS* sites positioned around the *oriC* region of the chromosome, therefore *ParB/parS* localization indirectly shows the localization of origin of replication. As for its homologs in plasmids, *Spo0J* alters the DNA conformation and binds co-operatively to non-*parS* sequences to form protein-DNA complexes that cover 20% of the *oriC* region of the chromosome (Lewis and Errington, 1997; Lin and Grossman, 1998; Marston and Errington, 1999). During cell division these assembled *Spo0J* proteins move along with the origin of replication (Lewis and Errington, 1997; Lin *et al.*, 1997; Webb *et al.*, 1997). Localization of *Spo0J/oriC* in vegetative cells is different from that in sporulating cells.

In vegetative cells, origins are located in different positions but preferentially towards one of the cell poles. The two chromosomal copies appear as a single nucleoid with two Spo0J/origin foci near the cell poles of newly born vegetative cells in *B. subtilis*. These foci remain separated during cell elongation. When initiation of the DNA replication commences, Spo0J/origin foci duplicate and segregate from each other, which is followed by cell growth, separation of nucleoids, and FtsZ ring formation at the center (Lin *et al.*, 1997). Thus, it has been suggested that initiation of replication and nucleoid separation are relatively synchronous in *B. subtilis* (Sharpe and Errington, 1998). In sporulating cells, two Spo0J foci move to the extreme poles of the cell (Glaser *et al.*, 1997; Lin *et al.*, 1997; Webb *et al.*, 1997). With the formation of the asymmetrically positioned septum, the remainder of the chromosomes are separated from each other and one is translocated into the prespore prior to mother cell engulfment of the prespore (Webb *et al.*, 1997).

Soj has two big roles in chromosome segregation. First, it assembles on the nucleoid and helps Spo0J proteins to condense into their centromere-like complexes. Second, it controls the nucleoid structure by assembling and disassembling into large nucleoid-associated structures by oscillating from one end of the cell to the other (Marston and Errington, 1999; Quisel *et al.*, 1999). It has been shown that conserved surface arginine residues are involved in mediating *in vivo* and *in vitro* nonspecific Soj-DNA interaction (Hester and Lutkenhaus, 2007). The increase in the Spo0J concentration on DNA stimulates the disassembly of Soj from the nucleoid and reassembles on another nucleoid. Thus, Spo0J is essential for the dynamic dissociation of Soj from the nucleoid. This dynamic localization of Soj is probably caused by the nucleotide binding and/or

hydrolysis behavior of the protein (Marston and Errington, 1999). Even though loss of Soj has little effect on chromosome segregation, it is required in conjunction with Spo0J/*parS* site for proper artificial plasmid partitioning in a heterologous *in vivo* assay (Hester and Lutkenhaus, 2007; Yamaichi and Niki, 2000).

Spo0J also plays a crucial role in recruiting SMC-ScpAB to the region around *oriC* (Gruber and Errington, 2009; Sullivan *et al.*, 2009; Minnen *et al.*, 2011). An *smc*-null mutant fails to condense nucleoids and forms approximately 28% anucleate vegetative cells in *B. subtilis* (Britton *et al.*, 1998). Segregation of sister *oriC* regions is also affected by the inactivation of SMC-ScpAB protein complex in *B. subtilis* under nutrient rich growth conditions and causes lethal defects in chromosome segregation. Therefore, the SMC-ScpAB complex presumably organizes newly replicated sister chromosomes by condensing them and preparing their segregation to opposite poles of the cell (Gruber *et al.*, 2014; Wang *et al.*, 2014). Wilhelm *et al.* (2015) showed that *spo0J* mutants are not only defective to form nucleoprotein complexes and spread from the *parS* sites, but also unable to load the SMC-ScpAB complex on the chromosome at the origin.

### **Chromosome segregation in *Caulobacter crescentus***

The chromosome within *C. crescentus* is highly organized in a fashion that is similar to the chromosome within *B. subtilis*. *C. crescentus* is a Gram-negative alpha-proteobacterium, which has a unique asymmetric cell division that always produces two types of daughter cells, a motile stalk cell and an immobile swarmer cell (Goley *et al.*, 2011). *C. crescentus* *oriC* region is located at one pole and *ter* region is located at the opposite pole of the cell. *oriC* region is attached to the flagellated pole by PopZ and ParB/*parS*. (See below for detailed descriptions of the functions of these elements.)

In *C. crescentus*, SMC is one of the key players of chromosome segregation. Unlike the single focus of *B. subtilis* SMC, *C. crescentus* SMC accumulates in multiple foci throughout the cell and a bright focus has been seen to localized near a cell pole in 30-40% of predivisional cells (Jensen and Shapiro, 2003). An *smc*-null mutation causes a conditional lethal temperature sensitive phenotype (Jensen and Shapiro, 1999; Britton *et al.*, 1998; Niki *et al.* 1991), and mislocalization of *oriC* and *ter* regions of the chromosome in 10-15% of the cells at the nonpermissive temperature (Jensen and Shapiro, 1999). Even though the roles of ScpA and ScpB in chromosome segregation still remain elusive, Shwartz and Shapiro (2011) showed that SMC co-immunoprecipitates in complex with ScpA and ScpB and proper chromosome segregation requires the ATPase activity of SMC to bind to chromosomal DNA.

In contrast to *E. coli* and *B. subtilis*, chromosome segregation and cell division are dependent of each other in *C. crescentus* (Du and Lutkenhaus, 2012). Even though there are no homologs of Min and NO systems in *C. crescentus*, it has genes encoding ParA and ParB homologs in the *oriC* region of the chromosome and these are essential for the bacterium (Mohl and Gober, 1997). There are two *parS* sites in *C. crescentus* (Livny *et al.*, 2007). ParB binds to these *parS* sequences downstream of *parAB* operon and is also capable of binding weakly to sequences with high AT nucleotide content. Over-expression of ParA produces elongated cells and localization defects of ParB whereas over-expression of ParB causes filamentous cells and multiple ParB foci that are mislocalised and scattered throughout the cell. When both proteins were over-expressed, an increased rate of production of anucleate cells and small defects on cell division and mislocalised/scattered ParB foci were observed (Bignell and Thomas, 2001; Mohl and

Gober, 1997). Thanbichler and Shapiro (2006) identified a bipolar gradient of the FtsZ inhibitor MipZ as an important factor for coupling cell division and chromosome segregation. MipZ is a member of ParA/MinD family of deviant Walker A type ATPases. An *in vivo* assay in *E. coli* showed that a MipZ gradient is stimulated by nonspecific DNA binding and the ATPase activity of the protein (Kiekebusch *et al.*, 2012).

*C. crescentus* has a polarly located protein, PopZ, which is essential for tethering the ParB/origin complexes to the cell poles. PopZ does not contain any known motif or domain, but according to bioinformatic analysis, PopZ homologs exist broadly in  $\alpha$ -proteobacterial genomes (Ebersbach *et al.*, 2008). Prior to S phase of DNA replication, a ParB focus bound to *parS* centromere sites is tethered to the old pole by interaction with PopZ, whereas FtsZ is restricted at the opposite pole of the cell and ParA is spread over the nucleoid (Bowman *et al.*, 2008; Mohl and Gober, 1997). ParB stimulates dimerization of ATP-bound MipZ by binding MipZ monomers and increases its concentration at the cell poles (Kiekebusch *et al.*, 2012; Thanbichler and Shapiro, 2006). Thus, ParB promotes non-specific DNA binding of MipZ. At the beginning of the cell cycle, a single ParB focus replicates and one of the ParB/origin complexes moves along with some MipZ to the opposite pole by the help of its interaction with ParA (Bowman *et al.*, 2008). ParB interaction with nucleoid-bound ParA causes its release from the nucleoid as monomers due to ATP hydrolysis, which is responsible for the segregation of the ParB/origin complex by a burnt bridge Brownian ratchet mechanism, which means that ParB/*oriC* disassembles ParA protofilaments and ratchets along a receding ParA structure and leaves the disassembled ParA dimers behind (Antal and Krapivsky, 2005; Ptacin *et al.*, 2010; Schofield *et al.*, 2010; Shebelut *et al.*, 2010). Ptacin *et al.* (2010) identified a



pole-specific protein, TipN, as a new component of the Par system in *C. crescentus*. TipN interacts with ParA *in vitro* and is essential for proper ParA localization and ParA-mediated ParB/*parS* segregation (Ptacin *et al.*, 2010). TipN might help to increase the local concentration of ParA by providing a binding site for ParA at the new pole (Ptacin *et al.*, 2010). Once the MipZ/ParB/origin complex reaches the new pole, the ParB focus binds to a new patch of PopZ and accompanying MipZ stimulates the release of FtsZ from the cell pole towards the midcell, which leads to midcell FtsZ ring formation where the bipolar MipZ gradient is the lowest (Figure 1.2, B) (Thanbichler and Shapiro, 2006).

Similar to *B. subtilis* and *E. coli*, FtsK is another key player in proper chromosome segregation in *C. crescentus*. FtsK was found to be localized at the division plane just before the cell division and after cell division it remained localized at the new cell pole of each progeny cell (Wang *et al.*, 2006). The C-terminal portion of the FtsK (FtsK<sub>C</sub>) is essential for the viability of the cells and 15-20% cells show segregation defects in cells depleted in FtsK<sub>C</sub>, whereas N-terminal region of the protein is important for localization of FtsK to the division plane, which is required for assembling or maintaining the FtsZ rings (Wang *et al.*, 2006). As mentioned above, *C. crescentus* chromosome segregation and cell division are dependent on each other in *C. crescentus* (Du and Lutkenhaus, 2012) and FtsK is one of the proteins that mediates an interdependence between chromosome segregation and cell division in *C. crescentus* (Wang *et al.*, 2006).

### **Chromosome segregation in *Corynebacterium glutamicum***

*C. glutamicum* is a unicellular high GC Gram-positive *Actinobacterium* that is known for its importance in biotechnology and as a model organism for mycolic acid

containing pathogens (Donovan and Bramkamp, 2014). However, the chromosome segregation aspect of this bacterium had not been studied in detail until recent years (Donovan *et al.*, 2010).

As in *B. subtilis* and *C. crescentus*, *C. glutamicum* has a chromosomal Par segregation system. It has a *parAB* operon, which is located close to the *oriC* region. There are three *parS* centromere-like sites that are located around the *oriC* region of the *C. glutamicum* chromosome (Donovan *et al.*, 2010; Livny *et al.*, 2007). *In vitro* assays have shown that ParB binds to *parS* sites and ParB-EGFP can be used to show the localization of origin of replication within the cell (Donovan *et al.*, 2010). Mutations in both *parA* and *parB* causes variable cell lengths, growth defects, multinucleoid cells, as well as anucleate cells (16% for  $\Delta parA$  and 11% for  $\Delta parB$ ).

Typically, organisms contain a single *parA* gene. However, *C. glutamicum*, like other Actinobacteria, has a second *parA*-like gene, *pldP* (ParA-like division protein), which is located on the opposite side of the chromosome without a neighboring *parB*-like gene. Even though there is 56% sequence similarity between products of *pldP* and *parA*, the mutants have different phenotypes. A *pldP* deletion mutation has no significant effect on chromosome segregation, but its loss causes various types of cell lengths from significantly longer to small and anucleate minicells, which suggests PldP has a role in cell division and it has been suggested that it acts as a division site selection protein (Donovan *et al.*, 2010). ParA localizes mostly close to the cell poles and colocalizes with the nucleoid in large patches, whereas PldP foci localize at the midcell (Donovan *et al.*, 2010). Similar to *Mycobacterium smegmatis* and *C. crescentus*, ParB foci localization is found to be close to the cell poles in non-dividing *C. glutamicum* cells (Bowman *et al.*,

2008; Donovan *et al.*, 2010; Maloney *et al.*, 2009; Mohl and Gober, 1997). Midcell localization of PldP in dividing cells suggested its potential direct interaction with FtsZ, which has also been confirmed by bacterial two-hybrid analysis (Donovan *et al.*, 2010). Even though PldP interacts with ParB in bacterial two-hybrid analysis, loss of PldP has no effect on ParB localization. However, ParA is necessary for polar localization of ParB, which suggests that ParA is required for the ParB/origin complex segregation to opposite poles of the cell (Donovan *et al.*, 2010).

A summary of the proposed model for chromosome segregation in *C. glutamicum* is given here. Prior to initiation of replication, ParB-origin nucleoprotein complex is localized to one cell pole by a ParB-DivIVA interaction. With the help of ParA, a duplicated new origin moves from the old origin towards the opposite cell pole after the initiation of replication and tethers to DivIVA. Tethering to DivIVA stimulates cell growth and helps the process of remaining DNA to segregate and condense to the opposite cell pole. After the DNA free zone in the midcell is created, polymerization of cell division protein FtsZ is initiated and Z ring formation occurs (Donovan *et al.*, 2012).

The proteins that are involved in chromosome segregation, such as the DNA translocase FtsK homolog and SMC-ScpAB protein complex in *C. glutamicum* have not been studied.

### **Chromosome segregation in *Streptomyces coelicolor***

Due to its large linear genome and complex life cycle, chromosome segregation in *S. coelicolor* may be more complex than unicellular bacteria dividing by binary fission (Bentley *et al.*, 2002). *S. coelicolor* is an advantageous organism for studying DNA

segregation since all of the tested segregation gene mutants are viable unlike other organisms (Dedrick *et al.*, 2009; Kois *et al.*, 2009).

This unique filamentous Gram-positive, sporulating soil bacterium has a large linear genome (8.67 Mbp) (Bentley *et al.*, 2002). It has one linear (SCP1) and one circular plasmid (SCP2) (Bentley *et al.*, 2004; Haug *et al.*, 2003). Compared to other prokaryotes it has an unusual life cycle. Branching filamentous hyphae grow from a germinating spore. Syncytial compartments are generated by widely-spaced cross-walls, which form in the vegetative mycelium where DNA is not condensed and septation is infrequent and not essential (McCormick *et al.*, 1994). Mature vegetative mycelium produces new aerial hyphae. Tip extension of the hyphae is provided by the polarity determinant DivIVA, the long coiled-coil protein Scy, and the filamentous FilP (Bagchi *et al.*, 2008; Flardh, 2010; Hempel *et al.*, 2008; Walshaw *et al.*, 2010). These three proteins form the tip-organizing center (TIPOC) that are believed to be responsible for the hyphal shape and/or tip extension and branching (Flardh *et al.*, 2012; Holmes *et al.*, 2013). At the end of aerial growth, these syncytial multigenomic aerial filaments synchronously divide and segregate chromosomes into a chain of uniformly-sized unicellular compartments (McCormick, 2009; McCormick and Flardh, 2012).

*S. coelicolor* has a chromosomal ParAB/*parS* segregation system. *Streptomyces* ParB binds to 24 *parS* sites near the origin of replication (*oriC*) (Jakimowicz *et al.*, 2002). In vegetative filaments and nascent aerial hyphae, ParB-EGFP localizes as a bright focus close to the tip with other foci being smaller and irregularly spaced through the length of the hyphae (Jakimowicz *et al.*, 2005). But during sporulation, evenly-spaced ParB-EGFP complexes assemble along the length of aerial hyphae, presumably organizing evenly-

spaced copies of the genome (Figure 1.3). The ParB-*parS* nucleoprotein complexes form before observable DNA condensation and septation and disassemble after these processes (Jakimowicz *et al.*, 2005). Even though the deletion of *parB*, or *parAB* operon, or elimination of the ParB DNA-binding motif are dispensable on colony growth and sporulation, these mutations resulted in anucleate spores about 15% in *parB* and 24% in *parA* mutants when compared to wild type cells (Jakimowicz *et al.*, 2002; Jakimowicz *et al.*, 2005). In nascent aerial hyphae, ParA accumulates first at the tips and then goes on to form helical filaments that spread along the aerial hyphae. ParA provides the assembly of ParB-*parS* nucleoprotein complexes *in vivo* and *in vitro* and both proteins play an important role in the accurate distribution of the chromosomes in the aerial hyphae. ParB enhances the ATPase activity of ParA and ATP binding is required for the dimerization of the protein but not the localization of the helical filaments in aerial hyphae (Jakimowicz *et al.*, 2007).

In addition to being part of the segregation complex and interacting with ParB, ParA has been shown to interact with two other proteins, Scy and ParJ (Ditkowski *et al.*, 2013; Ditkowski *et al.*, 2010). Scy, an intermediate filament-like protein, recruits ParA to hyphal tips and inhibits ParA polymerization, which also supports the idea that the TIPOC plays a role in developmental switch from aerial hyphal extension to sporulation. ParJ is one of the unique signature proteins that are widespread among Actinobacteria and are not found in any other bacteria (Gao *et al.*, 2009). Prior to septation during sporulation, ParJ controls ParA polymerization and causes the disassembly of the ParA polymers *in vitro* (Ditkowski *et al.*, 2010).

In addition to the partitioning proteins, SMC and FtsK proteins also play a role in

developmentally-associated chromosome segregation in *S. coelicolor*. Even though a *smc*-null mutation does not overtly affect DNA condensation, growth or morphology, it causes a slight defect in chromosome partitioning that resulted in 7-8% anucleate spores, whereas *scpAB*-null mutants showed bilobed nucleoids in spore compartments, which suggests they participate in the condensation of the DNA (Dedrick *et al.*, 2009, Kois *et al.*, 2009). As for homologs of *B. subtilis* and *C. crescentus*, ScpA interacts with ScpB and SMC *in vitro* (Kois *et al.*, 2009). A *smc scpAB* triple mutant produces 3% anucleate spores and 17% bilobed nucleoids in *S. coelicolor*, suggesting that SMC-ScpAB protein complex is not essential for chromosome condensation alone and might have another role in *S. coelicolor*. Double deletion mutants for *smc parA* and *smc parB* have also been tested and the additive phenotypes have been found (Dedrick *et al.*, 2009; Kois *et al.*, 2009). Interestingly, ParB-EGFP localization in a *smc*-null mutant appears to be smaller and less intensely fluorescent when compared to wild type ParB-EGFP foci in aerial filaments, which suggests that SMC may directly or indirectly help the formation of ParB/*parS* nucleoprotein complexes.

Unlike SMC, FtsK has a specific localization in *S. coelicolor* aerial filaments. FtsK localizes at the sporulation septa (Wang *et al.*, 2007; Ausmees *et al.*, 2007; Dedrick *et al.*, 2009). An *ftsK*-null mutant can cause large deletions in the chromosome and this probably causes the heterogeneity in colony formation when compared to the wild type strain (Wang *et al.*, 2007; Ausmees *et al.*, 2007; Dedrick *et al.*, 2009). Since there is no known NO system in *S. coelicolor*, *ftsK* deletion might cause the guillotine of the chromosome at the sporulation septa (Flardh, 2003). Even though the *ftsK*-null mutant has the same percentage of anucleate cells as for the in wild type strain, large

chromosome deletions during sporulation suggests a role for FtsK in developmentally-associated chromosome segregation (Wang *et al.*, 2007; Ausmees *et al.*, 2007; Dedrick *et al.*, 2009).

Even though Par proteins, FtsK, and SMC are all key players of the developmentally-associated chromosome segregation in *S. coelicolor*, the molecular machinery that underlies the chromosome partitioning has not been fully elucidated. Since a triple *parB smc ftsK* mutant results in only 10% anucleate spores, there must be other proteins that are involved in the chromosome partitioning system of *S. coelicolor*. Like other Actinobacteria, *Streptomyces* genome sequences reveal that in addition to *parA*, it has a second *parA*-like gene, called *parH*. Recent studies show that two other Actinobacteria [*Aggregatibacter actinomycetemcomitans* (*tadZ*) and *C. glutamicum* (*pldP*)] also have a second *parA*-like gene (Donovan *et al.*, 2010; Perez-Cheeks *et al.*, 2012). TadZ and PldP are found associated with biofilm formation on periodontal diseases and division site-selection, respectively (Donovan *et al.*, 2010; Perez-Cheeks *et al.*, 2012). Even though all the proteins that are described before (FtsK, SMC-ScpAB, ParAB) are associated with proper chromosome segregation, no single system is sufficient for efficient chromosome segregation.

My goal in this dissertation was to find additional proteins that participate in *Streptomyces* chromosome segregation. Specifically, my work continued Dedrick's preliminary study of the second ParA-like protein in the *S. coelicolor* genome (called ParH) (Dedrick, 2009), suggesting that ParH might be directly or indirectly involved in chromosome segregation. My study further describes and characterizes the role of ParH in chromosome segregation in *S. coelicolor*. In addition to the analysis of ParH, I

identified a novel protein (called HaaA) that interacts with both ParA and ParH. HaaA is also a unique signature protein in Actinobacteria. The role of HaaA in chromosome partitioning is partially characterized and will also be explained in this study.



## REFERENCES

- Abeles, A. L., Friedman, S. A., Austin, S. J. (1985). Partition of unit-copy miniplasmids to daughter cells. III. The DNA sequence and functional organization of the P1 partition region. *J Mol Biol.*, 185(2), 261-272.
- Ah-Seng, Y., Lopez, F., Pasta, F., Lane, D., Bouet, J. Y. (2009). Dual role of DNA in regulating ATP hydrolysis by the SopA partition protein. *J Biol Chem.*, 284(44), 30067-30075. doi: 10.1074/jbc.M109.044800.
- Antal, T., Krapivsky, P. L., (2005). "Burnt-bridge" mechanism of molecular motor motion. *Phys Rev E Stat Nonlin Soft Matter Phys.*, 72(4):046104.
- Aussel, L., Barre, F., Aroyo, M., Stasiak, A., Stasiak A. Z., & Sherratt, D. (2002). FtsK is a DNA motor protein that activates chromosome dimer resolution by switching the catalytic state of the XerC and XerD recombinases. *Cell*, 108, 195–205.
- Aylett, C. H., Lowe, J. (2012). Superstructure of the centromeric complex of TubZRC plasmid partitioning systems. *Proc Natl Acad Sci U S A*, 109(41), 16522-16527. doi: 10.1073/pnas.1210899109.
- Bagchi, S., Tomenius, H., Belova, L. M., Ausmees, N. (2008). Intermediate filament-like proteins in bacteria and a cytoskeletal function in *Streptomyces*. *Mol Microbiol.*, 70(4), 1037-1050. doi: 10.1111/j.1365-2958.2008.06473.x.
- Barilla, D., Carmelo, E., Hayes, F. (2007). The tail of the ParG DNA segregation protein remodels ParF polymers and enhances ATP hydrolysis via an arginine finger-like motif. *Proc Natl Acad Sci U S A*, 104(6), 1811-1816. doi: 10.1073/pnas.0607216104.

- Bentley, S. D., Brown, S., Murphy, L. D., Harris, D. E., Quail, M. A., Parkhill, J., . . . , Chater, K. F. (2004). SCP1, a 356,023 bp linear plasmid adapted to the ecology and developmental biology of its host, *Streptomyces coelicolor* A3(2). *Mol Microbiol.*, 51(6), 1615-1628.
- Bentley, S.D., Chater, K.F., Cerdeño-Tárraga, A.M., Challis, G.L., Thomson, N.R., James, K.D., . . . , Hopwood, D.A. (2002). Complete genome sequence of the model actinomycete *Streptomyces coelicolor* A3(2). *Nature*, 417(6885), 141-147. doi: 10.1038/417141a.
- Ben-Yehuda, S., Rudner, D.Z., and Losick, R. (2003). RacA, a bacterial protein that anchors chromosomes to the cell poles. *Science*, 299, 532-536.
- Bernhardt, T.G. and de Boer, P.A. (2005). SlmA, a nucleoid-associated, FtsZ binding protein required for blocking septal ring assembly over chromosomes in *E. coli*. *Mol. Cell*, 18, 555-564.
- Berry, C., O'Neil, S., Ben-Dov, E., Jones, A. F., Murphy, L., Quail, M. A., Parkhill, J. (2002). Complete sequence and organization of pBtoxis, the toxin-coding plasmid of *Bacillus thuringiensis* subsp. *israelensis*. *Appl Environ Microbiol.*, 68(10), 5082-5095.
- Bignell, C., Thomas, C. M. (2001). The bacterial ParA-ParB partitioning proteins. *J Biotechnol.*, 91(1), 1-34.
- Bigot S, Saleh OA, Lesterlin C, Pages C, El Karoui M, Dennis C, Grigoriev M, Allemand JF, Barre FX, Cornet F. (2005). KOPS: DNA motifs that control *E. coli* chromosome segregation by orienting the FtsK translocase. *EMBO J.*, 24(21), 3770-80.

- Bigot S, Sivanathan V, Possoz C, Barre F, Cornet F. (2007). FtsK, a literate chromosome segregation machine. *Mol Microbiol.*, 64(6), 1434–1441. doi: 10.1111/j.1365-2958.2007.05755.x.
- Bigot S, Corre J, Louarn J, Cornet F, Barre F. (2008). FtsK activities in Xer recombination, DNA mobilization and cell division involve overlapping and separate domains of the protein. *Mol Microbiol.*, 54, 876–886.
- Bouet, J. Y., Ah-Seng, Y., Benmeradi, N., Lane, D. (2007). Polymerization of SopA partition ATPase: regulation by DNA binding and SopB. *Mol Microbiol.*, 63(2), 468-481. doi: 10.1111/j.1365-2958.2006.05537.x.
- Bowman, G. R., Comolli, L. R., Zhu, J., Eckart, M., Koenig, M., Downing, K. H., Shapiro, L. (2008). A polymeric protein anchors the chromosomal origin/ParB complex at a bacterial cell pole. *Cell*, 134(6), 945-955.  
doi:10.1016/j.cell.2008.07.015.
- Britton, R.A., Lin, D.C., Grossman, A.D. (1998). Characterization of a prokaryotic SMC protein involved in chromosome partitioning. *Genes Dev.*, 12, 1254-1259.
- Bürmann, F., Shin, H.-C., Basquin, J., Soh, Y.-M., Giménez-Oya, V., Kim, Y.-G., Oh, B.-H., and Gruber, S. (2013). An asymmetric SMC-kleisin bridge in prokaryotic condensin. *Nat. Struct. Mol. Biol.*, 20, 371–379. doi:10.1038/nsmb.2488.
- Cervin, M. A., Spiegelman, G. B., Raether, B., Ohlsen, K., Perego, M., Hoch, J. A. (1998). A negative regulator linking chromosome segregation to developmental transcription in *Bacillus subtilis*. *Mol Microbiol.*, 29(1), 85-95.

- Cho H, McManus HR, Dove SL, Bernhardt TG. (2011). Nucleoid occlusion factor SlmA is a DNA-activated FtsZ polymerization antagonist. *Proc Natl Acad Sci U S A*, 108(9), 3773-8. doi: 10.1073/pnas.1018674108.
- Cui, Y., Petrushenko, Z.M. and Rybenkov, V.V. (2008). MukB acts as a macromolecular clamp in DNA condensation. *Nat. Struct. Mol. Biol.*, 15, 411-418.
- Dam, M., Gerdes, K. (1994). Partitioning of plasmid R1. Ten direct repeats flanking the *parA* promoter constitute a centromere-like partition site *parC*, that expresses incompatibility. *J Mol Biol.*, 236(5), 1289-1298.
- Davey, M. J., Funnell, B. E. (1994). The P1 plasmid partition protein ParA. A role for ATP in site-specific DNA binding. *J Biol Chem.*, 269(47), 29908-29913.
- Davey, M. J., Funnell, B. E. (1997). Modulation of the P1 plasmid partition protein ParA by ATP, ADP, and P1 ParB. *J Biol Chem.*, 272(24), 15286-15292.
- Davis, M. A., Martin, K. A., Austin, S. J. (1992). Biochemical activities of the *parA* partition protein of the P1 plasmid. *Mol Microbiol.*, 6(9), 1141-1147.
- de Boer, P. A., Crossley, R. E., Rothfield, L. I. (1989). A division inhibitor and a topological specificity factor coded for by the minicell locus determine proper placement of the division septum in *E. coli*. *Cell*, 56(4), 641-649.
- Dedrick, R.M., Wildschutte, H., and McCormick, J.R. (2009). Genetic interactions of *smc*, *ftsK* and *parB* genes in *Streptomyces coelicolor* and their developmental genome segregation phenotypes. *J. Bacteriol.*, 191, 320-332.
- Delbruck, H., Ziegelin, G., Lanka, E., Heinemann, U. (2002). An Src homology 3-like domain is responsible for dimerization of the repressor protein KorB encoded by

- the promiscuous IncP plasmid RP4. *J Biol Chem.*, 277(6), 4191-4198. doi: 10.1074/jbc.M110103200.
- Di Ventura, B., Knecht, B., Andreas, H., Godinez, W. J., Fritsche, M., Rohr, K., Sourjik, V. (2013). Chromosome segregation by the *Escherichia coli* Min system. *Mol Syst Biol.*, 9, 686. doi: 10.1038/msb.2013.44.
- Ditkowski, B., Holmes, N., Rydzak, J., Donczew, M., Bezulska, M., Ginda, K., Jakimowicz, D. (2013). Dynamic interplay of ParA with the polarity protein, Scy, coordinates the growth with chromosome segregation in *Streptomyces coelicolor*. *Open Biol.*, 3(3), 130006. doi: 10.1098/rsob.130006.
- Ditkowski, B., Troc, P., Ginda, K., Donczew, M., Chater, K. F., Zakrzewska-Czerwinska, J., Jakimowicz, D. (2010). The actinobacterial signature protein ParJ (SCO1662) regulates ParA polymerization and affects chromosome segregation and cell division during *Streptomyces* sporulation. *Mol Microbiol.*, 78(6), 1403-1415. doi: 10.1111/j.1365-2958.2010.07409.x.
- Donovan, C., Bramkamp, M. (2014). Cell division in *Corynebacterineae*. *Front Microbiol.*, 5, 132. doi: 10.3389/fmicb.2014.00132.
- Donovan, C., Schwaiger, A., Kramer, R., Bramkamp, M. (2010). Subcellular localization and characterization of the ParAB system from *Corynebacterium glutamicum*. *J Bacteriol.*, 192(13), 3441-3451. doi: 10.1128/JB.00214-10.
- Donovan, C., Sieger, B., Kramer, R., Bramkamp, M. (2012). A synthetic *Escherichia coli* system identifies a conserved origin tethering factor in Actinobacteria. *Mol Microbiol.*, 84(1), 105-116. doi: 10.1111/j.1365-2958.2012.08011.x.

- Du, S., Lutkenhaus, J. (2012). MipZ: one for the pole, two for the DNA. *Mol Cell*, 46(3), 239-240. doi: 10.1016/j.molcel.2012.04.024.
- Dubarry N, Barre F. (2010). Fully efficient chromosome dimer resolution in *Escherichia coli* cells lacking the integral membrane domain of FtsK. *EMBO J.*, 29, 597–605.
- Dubarry N, Possoz C, Barre FX. (2010). Multiple regions along the *Escherichia coli* FtsK protein are implicated in cell division. *Mol Microbiol.*, 78, 1088–1100.
- Dunham, T. D., Xu, W., Funnell, B. E., Schumacher, M. A. (2009). Structural basis for ADP-mediated transcriptional regulation by P1 and P7 ParA. *EMBO J.*, 28(12), 1792-1802. doi: 10.1038/emboj.2009.120.
- Ebersbach, G., Gerdes, K. (2001). The double par locus of virulence factor pB171: DNA segregation is correlated with oscillation of ParA. *Proc Natl Acad Sci U S A*, 98(26), 15078-15083. doi: 10.1073/pnas.261569598.
- Ebersbach G., Briegel A., Jensen G.J., Jacobs-Wagner C., (2008). A self-associating protein critical for chromosome attachment, division, and polar organization in *Caulobacter*. *Cell*, 134(6), 956-68. doi: 10.1016/j.cell.2008.07.016.
- Espeli O, Marians K. (2004). Untangling intracellular DNA topology. *Mol Microbiol.*, 52, 925–931.
- Flardh, K. (2003). Growth polarity and cell division in *Streptomyces*. *Curr Opin Microbiol.*, 6(6), 564-571.
- Flardh, K. (2010). Cell polarity and the control of apical growth in *Streptomyces*. *Curr Opin Microbiol.*, 13(6), 758-765. doi: 10.1016/j.mib.2010.10.002.

- Flardh, K., Richards, D. M., Hempel, A. M., Howard, M., Buttner, M. J. (2012). Regulation of apical growth and hyphal branching in *Streptomyces*. *Curr Opin Microbiol.*, 15(6), 737-743. doi: 10.1016/j.mib.2012.10.012.
- Galkin, V. E., Orlova, A., Rivera, C., Mullins, R. D., Egelman, E. H. (2009). Structural polymorphism of the ParM filament and dynamic instability. *Structure*, 17(9), 1253-1264. doi: 10.1016/j.str.2009.07.008.
- Gao, B., Sugiman-Marangos, S., Junop, M. S., Gupta, R. S. (2009). Structural and phylogenetic analysis of a conserved actinobacteria-specific protein (ASP1; SCO1997) from *Streptomyces coelicolor*. *BMC Struct Biol.*, 9, 40. doi: 10.1186/1472-6807-9-40.
- Gerard, E., Labedan, B., Forterre, P. (1998). Isolation of a *minD*-like gene in the hyperthermophilic archaeon *Pyrococcus* AL585, and phylogenetic characterization of related proteins in the three domains of life. *Gene*, 222(1), 99-106.
- Gerdes, K., Howard, M., Szardenings, F. (2010). Pushing and pulling in prokaryotic DNA segregation. *Cell*, 141(6), 927-942. doi: 10.1016/j.cell.2010.05.033.
- Gerdes, K., Moller-Jensen, J., Bugge Jensen, R. (2000). Plasmid and chromosome partitioning: surprises from phylogeny. *Mol Microbiol.*, 37(3), 455-466.
- Glaser, P., Sharpe, M. E., Raether, B., Perego, M., Ohlsen, K., Errington, J. (1997). Dynamic, mitotic-like behavior of a bacterial protein required for accurate chromosome partitioning. *Genes Dev.*, 11(9), 1160-1168.

- Goley, E.D., Yeh, Y.C., Hong, S.H., Fero, M.J., Abeliuk, E., McAdams, H.H., Shapiro, L., (2011). Assembly of the *Caulobacter* cell division machine. *Mol Microbiol.*, *80*, 1680-98.
- Golovanov, A. P., Barilla, D., Golovanova, M., Hayes, F., Lian, L. Y. (2003). ParG, a protein required for active partition of bacterial plasmids, has a dimeric ribbon-helix-helix structure. *Mol Microbiol.*, *50*(4), 1141-1153.
- Graham JE, Sherratt DJ, Szczelkun MD. (2010). Sequence-specific assembly of FtsK hexamers establishes directional translocation on DNA. *Proc Natl Acad Sci U S A*, *107*, 20263–20268.
- Grainge I, Lesterlin C, Sherratt DJ. (2011). Activation of XerCD-dif recombination by the FtsK DNA translocase. *Nucleic Acids Res.*, *39*(12), 5140-8.  
doi: 10.1093/nar/gkr078.
- Grenga L, Luzi G, Paolozzi L, Ghelardini P. (2008). The *Escherichia coli* FtsK functional domains involved in its interaction with its divisome protein partners. *FEMS Microbiol Lett.*, *287*, 163–167.
- Gruber S, Veening JW, Bach J, Blettinger M, Bramkamp M, Errington J. (2014). Interlinked sister chromosomes arise in the absence of condensin during fast replication in *B. subtilis*. *Curr Biol.*, *24*(3), 293-8. doi: 10.1016/j.cub.2013.12.049.
- Haug, I., Weissenborn, A., Brolle, D., Bentley, S., Kieser, T., Altenbuchner, J. (2003). *Streptomyces coelicolor* A3(2) plasmid SCP2\*: deductions from the complete sequence. *Microbiology*, *149*(2), 505-513.
- Hempel, A. M., Wang, S. B., Letek, M., Gil, J. A., Flardh, K. (2008). Assemblies of DivIVA mark sites for hyphal branching and can establish new zones of cell wall



- growth in *Streptomyces coelicolor*. *J Bacteriol*, 190(22), 7579-7583. doi: 10.1128/JB.00839-08.
- Hester, C. M., Lutkenhaus, J. (2007). Soj (ParA) DNA binding is mediated by conserved arginines and is essential for plasmid segregation. *Proc Natl Acad Sci U S A*, 104(51), 20326-20331. doi: 10.1073/pnas.0705196105.
- Hiraga, S. (1992). Chromosome and plasmid partition in *Escherichia coli*. *Annu Rev Biochem.*, 61, 283-306. doi: 10.1146/annurev.bi.61.070192.001435.
- Hirano, M., Anderson, D.E., Erickson, H.P., and Hirano, T. (2001). Bimodal Activation of SMC ATPase by intra- and inter-molecular interactions. *EMBO J.*, 20, 3238-3250.
- Holmes, N. A., Walshaw, J., Leggett, R. M., Thibessard, A., Dalton, K. A., Gillespie, M. D., Kelemen, G. H. (2013). Coiled-coil protein Scy is a key component of a multiprotein assembly controlling polarized growth in *Streptomyces*. *Proc Natl Acad Sci U S A*, 110(5), E397-406. doi: 10.1073/pnas.1210657110.
- Hu, Z., Gogol, E. P., Lutkenhaus, J. (2002). Dynamic assembly of MinD on phospholipid vesicles regulated by ATP and MinE. *Proc Natl Acad Sci U S A*, 99(10), 6761-6766. doi: 10.1073/pnas.102059099.
- Huang, L., Yin, P., Zhu, X., Zhang, Y., Ye, K. (2011). Crystal structure and centromere binding of the plasmid segregation protein ParB from pCXC100. *Nucleic Acids Res.*, 39(7), 2954-2968. doi: 10.1093/nar/gkq915.
- Hussain K, Begg KJ, Salmond GP, Donachie WD. (1987). ParD: a new gene coding for a protein required for chromosome partitioning and septum localization in *Escherichia coli*. *Mol Microbiol.*, 1(1), 73-81.

- Ireton, K., Gunther, N. W. t., Grossman, A. D. (1994). *spo0J* is required for normal chromosome segregation as well as the initiation of sporulation in *Bacillus subtilis*. *J Bacteriol.*, 176(17), 5320-5329.
- Jacob, F., Brenner, S. (1963). On the regulation of DNA synthesis in bacteria: the hypothesis of the replicon. *C R Hebd Seances Acad Sci.*, 256, 298-300.
- Jakimowicz, D., Chater, K., Zakrzewska-Czerwinska, J. (2002). The ParB protein of *Streptomyces coelicolor* A3(2) recognizes a cluster of *parS* sequences within the origin-proximal region of the linear chromosome. *Mol Microbiol.*, 45(5), 1365-1377.
- Jakimowicz, D., Gust, B., Zakrzewska-Czerwinska, J., Chater, K. F. (2005). Developmental-stage-specific assembly of ParB complexes in *Streptomyces coelicolor* hyphae. *J Bacteriol.*, 187(10), 3572-3580. doi: 10.1128/JB.187.10.3572-3580.2005.
- Jakimowicz, D., Zydek, P., Kois, A., Zakrzewska-Czerwinska, J., Chater, K. F. (2007). Alignment of multiple chromosomes along helical ParA scaffolding in sporulating *Streptomyces* hyphae. *Mol Microbiol.*, 65(3), 625-641. doi: 10.1111/j.1365-2958.2007.05815.x.
- Jensen, R. B., Gerdes, K. (1997). Partitioning of plasmid R1. The ParM protein exhibits ATPase activity and interacts with the centromere-like ParR-*parC* complex. *J Mol Biol.*, 269(4), 505-513. doi: 10.1006/jmbi.1997.1061.
- Jensen, R. B., Lurz, R., Gerdes, K. (1998). Mechanism of DNA segregation in prokaryotes: replicon pairing by *parC* of plasmid R1. *Proc Natl Acad Sci U S A*, 95(15), 8550-8555.

- Jensen, R.B. and Shapiro, L. (1999). The *Caulobacter crescentus* smc gene is required for cell cycle progression and chromosome segregation. *Proc. Natl. Acad. Sci. USA*, *96*, 10661-10666.
- Jensen, R.B. and Shapiro, L. (2003). Cell-cycle-regulated expression and subcellular localization of the *Caulobacter crescentus* SMC chromosome structural protein. *J. Bacteriol.*, *185*, 3068-3075.
- Kamada, K., Miyata, M., and Hirano, T. (2013). Molecular basis of SMC ATPase activation: role of internal structural changes of the regulatory subcomplex ScpAB. *Structure*, *21*, 581–594. doi:10.1016/j.str.2013.02.016.
- Khare, D., Ziegelin, G., Lanka, E., Heinemann, U. (2004). Sequence-specific DNA binding determined by contacts outside the helix-turn-helix motif of the ParB homolog KorB. *Nat Struct Mol Biol.*, *11*(7), 656-663. doi: 10.1038/nsmb773.
- Kiekebusch, D., Michie, K. A., Essen, L. O., Lowe, J., Thanbichler, M. (2012). Localized dimerization and nucleoid binding drive gradient formation by the bacterial cell division inhibitor MipZ. *Mol Cell*, *46*(3), 245-259. doi: 10.1016/j.molcel.2012.03.004.
- Kois, A., Swiatek, M., Jakimowicz, D., and Zakrzewska-Czerwinska, J. (2009). SMC protein-dependent chromosome condensation during aerial hyphal development in *Streptomyces*. *J. Bacteriol.*, *191*, 310-319.
- Koonin, E. V. (1993). A superfamily of ATPases with diverse functions containing either classical or deviant ATP-binding motif. *J Mol Biol.*, *229*(4), 1165-1174. doi: 10.1006/jmbi.1993.1115.

- Kunst, F., Ogasawara, N., Moszer, I., Albertini, A. M., Alloni, G., Azevedo, V., Danchin, A. (1997). The complete genome sequence of the Gram-positive bacterium *Bacillus subtilis*. *Nature*, 390(6657), 249-256. doi: 10.1038/36786.
- Larsen, R. A., Cusumano, C., Fujioka, A., Lim-Fong, G., Patterson, P., Pogliano, J. (2007). Treadmilling of a prokaryotic tubulin-like protein, TubZ, required for plasmid stability in *Bacillus thuringiensis*. *Genes Dev.*, 21(11), 1340-1352. doi: 10.1101/gad.1546107.
- Leonard, T. A., Butler, P. J., Lowe, J. (2005). Bacterial chromosome segregation: structure and DNA binding of the Soj dimer--a conserved biological switch. *EMBO J.*, 24(2), 270-282. doi: 10.1038/sj.emboj.7600530.
- Lesterlin C, Barre F, Cornet F. (2004). Genetic recombination and the cell cycle: what we have learned from chromosome dimers. *Mol Microbiol.*, 54, 1151–1160.
- Lewis, P. J., Errington, J. (1997). Direct evidence for active segregation of *oriC* regions of the *Bacillus subtilis* chromosome and co-localization with the Spo0J partitioning protein. *Mol Microbiol.*, 25(5), 945-954.
- Lim, G. E., Derman, A. I., Pogliano, J. (2005). Bacterial DNA segregation by dynamic SopA polymers. *Proc Natl Acad Sci U S A*, 102(49), 17658-17663. doi: 10.1073/pnas.0507222102.
- Lin, D. C., Grossman, A. D. (1998). Identification and characterization of a bacterial chromosome partitioning site. *Cell*, 92(5), 675-685.
- Lin, D. C., Levin, P. A., Grossman, A. D. (1997). Bipolar localization of a chromosome partition protein in *Bacillus subtilis*. *Proc Natl Acad Sci U S A*, 94(9), 4721-4726.

- Livny, J., Yamaichi, Y., Waldor, M. K. (2007). Distribution of centromere-like *parS* sites in bacteria: insights from comparative genomics. *J Bacteriol.*, *189*(23), 8693-8703. doi: 10.1128/JB.01239-07.
- Liu X, Wang X, Reyes-Lamothe R, Sherratt D. (2010). Replication-directed sister chromosome alignment in *Escherichia coli*. *Mol Microbiol.*, *75*(5), 1090–1097. doi: 10.1111/j.1365-2958.2009.06791.x.
- Löwe J, Ellonen A, Allen M, Atkinson C, Sherratt D, *et al.* (2008). Molecular mechanism of sequence-directed DNA loading and translocation by FtsK. *Mol Cell*, *31*, 498–509.
- Lutkenhaus, J. (2007). Assembly dynamics of the bacterial MinCDE system and spatial regulation of the Z ring. *Annu Rev Biochem.*, *76*, 539-562. doi: 10.1146/annurev.biochem.75.103004.142652.
- Lutkenhaus, J. (2012). The ParA/MinD family puts things in their place. *Trends Microbiol.*, *20*(9), 411-418. doi: 10.1016/j.tim.2012.05.002.
- Ma, L., King, G. F., Rothfield, L. (2004). Positioning of the MinE binding site on the MinD surface suggests a plausible mechanism for activation of the *Escherichia coli* MinD ATPase during division site selection. *Mol Microbiol.*, *54*(1), 99-108. doi: 10.1111/j.1365-2958.2004.04265.x.
- Maloney, E., Madiraju, M., Rajagopalan, M. (2009). Overproduction and localization of *Mycobacterium tuberculosis* ParA and ParB proteins. *Tuberculosis (Edinb)*, *89* Suppl 1, S65-69. doi: 10.1016/S1472-9792(09)70015-0.

- Marston, A. L., Errington, J. (1999). Dynamic movement of the ParA-like Soj protein of *B. subtilis* and its dual role in nucleoid organization and developmental regulation. *Mol Cell*, 4(5), 673-682.
- Massey T, Mercogliano C, Yates J, Sherratt D, Löwe J. (2006). Double-stranded DNA translocation: structure and mechanism of hexameric FtsK. *Mol Cell*, 23, 457–469.
- McCormick, J. R. (2009). Cell division is dispensable but not irrelevant in *Streptomyces*. *Curr Opin Microbiol.*, 12(6), 689-698. doi: 10.1016/j.mib.2009.10.004.
- McCormick, J. R., Flardh, K. (2012). Signals and regulators that govern *Streptomyces* development. *FEMS Microbiol Rev.*, 36(1), 206-231. doi: 10.1111/j.1574-6976.2011.00317.x.
- Million-Weaver, S., Camps, M. (2014). Mechanisms of plasmid segregation: have multicopy plasmids been overlooked? *Plasmid*, 75, 27-36. doi: 10.1016/j.plasmid.2014.07.002.
- Mohl, D. A., Gober, J. W. (1997). Cell cycle-dependent polar localization of chromosome partitioning proteins in *Caulobacter crescentus*. *Cell*, 88(5), 675-684.
- Moller-Jensen, J., Borch, J., Dam, M., Jensen, R. B., Roepstorff, P., Gerdes, K. (2003). Bacterial mitosis: ParM of plasmid R1 moves plasmid DNA by an actin-like insertional polymerization mechanism. *Mol Cell*, 12(6), 1477-1487.
- Mori, H., Kondo, A., Ohshima, A., Ogura, T., Hiraga, S. (1986). Structure and function of the F plasmid genes essential for partitioning. *J Mol Biol*, 192(1), 1-15.

- Mulder E, Woldringh CL. (1989). Actively replicating nucleoids influence positioning of division sites in *Escherichia coli* filaments forming cells lacking DNA. *J Bacteriol.*, *171*(8), 4303-14.
- Murayama, K., Orth, P., de la Hoz, A. B., Alonso, J. C., Saenger, W. (2001). Crystal structure of omega transcriptional repressor encoded by *Streptococcus pyogenes* plasmid pSM19035 at 1.5 Å resolution. *J Mol Biol.*, *314*(4), 789-796. doi: 10.1006/jmbi.2001.5157.
- Ni, L., Xu, W., Kumaraswami, M., Schumacher, M. A. (2010). Plasmid protein TubR uses a distinct mode of HTH-DNA binding and recruits the prokaryotic tubulin homolog TubZ to effect DNA partition. *Proc Natl Acad Sci U S A*, *107*(26), 11763-11768. doi: 10.1073/pnas.1003817107.
- Nielsen HJ, Ottesen JR, Youngren B, Austin SJ, Hansen FG. (2006). The *Escherichia coli* chromosome is organized with the left and right chromosome arms in separate cell halves. *Mol Microbiol.*, *62*(2), 331-8.
- Niki H, Jaffé A, Imamura R, Ogura T, Hiraga S. (1991). The new gene *mukB* codes for a 177 kd protein with coiled-coil domains involved in chromosome partitioning of *E. coli*. *EMBO J.*, *10*(1), 183-93.
- Nolivos S, Pages C, Rousseau P, Le Bourgeois P, Cornet F. (2010). Are two better than one? Analysis of an FtsK/Xer recombination system that uses a single recombinase. *Nucleic Acids Res.*, *38*, 6477–6489.
- Ogasawara, N., Yoshikawa, H. (1992). Genes and their organization in the replication origin region of the bacterial chromosome. *Mol Microbiol.*, *6*(5), 629-634.

- Pillet, F., Sanchez, A., Lane, D., Anton Leberre, V., Bouet, J. Y. (2011). Centromere binding specificity in assembly of the F plasmid partition complex. *Nucleic Acids Res.*, 39(17), 7477-7486. doi: 10.1093/nar/gkr457.
- Pinho, M. G., Kjos, M., Veening, J. W. (2013). How to get (a)round: mechanisms controlling growth and division of coccoid bacteria. *Nat Rev Microbiol.*, 11(9), 601-614. doi: 10.1038/nrmicro3088.
- Ptacin J, Nöllmann M, Bustamante C, Cozzarelli N. (2006). Identification of the FtsK sequence-recognition domain. *Nat Struct Mol Biol.*, 13, 1023–1025.
- Popp, D., Narita, A., Oda, T., Fujisawa, T., Matsuo, H., Nitani, Y., Maeda, Y. (2008). Molecular structure of the ParM polymer and the mechanism leading to its nucleotide-driven dynamic instability. *EMBO J.*, 27(3), 570-579. doi: 10.1038/sj.emboj.7601978
- Ptacin, J. L., Lee, S. F., Garner, E. C., Toro, E., Eckart, M., Comolli, L. R., Shapiro, L. (2010). A spindle-like apparatus guides bacterial chromosome segregation. *Nat Cell Biol.*, 12(8), 791-798. doi: 10.1038/ncb2083.
- Quisel, J. D., Grossman, A. D. (2000). Control of sporulation gene expression in *Bacillus subtilis* by the chromosome partitioning proteins Soj (ParA) and Spo0J (ParB). *J Bacteriol.*, 182(12), 3446-3451.
- Quisel, J. D., Lin, D. C., Grossman, A. D. (1999). Control of development by altered localization of a transcription factor in *B. subtilis*. *Mol Cell*, 4(5), 665-672.
- Radnedge, L., Youngren, B., Davis, M., Austin, S. (1998). Probing the structure of complex macromolecular interactions by homolog specificity scanning: the P1



- and P7 plasmid partition systems. *EMBO J.*, 17(20), 6076-6085. doi: 10.1093/emboj/17.20.6076.
- Raskin, D. M., de Boer, P. A. (1999). MinDE-dependent pole-to-pole oscillation of division inhibitor MinC in *Escherichia coli*. *J Bacteriol.*, 181(20), 6419-6424.
- Ravin, N. V., Rech, J., Lane, D. (2003). Mapping of functional domains in F plasmid partition proteins reveals a bipartite SopB-recognition domain in SopA. *J Mol Biol.*, 329(5), 875-889.
- Reyes-Lamothe R, Nicolas E, Sherratt DJ. (2012). Chromosome replication and segregation in bacteria. *Annu Rev Genet.*, 46, 121-43. doi: 10.1146/annurev-genet-110711-155421.
- Ringgaard, S., van Zon, J., Howard, M., Gerdes, K. (2009). Movement and equipositioning of plasmids by ParA filament disassembly. *Proc Natl Acad Sci U S A*, 106(46), 19369-19374. doi: 10.1073/pnas.0908347106.
- Rodionov, O., Yarmolinsky, M. (2004). Plasmid partitioning and the spreading of P1 partition protein ParB. *Mol Microbiol.*, 52(4), 1215-1223. doi: 10.1111/j.1365-2958.2004.04055.x.
- Rothfield, L., Taghbalout, A., Shih, Y. L. (2005). Spatial control of bacterial division-site placement. *Nat Rev Microbiol.*, 3(12), 959-968. doi: 10.1038/nrmicro1290.
- Salje, J., Gayathri, P., Lowe, J. (2010). The ParMRC system: molecular mechanisms of plasmid segregation by actin-like filaments. *Nat Rev Microbiol.*, 8(10), 683-692. doi: 10.1038/nrmicro2425.

- Schofield, W. B., Lim, H. C., Jacobs-Wagner, C. (2010). Cell cycle coordination and regulation of bacterial chromosome segregation dynamics by polarly localized proteins. *EMBO J.*, 29(18), 3068-3081. doi: 10.1038/emboj.2010.207.
- Schumacher, M. A. (2012). Bacterial plasmid partition machinery: a minimalist approach to survival. *Curr Opin Struct Biol.*, 22(1), 72-79. doi: 10.1016/j.sbi.2011.11.001.
- Schumacher, M. A., Funnell, B. E. (2005). Structures of ParB bound to DNA reveal mechanism of partition complex formation. *Nature*, 438(7067), 516-519. doi: 10.1038/nature04149.
- Schumacher, M. A., Piro, K. M., Xu, W. (2010). Insight into F plasmid DNA segregation revealed by structures of SopB and SopB-DNA complexes. *Nucleic Acids Res.*, 38(13), 4514-4526. doi: 10.1093/nar/gkq161.
- Sharpe, M. E., Errington, J. (1996). The *Bacillus subtilis* *soj-spo0J* locus is required for a centromere-like function involved in prespore chromosome partitioning. *Mol Microbiol.*, 21(3), 501-509.
- Sharpe, M. E., Errington, J. (1998). A fixed distance for separation of newly replicated copies of *oriC* in *Bacillus subtilis*: implications for co-ordination of chromosome segregation and cell division. *Mol Microbiol.*, 28(5), 981-990.
- Shebelut, C. W., Guberman, J. M., van Teeffelen, S., Yakhnina, A. A., Gitai, Z. (2010). *Caulobacter* chromosome segregation is an ordered multistep process. *Proc Natl Acad Sci U S A*, 107(32), 14194-14198. doi: 10.1073/pnas.1005274107.
- Shih, Y. L., Le, T., Rothfield, L. (2003). Division site selection in *Escherichia coli* involves dynamic redistribution of Min proteins within coiled structures that

- extend between the two cell poles. *Proc Natl Acad Sci U S A*, 100(13), 7865-7870. doi: 10.1073/pnas.1232225100.
- Sivanathan V, Allen M, de Bekker C, Baker R, Arciszewska L., (2006). The FtsK gamma domain directs oriented DNA translocation by interacting with KOPS. *Nat Struct Mol Biol.*, 13, 965–972.
- Stouf M, Meile JC, Cornet F., (2013). FtsK actively segregates sister chromosomes in *Escherichia coli*. *Proc Natl Acad Sci U S A*, 110(27), 11157-62. doi: 10.1073/pnas.1304080110.
- Surtees, J. A., Funnell, B. E., (1999). P1 ParB domain structure includes two independent multimerization domains. *J Bacteriol.*, 181(19), 5898-5908.
- Tang, M., Bideshi, D. K., Park, H. W., Federici, B. A., (2007). Iteron-binding ORF157 and FtsZ-like ORF156 proteins encoded by pBtoxis play a role in its replication in *Bacillus thuringiensis* subsp. israelensis. *J Bacteriol.*, 189(22), 8053-8058. doi: 10.1128/JB.00908-07.
- Thanbichler, M., Shapiro, L., (2006). MipZ, a spatial regulator coordinating chromosome segregation with cell division in *Caulobacter*. *Cell*, 126(1), 147-162. doi: 10.1016/j.cell.2006.05.038.
- Tinsley, E., Khan, S. A., (2006). A novel FtsZ-like protein is involved in replication of the anthrax toxin-encoding pXO1 plasmid in *Bacillus anthracis*. *J Bacteriol.*, 188(8), 2829-2835. doi: 10.1128/JB.188.8.2829-2835.2006.
- Tonthat NK, Milam SL, Chinnam N, Whitfill T, Margolin W, Schumacher MA., (2013). SImA forms a higher-order structure on DNA that inhibits cytokinetic Z-ring

- formation over the nucleoid. *Proc Natl Acad Sci U S A*, 110(26), 10586-91. doi: 10.1073/pnas.1221036110.
- van Baarle S, Celik IN, Kaval KG, Bramkamp M, Hamoen LW, Halbedel S., (2013). Protein-protein interaction domains of *Bacillus subtilis* DivIVA. *J Bacteriol.*, 195(5), 1012-21. doi: 10.1128/JB.02171-12.
- van den Ent, F., Moller-Jensen, J., Amos, L. A., Gerdes, K., Lowe, J. (2002). F-actin-like filaments formed by plasmid segregation protein ParM. *EMBO J.*, 21(24), 6935-6943.
- Walker JE, Saraste M, Runswick MJ, Gay NJ. (1982). Distantly related sequences in the alpha- and beta-subunits of ATP synthase, myosin, kinases and other ATP-requiring enzymes and a common nucleotide binding fold. *EMBO J.*, 1(8), 945-51.
- Walshaw, J., Gillespie, M. D., Kelemen, G. H. (2010). A novel coiled-coil repeat variant in a class of bacterial cytoskeletal proteins. *J Struct Biol.*, 170(2), 202-215. doi: 10.1016/j.jsb.2010.02.008.
- Wang L, Lutkenhaus J. (1998). FtsK is an essential cell division protein that is localized to the septum and induced as part of the SOS response. *Mol Microbiol.*, 29, 731-740.
- Wang, X., Liu, X., Possoz, C. and Sherratt, D.J. (2006). The two *Escherichia coli* chromosome arms locate to separate cell halves. *Genes Dev.*, 20, 1727-1731.
- Wang X, Tang OW, Riley EP, Rudner DZ. (2014). The SMC condensin complex is required for origin segregation in *Bacillus subtilis*. *Curr Biol.*, 24(3), 287-92. doi: 10.1016/j.cub.2013.11.050.

- Webb, C. D., Teleman, A., Gordon, S., Straight, A., Belmont, A., Lin, D. C., Losick, R. (1997). Bipolar localization of the replication origin regions of chromosomes in vegetative and sporulating cells of *B. subtilis*. *Cell*, 88(5), 667-674.
- Wiggins P, Cheveralls K, Martin J, Lintner R, Kondev J. (2010). Strong intranucleoid interactions organize the *Escherichia coli* chromosome into a nucleoid filament. *Proc Natl Acad Sci USA*, 107(11), 4991–4995. doi: 10.1073/pnas.0912062107.
- Wilhelm L, Bürmann F, Minnen A, Shin HC, Toseland CP, Oh BH, Gruber S. (2015). SMC condensin entraps chromosomal DNA by an ATP hydrolysis dependent loading mechanism in *Bacillus subtilis*. *eLife*, 4. doi: 10.7554/eLife.06659.
- Woldringh, C.L., Mulder, E., Valkenburg, J.A., Wientjes, F.B., Zaritsky, A., and Nanninga, N. (1990). Role of the nucleoid in the toporegulation of division. *Res Microbiol.*, 141, 39-49.
- Wu, L. J., and Errington, J. (1994). *Bacillus subtilis* SpoIIIE protein required for DNA segregation during asymmetric cell division. *Science*, 264, 572-575.
- Wu LJ, Errington J. (2003). RacA and the Soj-Spo0J system combine to effect polar chromosome segregation in sporulating *Bacillus subtilis*. *Mol Microbiol.*, 49(6), 1463-75.
- Wu, L.J. (2004). Structure and segregation of the bacterial nucleoid. *Curr Opin Genet Dev.*, 14, 126-132.
- Wu LJ, Errington J. (2011). Nucleoid occlusion and bacterial cell division. *Nat Rev Microbiol.*, 10(1), 8-12. doi: 10.1038/nrmicro2671.

- Yamaichi, Y., Niki, H. (2000). Active segregation by the *Bacillus subtilis* partitioning system in *Escherichia coli*. *Proc Natl Acad Sci U S A*, 97(26), 14656-14661. doi: 10.1073/pnas.97.26.14656
- Yates J, Aroyo M, Sherratt D, Barre F. (2003). Species specificity in the activation of Xer recombination at *dif* by FtsK. *Mol Microbiol.*, 49, 241–249.
- Yates J, Zhekov I, Baker R, Eklund B, Sherratt D, *et al.* (2006). Dissection of a functional interaction between the DNA translocase, FtsK, and the XerD recombinase. *Mol Microbiol.*, 59, 1754–1766.
- Yu XC, Tran AH, Sun Q, Margolin W. (1998). Localization of cell division protein FtsK to the *Escherichia coli* septum and identification of a potential N-terminal targeting domain. *J Bacteriol.*, 180, 1296–1304.

**Table 1.1. Elements that are found in Type I, II, and III plasmid partition systems.**

<b>Plasmids</b>	<b>NTPase*</b>	<b>CBP#</b>	<b>Centromere site</b>
<b>P1 (Type I)</b>	ParA	ParB	<i>parS</i>
<b>RP4 (Type I)</b>	KorA	KorB	<i>O<sub>B</sub></i>
<b>F1 (Type I)</b>	SopA	SopB	<i>sopC</i>
<b>R1 (TypeII)</b>	ParM	ParR	<i>parC</i>
<b>pXO1 (Type III) pBtoxis (Type III)</b>	TubZ	TubR	<i>tubC</i>

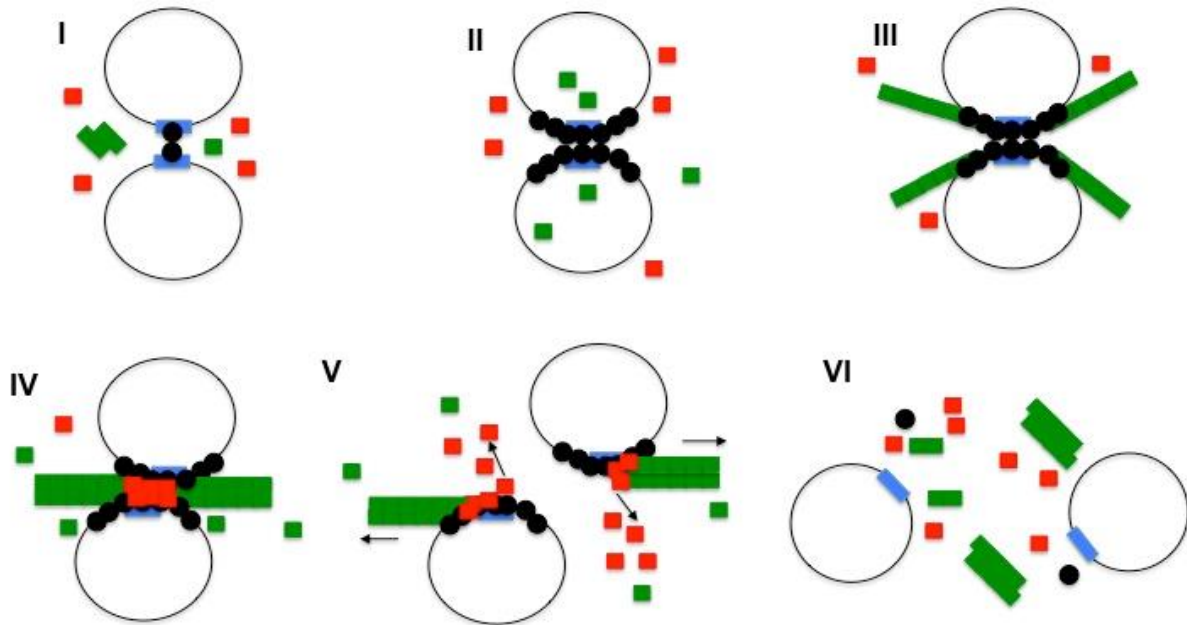
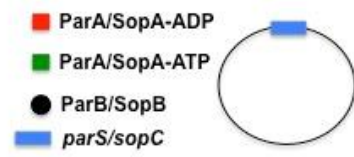
\*NTPase- Nucleotide triphosphatase; #CBP-Centromere binding protein

**Table 1.2. Elements that are found in bacterial chromosome segregation systems.**

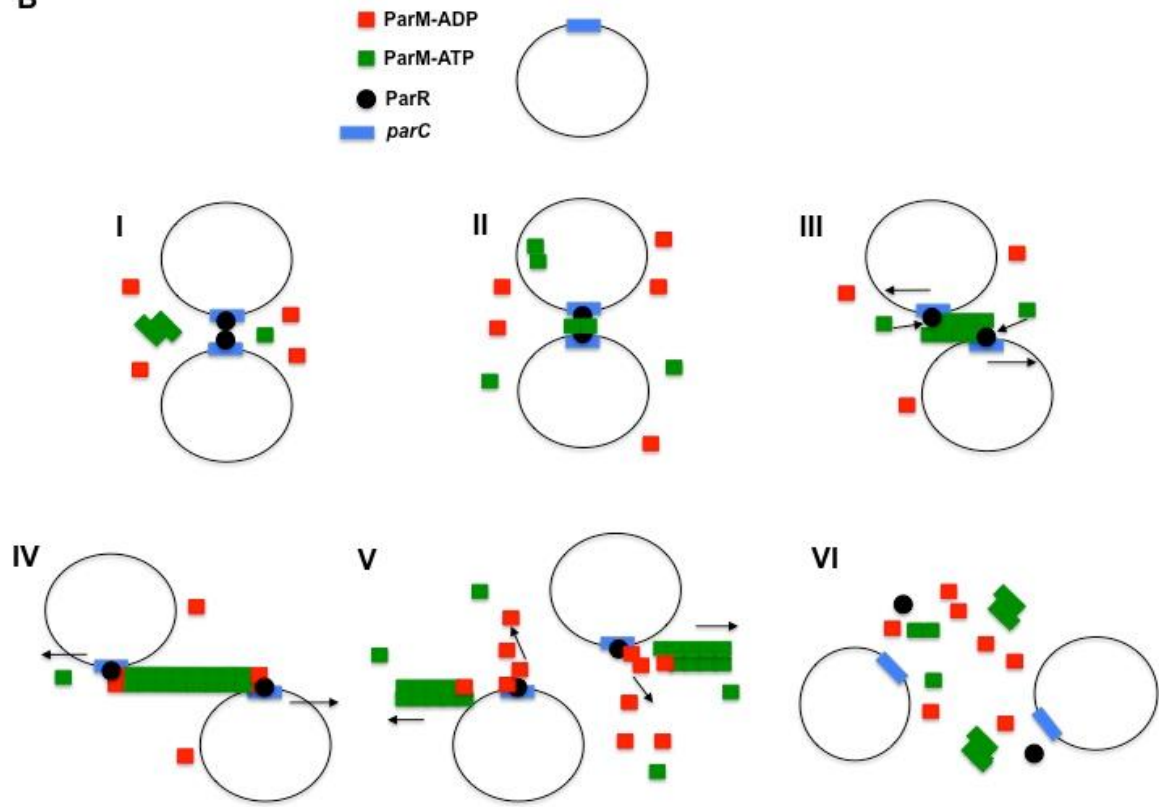
	<b>Segregation and condensation proteins (SMC/ScpAB)</b>	<b>DNA translocase (FtsK/SpoIIIE/Tra Family)</b>	<b>Par proteins (ParA/ParB/<i>parS</i>)</b>	<b>Other proteins or systems that are involved in chromosome segregation</b>
<i>E. coli</i>	MukB/MukEF	FtsK	–	MinCDE NO system
<i>B. subtilis</i>	SMC/ScpAB	SpoIIIE	SoJ/SpoOJ/ <i>parS</i>	RacA DivIVA
<i>C. crescentus</i>	SMC/ScpAB	FtsK	ParA/ParB/ <i>parS</i>	PopZ MipZ TipN
<i>C. glutamicum</i>	Not studied	Not studied	ParA/ <i>parB</i> / <i>parS</i>	PldP DivIVA
<i>S. coelicolor</i>	SMC/ScpAB	FtsK	ParA/ParB/ <i>parS</i>	ParJ Scy DivIVA ParH



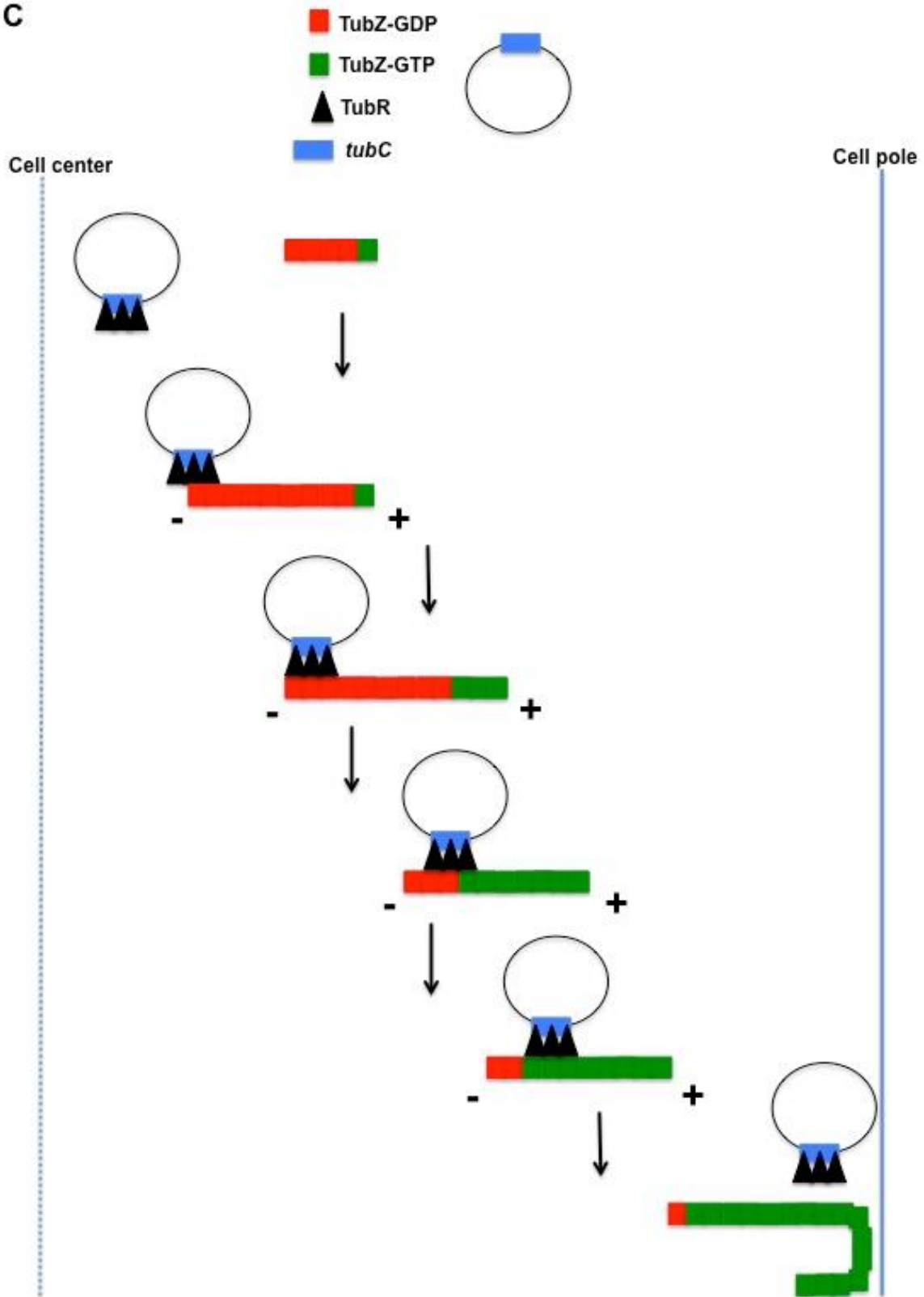
A



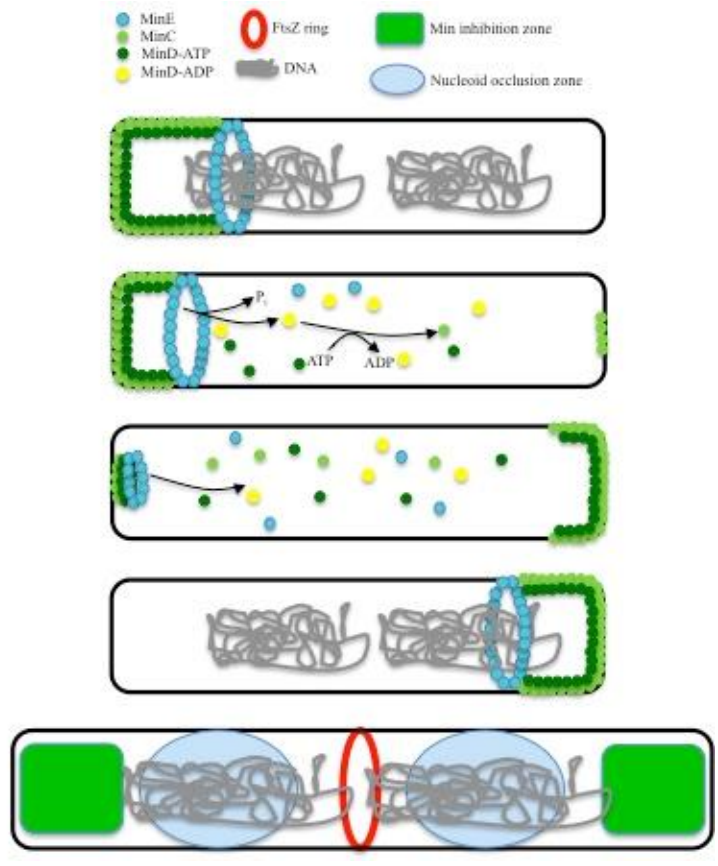
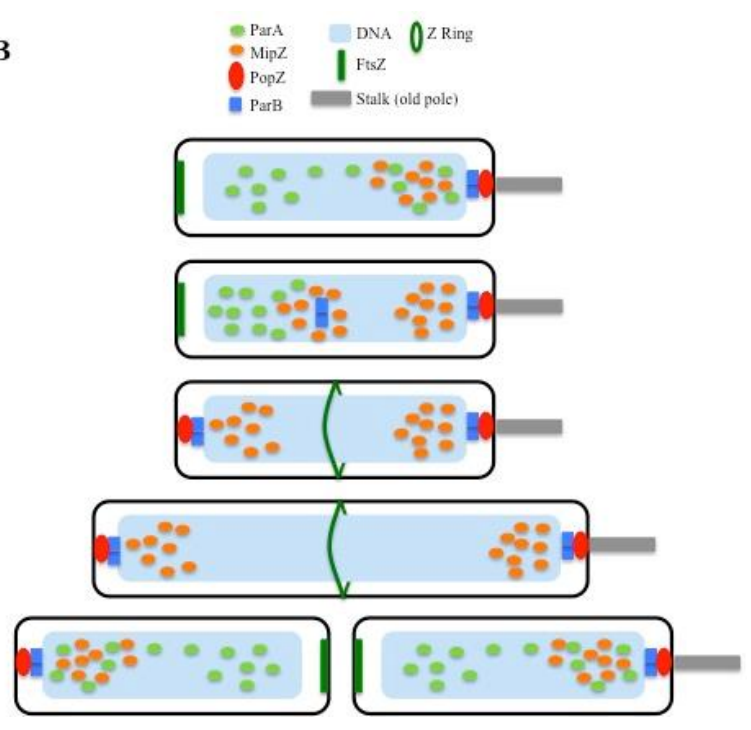
B



C



**Figure 1.1. Partitioning systems in plasmids.** Filamentation mechanisms of Type I, II, and III plasmid partitioning are illustrated in the figure and sample elements that are involved in each group are shown at the top of the panels. **A) In a Type I Par system,** centromere binding protein (CBP) ParB/SopB binds to *parS/sopC* centromere sites and brings the two plasmids together (I). CBP binding extends on the DNA and ParA ATPase binds to CBP in areas where CBP is not in a complex with centromeric DNA (II-III). ATPase protein polymerizes and filaments extend outwards in both directions until they meet a CBP/DNA nucleoprotein complex (arrows), which stimulates the ATPase activity (IV). ATP hydrolysis causes filaments to disassemble and disassembly pulls the plasmids apart in opposite directions (V-VI). **B) In a Type II par system,** when two plasmids meet in the cell, CBP binds to centromere sites and plasmids become tethered (I-II). The formation of nucleoprotein complex stabilizes the ends of ParM filaments. Monomers of the filament bind and nucleate on CBP ParR, then polymerizes at both ends of the extending ParM filament (III-IV). The extension of the filaments push sister plasmids apart (V-VI). **C) In a Type III par system,** CBP (TubR) binds to centromere sites and contacts the TubZ (GTPase protein). TubZ forms dynamic filaments, which grow at the plus (+) end by addition of TubZ-GTP and shrink from the minus (-) end by removal or loss of TubZ-GDP. TubR binds to the minus end of the TubZ (C-terminal end of a monomer at the end of the TubZ filament). TubR/DNA complexes are pulled along by the plus end until reaching the cell pole, where it dissociates from the TubZ filament when the filament bends after contact with the cell membrane at the pole. (Adapted from Baxter and Funnell, 2014 and Ni L. et al, 2010, and Weaver and Camps, 2014.)

**A****B**

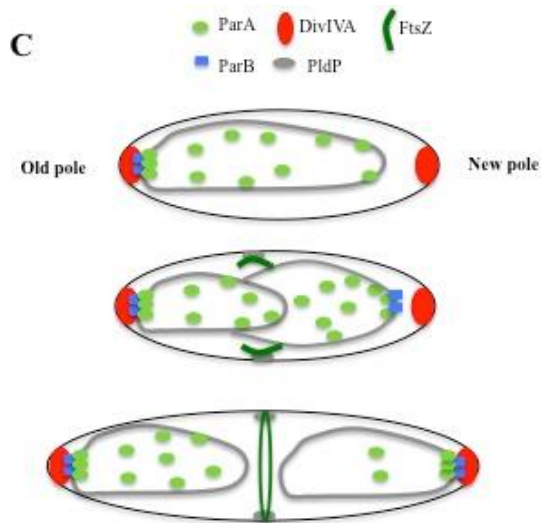


**Figure 1.2. Chromosome segregation models for *E. coli*, *C. crescentus*, and**

*C. glutamicum*. A) In *E. coli*, MinD-ATP binds to membrane and recruits MinC. FtsZ ring formation is inhibited by MinC, therefore a zone is formed at the poles of the cell that Z-ring can not be built. MinE forms a ring like structure and causes MinD to hydrolyze the ATP and release from the membrane that also causes MinC to release from the membrane. In the cytoplasm, MinD re-generates MinD-ATP and binds to the opposite pole. This process repeats itself and forms the MinCDE inhibition zone and helps chromosome segregates properly to each daughter cell. B) In *C. crescentus*, at the beginning of the cell cycle ParB/*oriC* is tethered to the old pole with the help of PopZ. ParB complexes are duplicated and along with MipZ, they migrate to the opposite pole by the help of ParA. When it reaches the opposite pole, ParB tethers to PopZ, which causes FtsZ to release from the pole and assemble in the midcell where the MipZ gradient is the lowest. C) In *C. glutamicum*, ParB/*oriC* binds to the pole through a DivIVA interaction. After replication, ParB binds to *parS* sites near the new *oriC* region where ParA binds and travels to the opposite pole. FtsZ starts to form a Z-ring and PldP regulates cell division by localizing at the cell division site. The new ParB/*oriC* is

tethered to the opposite cell pole by DivIVA, which stimulates the polar cell growth at the ends and would aid chromosomes to segregate. (Adapted from Pinho *et al.*, 2013, Du *et al.*, 2012, and Donovan *et al.*, 2014)

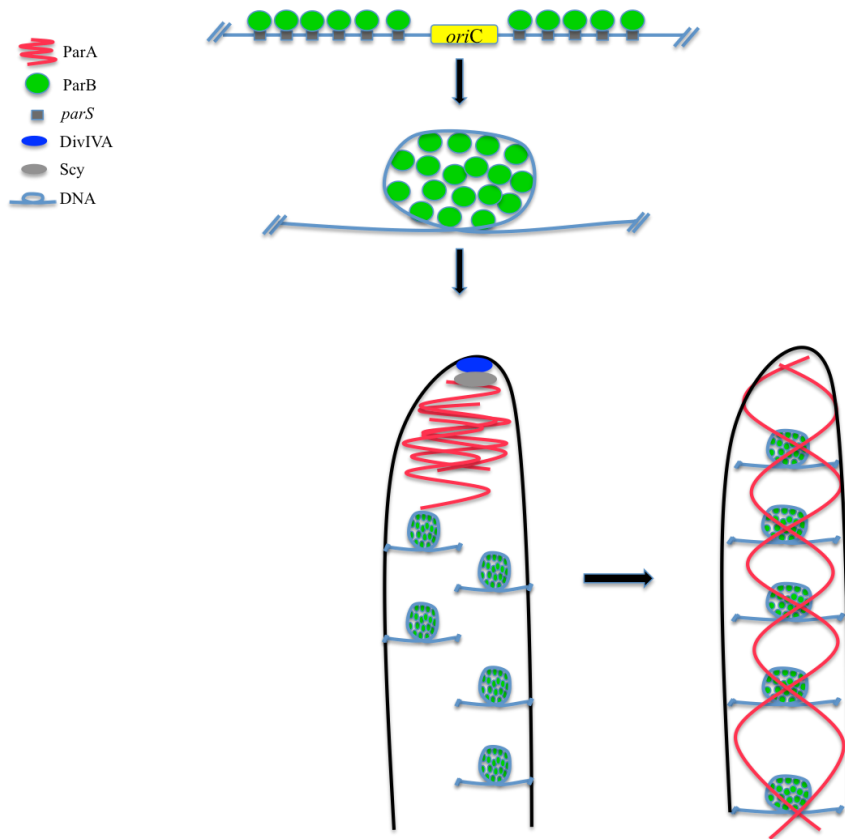


**Figure 1.3. Chromosome segregation model for *S. coelicolor*.** In nascent aerial hyphae, ParA accumulates first at the tips and then goes on to form helical filaments that spread along the aerial hyphae. ParA has been shown to interact with Scy and Scy has been shown to interact with polarity determinant protein DivIVA. Scy recruits ParA to hyphal tips and inhibits ParA polymerization. ParA provides the assembly of ParB-*parS* nucleoprotein complexes *in vivo* and *in vitro* and both proteins play an important role in the accurate distribution of the chromosomes in the aerial hyphae. ParB binds to *parS* sites near the origin of replication (*oriC*). Evenly-spaced ParB-*parS* complexes assemble along the length of aerial hyphae, presumably organizing evenly-spaced copies of the genome. The ParB-*parS* nucleoprotein complexes form before observable DNA condensation and septation and disassemble after these processes.



**CHAPTER 2: CHARACTERIZATION OF *STREPTOMYCES COELICOLOR*  
PARH IN DEVELOPMENTAL-ASSOCIATED CHROMOSOME  
SEGREGATION**

**ABSTRACT**

For *Streptomyces coelicolor*, there are five known components of developmental chromosome segregation: the *cis*-acting centromere-like sites (*parS*) and four characterized *trans*-acting proteins. ParA and ParB are conserved among other species, while the Actinobacterial signature protein ParJ (unique to Actinobacteria) and intermediate filament protein Scy are unique for *Streptomyces*. *parA* encodes a Walker-type ATPase that is required for efficient DNA segregation and proper placement of the ParB-*parS* nucleoprotein complexes. A paralogue of ParA, SCO1772 (named ParH) is encoded by the *S. coelicolor* genome. *parH* encodes a ParA-like ATPase protein that has 45% identical residues to ParA. Compared to ParA, ParH contains an N-terminal extension with an unusual amino acid composition. In this study I have identified ParH as a novel interaction partner of *S. coelicolor* ParB. The Walker A motif K99E substitution in ParH and removal of the N-terminal extension in ParH impaired interaction between them as judged by bacterial two-hybrid analyses. Also, no evidence was found that paralogs ParA and ParH can form a heterodimer. ParH-EGFP forms evenly-spaced localization patterns in aerial hyphae, which might suggest that ParH colocalizes with ParB in the aerial filaments of *S. coelicolor*. In aerial hyphae of the  $\Delta parH$  mutant, 5% of spores are anucleate compared to 1% of spores in wild type. The loss of ParH appears to result in abnormal positioning of a fraction of ParB-EGFP foci in aerial hyphae. The

*parH* mutant appears to be unable to properly organize the *oriC* regions within a subset of prespores, as judged by ParB-EGFP foci. I conclude that ParH is part of the partitioning system in *S. coelicolor* and appears to play a role in proper nucleoprotein complex positioning.

## INTRODUCTION

Bacterial chromosome segregation is an essential and tightly regulated process during the cell cycle of unicellular bacteria and is of central importance in microbial cell and molecular biology. An active partitioning system helps provide the proper segregation of chromosomes and low-copy plasmids into daughter cells in bacteria (Gerdes *et al.*, 2010). Most of the known information has come from the study of rod-shaped bacteria dividing by binary fission. After replication, chromosomal origin regions (*oriC*) migrate towards the cell poles by an active partitioning system (Errington, 2001; Jensen *et al.*, 2001; Lemon *et al.*, 2001; Sherratt, 2003)

Plasmid-encoded partition (*par*) loci of low-copy-number episomes have been a useful model to study the mechanisms of bacterial DNA segregation. Most bacterial chromosomes and low-copy-number plasmids have three main components of the partitioning system: one or more *cis*-acting centromere-like sites (*parS*), and two *trans*-acting proteins (ParA and ParB). *parB* encodes a protein that binds to the centromere-like regions and *parA* encodes a Walker-type ATPase that is essential for DNA segregation and required for the proper placement of the ParB-*parS* nucleoprotein complex within the cell (Hayes and Barilla, 2006; Leonard *et al.*, 2005; Schumacher, 2007).

Homologs of ParAB are encoded by most of the bacterial genomes with a few notable exceptions, such as *E. coli* and *Haemophilus influenza* (Mierzejewska and Jagura-Burdzy, 2012). In *B. subtilis*, Spo0J and Soj are the homologs of ParB and ParA, respectively. During vegetative growth, null mutations in *spo0J* (*parB*) resulted in 100-fold increase in the frequency of anucleate cells, but deletion of *soj* (*parA*) had no detectable effect on vegetative chromosome segregation (Ireton *et al.*, 1994).

Even though ParA and ParB appear to act together, they have multiple functions during chromosome segregation and cell division in *B. subtilis* (Gruber and Errington, 2009; Sullivan *et al.*, 2009). Spo0J (ParB) plays a role in recruiting the condensin SMC (structural maintenance of chromosomes) to origin of replication and Soj (ParA) is important in regulating the initiation of DNA replication by interacting with DnaA (Murray and Errington, 2008). In *C. crescentus*, individual deletion mutations in *parA* and *parB* are lethal and the gene products are involved in cell cycle progression and division (Thanbichler and Shapiro, 2006).

*S. coelicolor* is an advantageous organism for studying chromosome segregation since all of the tested segregation gene mutants are viable and double or triple mutants are not synthetic lethal or synthetic sick (Dedrick *et al.*, 2009). After replication and before developmentally- associated septation, ParAB proteins are essential for accurate distribution of the tens of chromosomes in syncytial aerial hyphae. There are a total of 24 *parS* sites near the origin of replication (Bentley *et al.*, 2002) on which ParB binds and forms nucleoprotein complexes (Jakimowicz *et al.*, 2002). In nascent aerial hyphae, ParA accumulates first at the distal tips and then goes on to form what appears to be helical filaments that spread along the aerial hyphae (Jakimowicz *et al.*, 2007). During sporulation, ParB-*parS* nucleoprotein complexes are evenly assembled along the aerial hyphae by the help of ParA (Jakimowicz *et al.*, 2005). ParB enhances the ATPase activity of ParA and ATP binding is required for the dimerization of ParA and ParB binding but not the localization of the helical filaments in aerial hyphae (Jakimowicz *et al.*, 2007). Even though these proteins are dispensable, deletion mutations in these genes resulted in anucleate spores about 15% in *parB* and 24% in *parA* mutants when compared to wild

type (Jakimowicz *et al.*, 2002; Jakimowicz *et al.*, 2005).

*S. coelicolor* is an unusual bacterium not only for its importance in biotechnology but also its complex life cycle and how it executes synchronous cell division and chromosome segregation during exospore formation. However, the molecular machinery that underlies the developmental chromosome segregation during morphological differentiation in *S. coelicolor* has not been fully elucidated. Studying the chromosome partitioning system of this organism might enlighten chromosome dynamics and its coordination with other cell cycle processes.

The goal of this study was to analyze the function of a ParA-like ATPase protein (ParH) and investigate protein-protein interactions between ParH with known segregation and condensation proteins to better understand its role in development-associated chromosome segregation in *S. coelicolor*. Bioinformatic analysis of ParA amino acid sequence revealed that a ParA-like ATPase was encoded in the *S. coelicolor* genome (Dedrick, 2009). Preliminary genetic data from Dedrick's dissertation (2009) suggested that a ParH plays a role in the proper localization of ParB-EGFP foci in the aerial filaments of *S. coelicolor*. Here, I confirmed these results and showed that loss of ParH affects chromosome segregation. Similar to some other ParA-like proteins in unicellular bacteria, ParH appears to bind to DNA in a heterologous *in vivo* assay. A bacterial two-hybrid system was used to screen protein-protein interactions and I identified a novel interaction between ParH and ParB for *S. coelicolor*. ParH forms homodimers according to a bacterial two-hybrid assay. A functional ATPase active site appears to be required for this interaction as in homologs of this type of Walker ATPase (Jakimowicz *et al.*, 2007). Possible interactions between other known segregation and condensation proteins

and ParH were also tested, but no evidence was found. However, I discovered novel interactions between ScpB (segregation and condensation protein B) and ParA, ScpB with SlzA (small leucine zipper type coiled-coil protein), and ParH with SlzA that might need further analysis to understand fully the link between chromosome segregation and condensation in *S. coelicolor*.

## **MATERIALS AND METHODS**

### **Bacterial strains, media, and growth conditions**

*E. coli* and *S. coelicolor* strains used in this study are listed in Table 2.1 and Table 2.2, respectively. *E. coli* strains were grown in either LB, SOB, or SOC media (Sambrook *et al.*, 1989) and were supplemented with final concentrations of ampicillin (100  $\mu\text{g ml}^{-1}$ ), apramycin (50  $\mu\text{g ml}^{-1}$ ), carbenicillin (100  $\mu\text{g ml}^{-1}$ ), chloramphenicol (25  $\mu\text{g ml}^{-1}$ ), kanamycin (50  $\mu\text{g ml}^{-1}$ ), or spectinomycin (50  $\mu\text{g ml}^{-1}$ ) when appropriate. TG1 and TOP10 were used for basic plasmid propagation. *E. coli* strains were grown at 37°C, except BW25113/pIJ790, which was grown at 30°C to ensure propagation of a temperature sensitive plasmid. *S. coelicolor* strains were grown at 30°C in ISP2 (yeast and malt extract medium) or YEME liquid medium or on minimal medium (MM), with either 0.5% glucose or 1% mannitol as the carbon source, R2YE, or soy flour mannitol agar (SFM) (Hopwood *et al.*, 1985; Kieser *et al.*, 2000) and were supplemented with the final concentrations of the following antibiotics when appropriate: apramycin (25  $\mu\text{g ml}^{-1}$ ), kanamycin (50  $\mu\text{g ml}^{-1}$ ), nalidixic acid (20  $\mu\text{g ml}^{-1}$ ), or spectinomycin (50  $\mu\text{g ml}^{-1}$ ).

### **Plasmids and general DNA techniques**

Cosmids and plasmids used in this study are listed in Table 2.3. Wizard Genomic DNA Purification Kit (Promega) was used for *S. coelicolor* total DNA preparations. QuikChange II Site-Directed Mutagenesis Kit (Stratagene) was used for creating point mutations. Redirect technology (Gust *et al.*, 2004) was used for  $\lambda$  RED-mediated recombination using mutagenic linear DNA cassettes in *E. coli*. Standard techniques were used for plasmid purification, creation of electrocompetent cells, and transformation (Sambrook *et al.*, 1989). DNA restriction enzymes (New England Biolabs), *Taq* DNA

Polymerase (New England Biolabs) and *Pfx* DNA polymerase (Invitrogen), plasmid purification and DNA cleanup kits (Qiagen and Zymo Research Corporation) were used according to the manufacturers' instructions.

### **Isolation of *parH*-null strains**

An insertion-deletion mutation for *parH* (*SCO1772*) was created by using *in vivo* *E. coli*  $\lambda$  Red-mediated recombination (Dedrick, 2009). Oligonucleotides *parA2Fwd* and *parA2Rev* were used to amplify and add *parH* (*parA2*) homology to an *aac(3)IV* disruption cassette isolated from pIJ733. The mutagenic PCR product was transformed into the *E. coli* strain BW25113/pIJ790/SCI51 to create cosmid pRMD12 (Dedrick, 2009). This cosmid derivative pRMD12 lacking *parH* ( $\Delta$ *parH::aac(3)IV*) was introduced into the chromosome of *S. coelicolor* strain M145, J3306, and J3310 via homologous recombination after conjugation, selecting for apramycin resistance and screening for kanamycin sensitivity, resulting in MH5 and MH6 (this study), and RMD29 strains (Dedrick, 2009), respectively, and PCR was used to verify the candidates. Strains J3306 (*parA*-null, unmarked) and J3310 (*parB-egfp*, unmarked) were a gift from D. Jakimowicz (Jakimowicz *et al.*, 2005).

### **Creation of the ParH-EGFP expressing strain**

The ParH-EGFP expressing strain (RMD30) was constructed by using *in vivo* *E. coli*  $\lambda$  Red-mediated recombination (Dedrick, 2009; Gust *et al.*, 2004). Oligonucleotides *parA2egfpFwd* and *parA2egfpRev* were used to amplify and add *parH* (*parA2*) homology to the *egfp-aac(3)IV-oriT* cassette of the cosmid H24-ParB-EGFP (Jakimowicz *et al.*, 2005). The mutagenic PCR product was transformed into the *E. coli* strain BW25113/pIJ790/SCI51 to create cosmid I51*parA2-egfp*. This cosmid was



introduced into the chromosome of *S. coelicolor* strain M145 via homologous recombination after conjugation, selecting for apramycin resistance and screening for kanamycin sensitivity and strain was named RMD30.

### **Creation of the ParB-mCherry and ParH-EGFP expressing strain**

In an attempt to determine the co-localization of ParB-mCherry and ParH-EGFP, cosmid I51*parA2-egfp* was introduced into the chromosome of *S. coelicolor* strain J3316 (*parB-mCherry*, unmarked) via homologous recombination after conjugation, selecting for apramycin resistance and screening for kanamycin sensitivity. *S. coelicolor* strain J3316 was a gift from Dr. Dagmara Jakimowicz (University of Wroclaw, Poland). PCR was used to verify the candidate and named MH4.

### **Creation of *parH* genes expressing K99E, R273E, and $\Delta$ 20-80 variants of ParH**

Genes expressing K99E and R273E variants of ParH contain a point mutation for a codon in the ATPase active site and a codon for a conserved putative DNA-binding arginine residue in *parH*, respectively. Plasmid pRJ1, which has the coding sequence as a source of *parH*, was used to make point mutations by using Stratagene Quickchange site-directed mutagenesis kit. Briefly, by following the manufacturer's protocol (Stratagene), the primers K99E Fwd and K99E Rev, R273E Fwd and R273E Rev were used to make point mutations in the ATPase active site (K99E) and in a surface arginine residue (R273E), respectively, to change these positively charged residues (lysine or arginine) into negatively charged glutamic acid. These plasmids were named as pRJ3 and pTR1, respectively. (pRJ3 was created by pre-doctoral rotation student Rachel Monaghan.) pRMD16 was used as a vector plasmid, which has the entire *parH* gene with promoter, an origin of transfer for conjugation, and *int* and *attP* of  $\Phi$ C31. This integration vector

was used to create the *parH* variants from pRJ3 and pTR1 by using *MluI* and *AscI* restriction enzyme digestion and ligation to substitute a 897 kb fragment containing the independent mutations. Since there are two *MluI* sites in pRMD16, construction had to be completed in two steps. The first step was the ligation of the altered *parH* as a 897 kb *MluI-AscI* fragment from pRJ3 and pTR1 with the 4,845 kb *MluI-AscI* fragment of the vector plasmid pRMD16 creating pRJ4 and pTR2. The second step was to ligate the 3,347 kb *MluI* fragment isolated from pRDM16 in the correct orientation into pRJ4 and pTR2, respectively. The final plasmids, pRJ5 [*parH* (K99E)] and pTR3 [*parH* (R273E)] were used to introduce the *parH* variants into RMD29 ( $\Delta parH::acc(3)IV parB-egfp$ ) by conjugation and site specific recombination into the  $\Phi C31 attB$  site.

A  $\Delta 20-80$  variant of ParH, which includes an in-frame deletion of the *parH* codons for 60 amino acids of the 61 amino acid N-terminal extension of ParH (GAPRNLNDHGPAK), was constructed by using oligonucleotides ParH60Fdel and ParH240Rdel to amplify and add *parH* homology to an *aac(3)IV* disruption cassette pIJ733. In addition, *SwaI* recognition sites were included in the primers and were inserted flanking the apramycin resistance gene. The mutagenic PCR product was transformed in to the *E. coli* strain BW25113/pIJ790/SCI51, resulting plasmid pMH39. Then, pMH39 was digested with *SwaI* restriction enzyme and ligated to remove the disruption cassette and was named pMH40. A *SwaI* cut site is left in place of 60 codons of *parH*. The K99E (AAG to GAG) and R273E (CGC to GAG) point mutations and in-frame deletion of codons 20-80 (GGCGCGCCCCGCAACttaaGATCACGGCCCCGCCAA) were verified by sequence analysis.

### **Analysis of *in vivo* DNA binding ability of ParH by GFP-ParH localization in *E. coli***

For analysis of the *in vivo* localization of GFP-ParH in a heterologous system, pSEB181 ( $P_{lac-gfp}$ ) was obtained from Dr. Joe Lutkenhaus (University of Kansas). This plasmid was previously used to make genes expressing various GFP-Soj (*B. subtilis* ParA) fusions (Zhou *et al.*, 2004). Oligomers XbaI-ParHFwd and HindIII-ParHRev were designed to add XbaI and HindIII restriction enzyme recognition sites to *parH* and its mutants (K99E, R273E, and  $\Delta 20-80$ ) and cloned into TOPO vector pCR2.1 creating pTR4, pTR5, pTR6, respectively. These plasmids and pSEB181 were digested and used to make *gfp-parH* fusions and were called pMH1 (WT), pMH2 (K99E), pMH3 (R273E), and pMH109 ( $\Delta 20-80$ ), respectively.

For analysis of the expression of GFP-ParH and variants, cultures of TG1 bearing pMH1 [ $P_{lac-gfp-parH}$ ], pMH2 [ $P_{lac-gfp-parH(K99E)}$ ], pMH3 [ $P_{lac-gfp-parH(R273E)}$ ], pMH109 [ $P_{lac-gfp-parH(\Delta 20-80)}$ ], as well as controls pSEB181 [ $P_{lac-gfp}$ ] and pSEB200 [ $P_{lac-gfp-soj}$ ] were grown overnight at 37°C in LB-spec. Samples were diluted 1:100 into 20 ml LB-spec and grown to an OD<sub>540</sub> of greater than 0.1. GFP-fusion expression was induced by the addition of 1 mM IPTG, and the cultures were allowed to grow for 45 minutes. One ml from each sample was immediately fixed for microscopy. Cells were harvested by centrifuging for 5 mins at 4°C. The pellet was resuspended in 1 ml of ice-cold lysis buffer (0.1 M Tris, pH8, 60 mM NaCl, 14 mM MgCl<sub>2</sub>) containing 10  $\mu$ l of Halt proteinase inhibitor cocktail (Thermo Fisher Scientific. Springfield, NJ) to prevent protein degradation. Sonication was performed on ice with 10 second bursts at 10 Watts and 20 second cooling for a total of 6 times for 3 minutes using a Sonic Dismembrator (Fisher Scientific. Springfield, NJ). The cell extracts were centrifuged at 4°C at 12,000Xg

for 10 minutes to remove unbroken cells, cell debris, and DNA. The supernatant was collected containing the soluble whole cell extract. Whole cell extracts were fractionated on 12% SDS-PAGE gels and GFP fluorescence was visualized by Li-cor Odyssey Fc imaging system.

Fluorescence microscopy to analyze the localization of GFP-ParH and derivatives was performed with an aliquot of the IPTG-induced *E. coli* strains isolated at the same time as the expression analysis above. Details of the fluorescence microscopy are given in the fluorescence microscopy section later in this chapter.

### **Creation of plasmids expressing fusions to ParH, ParH-variants, SMC, ScpA and ScpB for use in a bacterial two-hybrid assay**

Plasmids were created according to the previously described bacterial two-hybrid protocol (Karimova *et al.*, 2000). Briefly, primers listed on Table 2.4 for the genes of interest were used to amplify and add flanking *KpnI* restriction sites to *parH*, *parH*-variants, *smc*, *scpA*, and *scpB* using pRJ1, pRJ5, pTR3, pTR4, St7A1, or StI51 as a template.

The PCR products were cloned into TOPO vector pCR2.1 and completely sequenced to verify the integrity of the inserts. Each verified plasmid was separately digested with *KpnI* and ligated into *KpnI*-digested and dephosphorylated bacterial-two hybrid vectors pUT18, pUT18C, pKT25, and pKNT25. Diagnostic restriction enzyme digestion and sequence analysis were used to verify the orientation and reading frame of each two-hybrid construct before pairs to be tested were co-transformed into the *E. coli* strain BTH101. The visualization of possible protein-protein interaction was performed following the manufacturer's protocol with the following modifications. Co-

transformants were grown on LB agar containing ampicillin ( $100 \mu\text{g ml}^{-1}$ ), and kanamycin ( $50 \mu\text{g ml}^{-1}$ ) and incubated overnight at  $37^\circ\text{C}$ . Individual colonies from these plates were picked and patched on MacConkey agar containing 1% maltose, 0.5 mM IPTG, ampicillin ( $100 \mu\text{g ml}^{-1}$ ), and kanamycin ( $50 \mu\text{g ml}^{-1}$ ) and incubated overnight at  $30^\circ\text{C}$  before visual observations. The strains containing positive interacting clones were confirmed if they contained the correct genes by PCR.

Beta-galactosidase assays in single determinations were performed by following manufacturer's recommendations on overnight cultures of three independent isolates of each strain (Euromedex). The activity units were averaged from the 3 determinations.

### **Fluorescence Microscopy**

*S. coelicolor* strains were prepared for confocal microscopy using cover slips that were embedded at a  $45^\circ$  angle in the agar medium and incubated for the indicated lengths of time and either fixed with 4.375% glutaraldehyde and 0.028% paraformaldehyde or 100% methanol or unfixed, and analyzed using a TCS SP2 Spectral Confocal Microscope System (Leica), confocal microscope (Nikon A1<sup>+</sup>), or epi-fluorescence wide-field microscope (Nikon Eclipse Ni-U) with a 100X oil or 63X immersion lenses and 488- and 543-nm lasers. A standardized amount of spores and three independent inoculations on cover slips were used for characterization of all strains used in this study. Volocity Demo program (Perkin Elmer Inc, Version 6.1.1) was used to crop images, optimize contrast, and add scale bars.

*E. coli* strains prepared for confocal microscopy were fixed at room temperature by adding 1% formaldehyde (final concentration) for 10 min to a sample of a culture growing exponentially in LB (Hester *et al.*, 2007). The coverslips were washed three

times with PBS, allowed to air dry, and mounted in 50% glycerol containing 10  $\mu\text{g}/\text{mL}$  wheat germ agglutinin, Alexa Fluor 633 conjugate (Invitrogen) and analyzed using a TCS SP2 Spectral Confocal Microscope System (Leica) with a 100X oil lens and 488 nm and 633 nm lasers. Images were processed to adjust the brightness and contrast using Volocity Demo (Perkin Elmer Inc, Version 6.1.1) program.

## RESULTS

### ***S. coelicolor* possesses a gene to express a second ParA-like ATPase**

A previous study in our laboratory revealed a potential *parA*-like gene upon BLAST analysis of the ParA amino acid sequence (Dedrick, 2009). The amino acid sequence encoded by *sco1772* was found to be homologous to the ParA-family of proteins that has a conserved ATPase domain, such as the MinD family of ATPases. *sco1772* is 1,023 bp and is predicted to encode a 340 amino-acid protein. SCO1772 has 44.8% (111/248) identical residues and 63.3% (157/248) similarity to ParA of *S. coelicolor* (Figure 2.1). Due to its homology to ParA, it will be referred to as ParH (ParA homolog) from this point on. Relative to its paralog ParA, ParH has a 61 amino acid extension inserted near the N-terminus and ParA has 22 amino acid extension at the C-terminus. The composition of this additional N-terminal sequence in ParH is unusual with 8 aromatic (3F and 5Y) and 11 proline residues and highly conserved (Figure 2.1 and Figure 2.2), whereas the composition of the additional sequence in ParA is more variable amongst other *Streptomyces* (Figure 2.3).

*parH* is located one gene upstream of the operon encoding SMC-associated proteins called ScpA and ScpB (Figure 2.4) (Dedrick *et al.*, 2009), which help compact and organize the chromosome in a complex with SMC (structural maintenance of chromosomes) proteins and is important for chromosome segregation (Dedrick *et al.*, 2009; Kois *et al.*, 2009; Lindow *et al.*, 2002; Soppa *et al.*, 2002). The proximity of *parH* to *scpAB* may indicate that it might also have a role in chromosome segregation. In contrast to ScpAB, a BLAST search of the protein encoded downstream of *parH*, SCO1771, revealed that it has no known conserved domains, however homologs are

highly conserved amongst *Streptomyces* species (data not shown). Interestingly, the open reading frame of *parH* overlaps with *sco1771*, which may indicate that these two genes are transcribed as a bicistronic operon (Figure 2.4). On the other hand, the upstream gene *sco1773* encodes L-alanine dehydrogenase, which is required for maturation of spores and under the regulation of the developmental gene *whiH* (Salerno *et al.*, 2013).

Interestingly, the *parH* homolog in *S. venezuelae* (*sven1405*) is a direct WhiA target and its expression depends on *whiA*, which is involved in the regulation of key steps in aerial growth, initiation of cell division, and chromosome segregation (Bush *et al.*, 2013).

The genome sequences of all 7 *Streptomyces* species that are presented on the *Streptomyces* genome database and 2 other Actinobacteria reveal that all have a *parA* and *parA*-like gene (<http://strepdb.streptomyces.org.uk>). Recent studies also showed that besides *Streptomyces* species, *C. glutamicum* and *Aggregatibacter actinomycetemcomitans* have a *parA*-like gene, *pldP* and *tadZ*, respectively (Donovan *et al.*, 2010; Perez-Cheeks *et al.*, 2012). PldP plays a role in division-site selection and TadZ is important in the biofilm formation in periodontal diseases.

An alignment of a total of 27 ParA, ParA-like and other deviant Walker A ATPase (KGGVGK nucleotide-binding motif) proteins (MinD/MipZ) shows that these proteins are homologs. Cell division site MinD proteins form a separate family according to their sequence similarity and their functions (spatial regulation of cell division) in the cell (Lutkenhaus and Sundaramoorthy, 2003). The 27 aligned sequences show higher identity towards the C-terminus. This may suggest that the C-terminal portion of these proteins has a specific and conserved function. The aligned amino acid sequences of these proteins were used to construct a phylogenetic tree by Clustal W2 alignment



phylogeny program and a phylogenetic neighbor-joining tree, MEGA 5.2.1 phylogeny program (Figure 2.5). The phylogenetic tree reveals an obvious evolutionary relation between ParA and ParA-like proteins.

### **Deletion of ParH affects chromosome segregation**

To analyze the function of the putative partitioning protein ParH of *S. coelicolor*, a deletion-insertion mutant was created using a PCR-directed mutagenesis. Previously, Dedrick constructed the strain (RMD25) and found 3% (3% of 1633 total spores compared to 1% of wild type spores) anucleate spores for the *parH*-null strain (Dedrick, 2009). Unfortunately, the strain was lost from the collection and was re-isolated here (MH5). As with the previous isolate, phase-contrast microscopy revealed that the mutant strain was able to sporulate and the spores were similar to wildtype strain M145 in regards to shape and size. Propidium iodine stain was used to visualize DNA segregation in the  $\Delta parH$  strain (MH5) and a frequency of 5% anucleate spores (5% of 3090 total spores compared to 1.7% of 3006 total spores for wild type) was found (Figure 2.6 C). In addition to this slight chromosome segregation defect, the *parH*-null mutation (MH5) also caused infrequent branching spore chains in the aerial filaments of *S. coelicolor* (Figure 2.6 C). To further analyze the role of ParH in chromosome segregation, an unmarked *parA* deletion strain (Jakimowicz, 2007) was used to create a double deletion-insertion mutant for *parA* and *parH* by introducing the *parH*-null mutation into the *parA* deletion strain. The *parA parH* double null mutant (MH6) has 17% anucleate spores (17% of 3102 total spores) as compared to 20% of *parA* (20% of 2967 total spores) mutant strain, which showed that the segregation phenotypes were not additive (Figure 2.6 D).

### **Localization of ParB-EGFP is slightly disrupted in *parH* deletion mutant**

The *Streptomyces* ParB binds *parS* sites near the origin of replication (*oriC*) (Jakimowicz *et al.*, 2002). In vegetative filaments and nascent aerial hyphae, ParB-EGFP localizes as a bright focus close to the hyphal tip and other foci being smaller and irregularly spaced through the length of the hyphae (Jakimowicz *et al.*, 2005). But, during sporulation, large evenly-spaced ParB-EGFP foci assemble along the length of aerial hyphae, presumably uniformly organizing the copies of the genome along the length of the hyphae. The ParB-*parS* nucleoprotein complexes form before observable DNA condensation and septation, and disassemble after these processes (Jakimowicz *et al.*, 2005).

To further analyze the role of ParH in chromosome partitioning, a *parH* mutant strain RMD29 ( $\Delta parH::acc(3)IV parB-egfp$ ) was constructed by introducing the  $\Delta parH$  mutation into J3310 (*parB-egfp*) strain (Dedrick, 2009). This mutant strain appeared to be similar to the wild type as it produced a gray pigment associated with mature spore formation and the spores were similar to wildtype strain M145 in regards to shape and size (Dedrick, 2009). Preliminary, confocal fluorescence microscopy results revealed that centromere-binding protein ParB-EGFP localized normally throughout the life cycle of *S. coelicolor* until the maturation of spores (Dedrick, 2009). I repeated the fluorescence microscopy analysis and found that as certain prespores mature, the organization of the ParB-EGFP foci was disrupted in some spores. To quantitate the phenotype of the disrupted ParB-EGFP localization, the distances between ParB-EGFP foci were measured in wild type and *parH* null mutant strains (Figure 2.7). For this analysis a ParB-EGFP interfocal distance of less than 0.4  $\mu\text{m}$  was considered as a disrupted ParB-EGFP

localization. To provide a quantitative evidence for the ParB-EGFP foci localization disruption, samples from different time points of development (24, 40, 48, and 56 hours growth on plates) were prepared and the subtle phenotype was observed mainly between 48 and 56 hour time points. The average ParB-EGFP interfocal distance in a wild type strain was found to be approximately 1  $\mu\text{m}$  coinciding with the approximate length of a spore compartment. However, in strain RMD29, the interfocal distance of ParB-EGFP was either laterally or vertically close to each other in 6% prespores. The total percentage of disrupted ParB-EGFP in *parH* null strain was found to be approximately 6% compared to 1% of the wild type strain ( $p=0.0052$ , chi-square test) (Table 2.5). These data and together with the observation of evenly-spaced ParH-EGFP localization, suggested that ParH might play a direct or indirect role in positioning of ParB foci.

To further analyze the function of ParH, site-directed mutagenesis was used to change the codon for a conserved lysine residue in the ATPase Walker A box of ParH to glutamic acid (opposite charge substitution). This lysine residue is required for ATPase function and dimer formation in other similar ATPase proteins because the ATPase site is formed at the dimer interface (Jakimowicz *et al.*, 2007, Lutkenhaus *et al.*, 2003). In addition to the lysine mutation, I analyzed a second mutation, which was created by using site-directed mutagenesis by a previous rotation student R. Monaghan. The mutation altered a surface arginine residue (R273E), which is conserved among other chromosomal *parA*-like gene homologs and is involved in non-specific DNA binding for *B. subtilis* Soj (Hester and Lutkenhaus, 2007). These variants under the control of the native *parH* promoter were introduced by site-specific recombination into the  $\phi\text{C31 att}$  site into an *S. coelicolor* strain containing  $\Delta\text{parH}$ , making the genes with the point

mutation the only source of *parH* into the strain expressing ParB-EGFP to see if there was an effect on segregation and localization of ParB-EGFP foci. The preliminary microscopy results showed the aberration of ParB-EGFP foci in *parH*(K99E), but not in *parH*(R273E) strains (data is not shown). Although interfocal distance in these strains was not measured as accurately as in *parH*-null strain, I concluded that the Walker-type ATPase activity of ParH is needed for ParH to directly or indirectly influence proper ParB-EGFP foci localization.

### **ParH-EGFP localizes at evenly spaced intervals within aerial filaments**

To determine the *in vivo* localization pattern of ParH, a ParH-EGFP translational fusion strain was created using a PCR-directed mutagenesis. *parH-egfp* was integrated at the native location in the chromosome, expressed as the only source of ParH, and analyzed by fluorescence microscopy (Dedrick, 2009). ParH-EGFP protein appeared to be fully functional; the strain was able to sporulate and the spores were similar to wildtype strain M145 in regards to shape and size.

Previously, using confocal microscopy in a preliminary analysis to show the localization of ParH-EGFP, Dedrick treated the samples with anti-gfp antibody to enhance the EGFP signal probably due to low expression levels of the ParH. Dedrick showed that ParH-EGFP localization has no distinct pattern in vegetative filaments (Dedrick, 2009). But, in infrequent predivisional aerial filaments, some of the aerial hyphae revealed a bright band or several evenly-spaced bands in the apical compartment and some of them showed increased ParH fluorescence toward the tip of these filaments (Dedrick, 2009). With the observation of several localization patterns, Dedrick concluded that ParH-EGFP localization might be dynamic. However, despite numerous attempts

without enhancing with anti-gfp antibody, I have not been able to observe the same results.

Recently, I observed the same strain with epi-fluorescence wide-field microscope (Nikon Eclipse Ni-U) and a new confocal microscope (Nikon A1<sup>+</sup>). Epi-fluorescence and confocal microscopy results showed that ParH-EGFP localized in evenly spaced intervals within predivisional aerial filaments (Figure 2.7). ParH-EGFP fluorescence was not observed in vegetative filaments or mature aerial filaments with spore compartments. Epi-fluorescence and a new confocal microscopes appeared to be better to observe the localization of ParH-EGFP and provided better-quality imaging. Probably the ParH expression is very low and newer equipment was necessary to visualize ParH-EGFP localization. This data suggested that ParH might co-localize with evenly-spaced ParB-*parS* complexes.

To investigate potential co-localization of ParH with ParB-EGFP foci, I constructed a strain expressing a translational ParH-mCherry fusion. In order to construct a gene to express a ParH-mCherry fusion, an *in vivo* recombination system was used to create the fusion in one step in *E. coli* (Datsenko and Wanner, 2000; Gust *et al.*, 2004). Then, *parH*-mCherry, as the only source of *parH*, was introduced by conjugation into a *S. coelicolor* strain with a *parH*-null mutation strain expressing ParB-EGFP and verified by PCR using *S. coelicolor* chromosomal DNA as template. This strain expressing ParH-mCherry and ParB-EGFP was analyzed by scanning laser confocal microscopy.

Unfortunately, the ParH-mCherry fluorescence was too weak to be able to clearly see ParH-mCherry localization (data not shown). Since ParB has a brighter signal than ParH in the aerial hyphae, as judged by EGFP fusion signals, a strain expressing ParB-mCherry

and ParH-EGFP (MH4) was constructed with the same method and analyzed by the scanning laser confocal microscopy (Figure 2.9). A ParB-mCherry expressing strain was obtained from Dr. Dagmara Jakimowicz (University of Wroclaw, Poland). Both mCherry and EGFP signals were not very strong. ParH-EGFP and ParB-mCherry did not appear to co-localize in the aerial filaments of *S. coelicolor*, as judged by the scanning laser confocal pictures. However, due to the weakness of the fluorescence signal I cannot definitively say that these two proteins do not co-localize.

Recently, I checked the same strain, MH4 with an epi-fluorescence wide-field microscope. Preliminary analysis showed that I was able to observe the co-localization, but unfortunately was unable to capture the image due to quick bleaching of the samples. These preliminary results would need to be confirmed by further analysis in the future.

#### **ParH binds to nucleoid in a heterologous *in vivo* assay**

Even though the DNA binding property of *S. coelicolor* ParA has not been studied, most chromosomally encoded ParA and ParA-like proteins can bind to DNA in a nonspecific manner, such as ParA of *C. crescentus*, Soj (ParA) from *Thermus thermophilus*, and Soj of *B. subtilis* (Easter and Gober, 2002; Hester and Lutkenhaus, 2007; Leonard *et al.*, 2005), as well as the ParA-like PomZ from *Myxococcus xanthus* (Treuner-Lange *et al.*, 2012).

For *B. subtilis*, a GFP-Soj (ParA) fusion expressed in *E. coli* was used as an *in vivo* assay to see the localization of the protein with the nucleoid as one way to show its ability to bind DNA (Hester and Lutkenhaus, 2007). In their model, polymerization of Soj occurs by non-specific binding on a DNA scaffold. A conserved surface arginine to glutamic acid (opposite charge substitution) mutant fails to localize to nucleoid. The

same assay was used to investigate *in vivo* DNA binding ability of ParH. pSEB181 ( $P_{lac}$ -*gfp*) (Zhou and Lutkenhaus, 2004) was used to make fusion genes expressing GFP-ParH, GFP-ParH(K99E), GFP-ParH(R273E), and ParH( $\Delta$ 20-80). For analysis of the localization of GFP-ParH and its variants, images were taken by a scanning laser confocal microscope (Figure 2.10). Cell envelopes were counter labeled with WGA Alexa Fluor 633 conjugate, which binds to peptidoglycan. It showed that the positive control GFP-Soj localizes in foci on the nucleoid as it was published (Hester and Lutkenhaus, 2007). Similar to the GFP-Soj control, GFP-ParH<sup>+</sup> appears to localize on the nucleoid of the cells in *E. coli*. Localization of GFP-ParH<sup>+</sup> is affected in GFP-ParH(K99E), GFP-ParH(R273E), and GFP-ParH( $\Delta$ 20-80). Both GFP-ParH(K99E) and GFP-ParH( $\Delta$ 20-80) appear to localize at the poles and GFP-ParH(R273E) appear to either localize at the poles or diffuse in the cytoplasm of the cells in *E. coli* (Figure 2.10). Localization patterns are specific for the ParH proteins. GFP control shows that the fluorescent protein is located throughout the cytoplasm.

Whole cell protein extracts of the fusion-containing strains were fractionated on a SDS-PAGE gel and GFP fluorescence was visualized by Fuji FLA-5100 2-dimensional scanner (Figure 2.11). GFP-ParH<sup>+</sup> and GFP-ParH(R273E) were stable as in the GFP-Soj control. However, the GFP-ParH(K99E) and GFP-ParH( $\Delta$ 20-80) protein were not as stable as the wild type and appeared to be partially degraded due to possible misfolding in *E. coli* (Figure 2.11 lanes K99E and  $\Delta$ 20-80).

## ***S. coelicolor* ParA-like protein ParH interacts with centromere-binding protein ParB in a bacterial two-hybrid assay**

Until recently, ParB was the only identified interacting partner of ParA in *S. coelicolor* (Jakimowicz *et al.*, 2007). ParJ and Scy were found to be involved in the partitioning system as a ParA-interacting protein of *S. coelicolor* in a screen of a random library by using a bacterial two-hybrid system (BTH) (Ditkowski *et al.*, 2010; Ditkowski *et al.*, 2013). Scy has been proposed to recruit ParA to the aerial hyphae tips. ParA polymerization is regulated by both Scy and ParJ, which affect DNA segregation and cell division during sporulation (Ditkowski *et al.*, 2013; Ditkowski *et al.*, 2010). Since ParA binds to ParB/*parS* nucleoprotein complexes and there is 45% identity between ParA and ParH, and some disruption of ParB-EGFP localization in *parH*-null mutant rendered ParH a candidate to investigate interactions between known segregation proteins, such as ParA, ParB and ParJ.

Donovan *et al.*, (2010) also showed that in a closely related unicellular Actinomycete bacterium *C. glutamicum* PldP (a ParH-like protein) interacts in a bacterial two-hybrid system with itself, ParA and ParB. In addition, ParB-*parS* complexes interact directly with polar-growth protein DivIVA at the cell poles (Donovan *et al.*, 2012). However, PldP localizes within *C. glutamicum* with FtsZ rings at the site of cell division (Donovan *et al.*, 2010). Since, PldP is closely related to ParH, putative dynamic localization of ParH could be affected by interaction with ParB or FtsZ in *S. coelicolor*.

A bacterial two-hybrid system was used to attempt to find which, if any, known segregation proteins interact with ParH. This system is an *in vivo* screening and selection method for identification of interacting proteins in a heterologous analysis. This system



requires the co-expression of the fusion proteins of interest to either T25 or T18 subdomains of *Bordetella pertussis* adenylate cyclase in an *E. coli cya* mutant (Karimova, *et al.*, 2000). Plasmids carrying *parA*, *parB*, and *parJ* genes fused with either sequence expressing T25 or T18 subdomain in reporter strains were obtained from Dr. Dagmara Jakimowicz (University of Wroclaw, Poland). These plasmids were co-transformed with the plasmids that encode *parH* fusions into an *E. coli cya* screening strain followed by plating on MacConkey indicator plates. When pairs of ParH, ParA, ParB, ParJ fusions were coexpressed and screened for an interaction, ParH was found to be able to interact with ParB (Figure 2.12). ParH also interacted with itself in this assay (see next section for detailed information). Interestingly, ParH did not interact with ParA, which shows that these proteins, despite the close sequence identity, do not appear to form hetero-dimers in this assay (Figure 2.12).

Since the data showed an interaction between ParH and ParB, the same bacterial two-hybrid system was used to test three *parH* mutants to find if a functional ATPase active site, conserved surface arginine residue, or N-terminal  $\Delta$ 20-80 might be involved in ParB interaction. Previously constructed *parH* gene variants were cloned into the reporter plasmids in bacterial two-hybrid system. The ATPase deficient K99E and N-terminal in-frame variants of ParH impaired interaction with ParB, but a surface arginine substitution did not have any affect on ParH-ParB interaction (Figure 2.13). These 2 results showing no interaction potentially could be explained due to inability to form a dimer and unstable protein (Figure 2.11 Lanes K99E and  $\Delta$ 20-80) for the mutation in ATPase active site, which could be required for forming homodimers and improper folding of the protein, respectively. Since ParB-EGFP foci disruption in *parH* (K99E)

(ATPase active site) variant have been observed, the data are consistent with an interpretation that ATPase activity is required for the proper localization of ParB-EGFP foci in the midcell and it may also be involved in the interaction of ParH and ParB.

### **ParH forms homodimers as do homologs of this type of Walker ATPases**

Similar to ParA, ParB, and ParJ in *S. coelicolor*, ParH also interacts with itself, as do homologs of this type of deviant Walker ATPases, such as MinD and Soj (Ditkowski *et al.*, 2010, Hu *et al.*, 2002, Jakimowicz *et al.*, 2007, Leonard *et al.*, 2005, Suefuji *et al.*, 2002). Previously, it has been shown that the intact Walker A motif was required for the formation of the ParA dimers which was also detected by the bacterial two-hybrid analysis (Jakimowicz *et al.*, 2007). *parH* gene variants that encode R273E, K99E, and  $\Delta$ 20-80 mutations were used in this system to see if these mutations affect the formation of ParH dimers. Both the ATPase deficient and N-terminal in-frame variants ( $\Delta$ 20-80) impaired the interaction of ParH with itself (Figure 2.13). R273E variant was used as a positive control and did not affect the dimerization of ParH. The result for *parH* gene variant that encodes K99E was consistent with the ATPase active site required for dimerization of the protein and N-terminal in-frame variant ( $\Delta$ 20-80) might affect the stability and proper folding of the protein, thus dimerization of the protein.

### **ParH does not appear to interact with proteins that make up the bacterial condensin SMC, ScpA, and ScpB complexes**

*parH* is located one gene upstream of the operon encoding SMC-associated proteins called ScpA and ScpB, which help compact and organize the chromosome in a complex with SMC (structural maintenance of chromosomes) proteins (Lindow *et al.*, 2002; Soppa *et al.*, 2002). SMC is involved in development-specific DNA segregation

and 8% of the spores are anucleate in an *smc* null mutant (Dedrick *et al.*, 2009). The similarity of ParH to ParA and proximity of *parH* to *scpAB* is what originally suggested a potential role of ParH in chromosome segregation. To see if ParH interacts with condensation proteins SMC, ScpA and/or ScpB, the *smc*, *scpA* or *scpB* genes were cloned into reporter plasmids. No interaction was found between ParH and these individual condensation proteins (Figure 2.14, B). I also tested other partitioning proteins with SMC, ScpA, and ScpB to see if they interact in the bacterial two-hybrid assay. I only found evidence to support that ParA interacts with ScpB. A summary of interactions determined in this study is given in Figure 2.14, A. This data suggests that ParA may help coordinate the activity of condensins as well as influencing the evenly-spaced localization of ParB nucleoprotein complexes in pre-divisional *S. coelicolor* aerial hyphae. Results may be analogous to the fact that Spo0J (ParB) recruits SMC to the region of *oriC* in *B. subtilis* (Gruber and Errington, 2009; Sullivan *et al.*, 2009; Minnen *et al.*, 2011).

### **Small leucine zipper (*slzA*) interacts with ScpB and ParH**

SlzA is a small leucine zipper type coiled-coil protein (SCO5576a) that encodes a 69 amino acid protein product (C. Guerrero and J. R. McCormick, unpublished data; Kotun, 2013). It was discovered in this laboratory and is highly conserved among *Streptomyces* species as well as other Actinobacteria. *slzA* is located 300 bp upstream of the DNA segregation and condensation gene *smc*. The proximity of *slzA* to *smc* suggested that SlzA may have a function in chromosome condensation and segregation. Unfortunately, no obvious condensation or segregation phenotype was observed in *slzA* null mutant (Kotun, 2013). Consistent with a potential role in developmental segregation,

in *S. venezuelae*, SlzA (SVEN5271) is one of many targets of WhiA, a transcriptional regulator whose expression is highly upregulated during sporulation (Bush *et al.*, 2013). I used plasmids carrying *slzA* fusion genes (Kotun, 2013) in bacterial two-hybrid system to see if SlzA interacts with partitioning and/or segregation and condensation proteins. Interestingly, my results have shown that SlzA interacted with both ParH and ScpB (Figure 2.14, B). This may suggest that SlzA plays a role in segregation and/or condensation in *S. coelicolor*, where either ParH and/or ScpB uses SlzA as a linker, while ParA is capable of direct interaction with ScpB during development in the aerial hyphae.

## DISCUSSION

The bacterial ParAB proteins are essential for accurate distribution of the chromosomes into daughter cells. One demonstrated role of ParA in *S. coelicolor* is to assemble into long helical filaments in pre-developmental aerial hyphae. The ParA filaments are believed to be responsible, at least in part, for proper positioning of ParB-*parS* complexes (Jakimowicz *et al.*, 2007). The phenotypes of *parA* and *parB* mutants are 24% and 15% of anucleate spores, respectively. Even though these proteins are not essential for the survival of the bacterium under laboratory conditions, the phenotypes point out the central roles of the proteins in proper developmental genome segregation. The purpose of this study was to consider additional key elements of chromosome segregation and identify additional proteins that may interact with ParA or ParB in *S. coelicolor*.

Prior to this present study, Dedrick discovered an additional ParA-encoding gene (*sco1772*, named ParH) through BLAST analysis using the ParA amino acid sequence. ParH has 45% identical residues to ParA of *S. coelicolor*, and it has a 61 amino acid extension inserted near the N-terminus and ParA has a 22 amino acid extension at the C-terminus (Figures 2.1 and 2.3). Interestingly, the composition of this additional sequence at the N-terminus of ParH is unusual and rich in aromatic residues (3F and 5Y). Statistical studies have shown that, a small group of aromatic residues are important in protein-protein interactions and phenylalanine and tyrosine are among this small subset of aromatic amino acids (Bogan and Thorn, 1998; Wells, 1991). Therefore, in addition to its homology to ParA, having this aromatic residue rich N-terminal extension makes ParH potentially more interesting protein to analyze its function and role in chromosome

segregation in *S. coelicolor*. Although a strain expressing a  $\Delta 20-80$  variant of *parH* in *S. coelicolor* was constructed, the phenotype of the strain has not been analyzed yet. Perhaps as for a FtsK C-terminal truncation mutant (Dedrick *et al.*, 2009), the phenotype of this N-terminal in-frame deletion variant may produce more anucleate spores than in the *parH*-null mutant strain.

One of the common properties of ParA as well as other ParA-like proteins is they have a conserved deviant Walker A (KGGVGK) nucleotide-binding motif (Lutkenhaus and Sundaramoorthy, 2003). According to the crystal structure of Soj, this family of proteins forms a dimer and the nucleotide-binding sites are between the dimer interface of each monomer and nucleotide binding is required for dimer formation (Leonard *et al.*, 2005). Although the very N-terminal sequences of these proteins are not as highly conserved, the deviant Walker A nucleotide-binding motif is within the N-terminal region and these proteins show higher identity towards their C-terminal domain, which may suggest that these proteins have an evolutionary conserved function.

Due to its homology to ParA, loss of ParH was expected to have a defect in chromosome segregation in *S. coelicolor*. Microscopic analysis of a *parH* deletion strain revealed a frequency of 5% anucleate spores. Even though it seems as a subtle phenotype, compared to the phenotypes of some mutants for other segregation/condensation genes ( $\Delta smc$  is 8%,  $\Delta smc \Delta scpAB$  is 3%,  $\Delta ftsK$  is 0.8%), *parH* deletion mutant has higher frequency of anucleate spores than *scpAB* and *ftsK* deletion mutants. Therefore, I concluded that ParH has a direct or indirect role in the chromosome segregation of *S. coelicolor*. In addition to the slight chromosome segregation defect, I also observed infrequent branching in spore chains of aerial filaments of *parH* deletion strain. Since

other ParH-like proteins in other organisms, such as *C. glutamicum* plays a role in cell division (Donovan *et al.*, 2010), this branching phenotype in *parH* deletion strain suggests the possible role of ParH in cell division.

Previous preliminary analysis of the *in vivo* localization pattern of ParH revealed that ParH-EGFP showed no distinct pattern in vegetative filaments. Interestingly, several potential localization patterns in predivisional aerial filaments were observed (Dedrick, 2009). In this analysis, some small subset of the aerial filaments showed a bright band or several evenly-spaced bands and some of them showed diffused fluorescence at the tip of the filaments (Dedrick, 2009). The weak signal was enhanced by immunofluorescence microscopy using a FITC labeled GFP antibody. Based on the observed bands and increased fluorescence at the tips, I thought ParH might colocalize with FtsZ or over ParB foci or polymerize into helical filaments like ParA forms in predivisional aerial filaments. My recent preliminary epi-fluorescent (Nikon Eclipse Ni-U) and confocal (Nikon A1<sup>+</sup>) microscopy results, without enhancing the signal by immunofluorescence, instead showed that ParH-EGFP localized as evenly spaced foci intervals within predivisional aerial filaments similar to the pattern of ParB-EGFP of *S. coelicolor* (Figure 2.6). ParH-EGFP fluorescence was not observed in vegetative filaments or mature aerial filaments with spore compartments. The results were convincing since three different inoculations were used for sample preparation and the same localization pattern were observed in all samples. Probably the older confocal (Leica) microscope imaging was not sensitive enough to detect the low expression of ParH and samples were bleaching quickly. Epi-fluorescence microscope and a newer confocal microscope might be a better way to observe the localization of ParH-EGFP and provides improved results. The

observation of evenly-spaced ParH was reminiscent of the pattern observed for ParB and suggested that ParH might be colocalizing with ParB/*parS* complexes in aerial filaments and assist ParA directly or indirectly for proper localization of ParB/*parS* complexes. Unfortunately, I failed to see the colocalization of ParH-EGFP and ParB-mCherry in the aerial filaments due to weakness of the fluorescence signals. It is also possible that this event may happen for a very short period of time and observation time points failed to catch those events. Although, recently I analyzed the same strain with the epifluorescence wide-field microscope and was able to observe the co-localization, but unfortunately unable to capture the image due to quick bleaching of the samples. The preliminary evidence may suggest that ParH and ParB do colocalize in predivisional aerial hyphae.

Even though ParH and ParB may or may not colocalize in aerial filaments of *S. coelicolor*, I observed a mildly disrupted pattern of ParB-EGFP foci localization in a *parH*-null strain. Instead of typical evenly-spaced localization in each predivisional hyphae with the average ParB-EGFP interfocal distance 1  $\mu\text{m}$  apart, the distance between the two ParB-EGFP foci were either laterally or vertically closer to each other in a subset of hyphae. The total percentage of disrupted ParB-EGFP in a *parH*-null strain was approximately 6% compared to 1% of the wild type strain. This suggested that the deletion of *parH* was directly or indirectly playing a role in the proper localization of ParB-*oriC* regions in the aerial filaments of *S. coelicolor*.

Since loss of ParH mildly affects the localization of ParB-*oriC*, ParH might help ParB-*oriC* to stay evenly distributed along the aerial hyphae until septation begins. In addition, ParA and ParA-like proteins in other organisms are known for their non-specific



DNA-binding properties, as in ParA of *C. crescentus* and Soj in *Thermus thermophilus* and *B. subtilis* (Easter and Gober, 2002; Hester and Lutkenhaus, 2007; Leonard *et al.*, 2005). Even though it is still not known if ParA binds to DNA in *S. coelicolor*, I wanted to know whether ParH binds to DNA in a non-specific manner and help the localization of ParB-*oriC* localization. I used GFP-ParH fusions expressed in *E. coli* cells as an *in vivo* assay to see the localization of the protein with the nucleoid as one way to show its ability to bind DNA. My analysis showed that GFP-ParH localizes over the nucleoid of the cells in *E. coli*. Interestingly, a mutation at the ATPase active site affected the localization of ParH in *E. coli*. Although, this might have been caused by a partially degraded or unstable protein, it is also possible that ATPase activity might be important for DNA-binding of the protein. Even if the mutation at the ATPase active site causes instability and makes the results seem unreliable, it does not affect the purpose of this assay. The purpose of this assay was to show the DNA-binding ability of ParH. I used GFP-Soj as a positive control and it localized over the nucleoid same as in GFP-ParH.

One of the purposes of this study was to investigate interactions between ParH and known segregation and condensation proteins. I used a bacterial two-hybrid system to identify protein-protein interactions. Even though I failed to show the colocalization of ParH and ParB in *S. coelicolor*, I found that these two proteins were interacting partners in a bacterial two-hybrid system. This result was not surprising, since ParH has 45% identical amino acid sequence to ParA in *S. coelicolor* and ParA interacts with ParB in a bacterial two-hybrid system. In addition, *C. glutamicum* both ParA and PldP (a ParH-like protein) interacts with ParB in a bacterial two-hybrid system as well (Donovan *et al.*, 2010). Interestingly, ATPase active site and N-terminal extension of ParH was found to

be required for dimerization of the protein since these two mutations impaired ParH-ParB interaction, as judged by the two-hybrid system. These outcomes could have been the results of an unstable or improper folding of the protein. False-negative or false-positive outcomes of the bacterial two-hybrid system should also be taken into consideration. An independent assay, such as co-immunoprecipitation assay can be used to re-test ParA and ParH interaction and confirm ParB-ParH interaction.

Interactions between ParH and other known segregation/condensation (ParA, ParJ, SMC, ScpA, ScpB, FtsK) and division protein FtsZ were also tested, but I did not observe any interactions between them. These conclusions should not discard the false-negative outcomes of the bacterial two-hybrid system. Interestingly, I found interactions between ScpB-ParA, ScpB-SlzA, and SlzA-ParH. Interaction between ScpB and ParA was noteworthy since I tried to find the link between condensation and segregation of the chromosomes and ParA might help coordinate the activity of condensins. On the other hand, even though SlzA has no obvious segregation and condensation defects, its close proximity to *smc* and interaction with ScpB and ParH makes SlzA a possible segregation/condensation protein and a link between partitioning and condensation in *S. coelicolor*.

## REFERENCES

- Bentley, S. D., Chater, K. F., Cerdeno-Tarraga, A. M., Challis, G. L., Thomson, N. R., James, K. D., Hopwood, D. A. (2002). Complete genome sequence of the model actinomycete *Streptomyces coelicolor* A3(2). *Nature*, 417(6885), 141-147. doi: 10.1038/417141a.
- Bogan, A. A., Thorn, K. S. (1998). Anatomy of hot spots in protein interfaces. *J Mol Biol*, 280(1), 1-9. doi: 10.1006/jmbi.1998.1843.
- Bush, M. J., Bibb, M. J., Chandra, G., Findlay, K. C., Buttner, M. J. (2013). Genes required for aerial growth, cell division, and chromosome segregation are targets of WhiA before sporulation in *Streptomyces venezuelae*. *mBio*, 4(5), e00684-00613. doi: 10.1128/mBio.00684-13.
- Datsenko, K. A., Wanner, B. L. (2000). One-step inactivation of chromosomal genes in *Escherichia coli* K-12 using PCR products. *Proc Natl Acad Sci U S A*, 97(12), 6640-6645. doi: 10.1073/pnas.120163297.
- Dedrick, R. M., Wildschutte, H., McCormick, J. R. (2009). Genetic interactions of *smc*, *ftsK*, and *parB* genes in *Streptomyces coelicolor* and their developmental genome segregation phenotypes. *J Bacteriol*, 191(1), 320-332. doi: 10.1128/JB.00858-08.
- Ditkowski, B., Holmes, N., Rydzak, J., Donczew, M., Bezulska, M., Ginda, K., Jakimowicz, D. (2013). Dynamic interplay of ParA with the polarity protein, Scy, coordinates the growth with chromosome segregation in *Streptomyces coelicolor*. *Open Biol*, 3(3), 130006. doi: 10.1098/rsob.130006.
- Ditkowski, B., Troc, P., Ginda, K., Donczew, M., Chater, K. F., Zakrzewska-Czerwinska, J., Jakimowicz, D. (2010). The actinobacterial signature protein ParJ (SCO1662)

- regulates ParA polymerization and affects chromosome segregation and cell division during *Streptomyces* sporulation. *Mol Microbiol*, 78(6), 1403-1415. doi: 10.1111/j.1365-2958.2010.07409.x.
- Donovan, C., Schwaiger, A., Kramer, R., Bramkamp, M. (2010). Subcellular localization and characterization of the ParAB system from *Corynebacterium glutamicum*. *J Bacteriol*, 192(13), 3441-3451. doi: 10.1128/JB.00214-10.
- Donovan, C., Sieger, B., Kramer, R., Bramkamp, M. (2012). A synthetic *Escherichia coli* system identifies a conserved origin tethering factor in *Actinobacteria*. *Mol Microbiol*, 84(1), 105-116. doi: 10.1111/j.1365-2958.2012.08011.x.
- Easter, J., Jr., Gober, J. W. (2002). ParB-stimulated nucleotide exchange regulates a switch in functionally distinct ParA activities. *Mol Cell*, 10(2), 427-434.
- Errington, J. (2001). Septation and chromosome segregation during sporulation in *Bacillus subtilis*. *Curr Opin Microbiol*, 4(6), 660-666.
- Fuchino, K., Bagchi, S., Cantlay, S., Sandblad, L., Wu, D., Bergman, J., Ausmees, N. (2013). Dynamic gradients of an intermediate filament-like cytoskeleton are recruited by a polarity landmark during apical growth. *Proc Natl Acad Sci U S A*, 110(21), E1889-1897. doi: 10.1073/pnas.1305358110.
- Gerdes, K., Howard, M., Szardenings, F. (2010). Pushing and pulling in prokaryotic DNA segregation. *Cell*, 141(6), 927-942. doi: 10.1016/j.cell.2010.05.033.
- Gruber, S., Errington, J. (2009). Recruitment of condensin to replication origin regions by ParB/SpoOJ promotes chromosome segregation in *B. subtilis*. *Cell*, 137(4), 685-696. doi: 10.1016/j.cell.2009.02.035.

- Gust, B., Chandra, G., Jakimowicz, D., Yuqing, T., Bruton, C. J., Chater, K. F. (2004). Lambda red-mediated genetic manipulation of antibiotic-producing *Streptomyces*. *Adv Appl Microbiol*, 54, 107-128. doi: 10.1016/S0065-2164(04)54004-2.
- Hayes, F., Barilla, D. (2006). The bacterial segrosome: a dynamic nucleoprotein machine for DNA trafficking and segregation. *Nat Rev Microbiol*, 4(2), 133-143. doi: 10.1038/nrmicro1342.
- Hester, C. M., Lutkenhaus, J. (2007). Soj (ParA) DNA binding is mediated by conserved arginines and is essential for plasmid segregation. *Proc Natl Acad Sci U S A*, 104(51), 20326-20331. doi: 10.1073/pnas.0705196105.
- Hu, Z., Gogol, E., Lutkenhaus, J., (2002). Dynamic assembly of MinD on phospholipid vesicles regulated by ATP and MinE. *Proc Natl Acad Sci USA*, 99, 6761–6766.
- Ireton, K., Gunther, N. W. t., Grossman, A. D. (1994). *spo0J* is required for normal chromosome segregation as well as the initiation of sporulation in *Bacillus subtilis*. *J Bacteriol*, 176(17), 5320-5329.
- Jakimowicz, D., Chater, K., Zakrzewska-Czerwinska, J. (2002). The ParB protein of *Streptomyces coelicolor* A3(2) recognizes a cluster of *parS* sequences within the origin-proximal region of the linear chromosome. *Mol Microbiol*, 45(5), 1365-1377.
- Jakimowicz, D., Gust, B., Zakrzewska-Czerwinska, J., Chater, K. F. (2005). Developmental-stage-specific assembly of ParB complexes in *Streptomyces coelicolor* hyphae. *J Bacteriol*, 187(10), 3572-3580. doi:10.1128/JB.187.10.3572-3580.2005.

- Jakimowicz, D., Zydek, P., Kois, A., Zakrzewska-Czerwinska, J., Chater, K. F. (2007). Alignment of multiple chromosomes along helical ParA scaffolding in sporulating *Streptomyces* hyphae. *Mol Microbiol*, 65(3), 625-641. doi: 10.1111/j.1365-2958.2007.05815.x.
- Jensen, R. B., Wang, S. C., Shapiro, L. (2001). A moving DNA replication factory in *Caulobacter crescentus*. *EMBO J*, 20(17), 4952-4963. doi: 10.1093/emboj/20.17.4952.
- Karimova, G., Ullmann, A., Ladant, D. (2000). *Bordetella pertussis* adenylate cyclase toxin as a tool to analyze molecular interactions in a bacterial two-hybrid system. *Int J Med Microbiol*, 290(4-5), 441-445. doi: 10.1016/S1438-4221(00)80060-0.
- Kois, A., Swiatek, M., Jakimowicz, D., and Zakrzewska-Czerwinska, J. (2009). SMC Protein-Dependent Chromosome Condensation during Aerial Hyphal Development in *Streptomyces*. *J Bacteriol*, 191, 310-319.
- Lemon, K. P., Kurtser, I., Grossman, A. D. (2001). Effects of replication termination mutants on chromosome partitioning in *Bacillus subtilis*. *Proc Natl Acad Sci U S A*, 98(1), 212-217. doi: 10.1073/pnas.011506098.
- Leonard, T. A., Butler, P. J., Lowe, J. (2005). Bacterial chromosome segregation: structure and DNA binding of the Soj dimer-a conserved biological switch. *EMBO J*, 24(2), 270-282. doi: 10.1038/sj.emboj.7600530.
- Leonard, T. A., Moller-Jensen, J., Lowe, J. (2005). Towards understanding the molecular basis of bacterial DNA segregation. *Philos Trans R Soc Lond B Biol Sci*, 360(1455), 523-535. doi: 10.1098/rstb.2004.1608.

- Lindow, J. C., Kuwano, M., Moriya, S., Grossman, A. D. (2002). Subcellular localization of the *Bacillus subtilis* structural maintenance of chromosomes (SMC) protein. *Mol Microbiol*, 46(4), 997-1009.
- Lutkenhaus, J. (2007). Assembly dynamics of the bacterial MinCDE system and spatial regulation of the Z ring. *Annu Rev Biochem*, 76, 539-562. doi: 10.1146/annurev.biochem.75.103004.142652.
- Lutkenhaus, J., Sundaramoorthy, M. (2003). MinD and role of the deviant Walker A motif, dimerization and membrane binding in oscillation. *Mol Microbiol*, 48(2), 295-303.
- McCormick, J. R. (2009). Cell division is dispensable but not irrelevant in *Streptomyces*. *Curr Opin Microbiol*, 12(6), 689-698. doi: 10.1016/j.mib.2009.10.004.
- Mierzejewska, J., Jagura-Burdzy, G. (2012). Prokaryotic ParA-ParB-*parS* system links bacterial chromosome segregation with the cell cycle. *Plasmid*, 67(1), 1-14. doi: 10.1016/j.plasmid.2011.08.003.
- Murray, H., Errington, J. (2008). Dynamic control of the DNA replication initiation protein DnaA by Soj/ParA. *Cell*, 135(1), 74-84. doi: 10.1016/j.cell.2008.07.044.
- Perez-Cheeks, B. A., Planet, P. J., Sarkar, I. N., Clock, S. A., Xu, Q., Figurski, D. H. (2012). The product of *tadZ*, a new member of the *parA/minD* superfamily, localizes to a pole in *Aggregatibacter actinomycetemcomitans*. *Mol Microbiol*, 83(4), 694-711. doi: 10.1111/j.1365-2958.2011.07955.x.
- Salerno, P., Persson, J., Bucca, G., Laing, E., Ausmees, N., Smith, C. P., Flardh, K. (2013). Identification of new developmentally regulated genes involved in

- Streptomyces coelicolor* sporulation. *BMC Microbiol*, 13, 281. doi: 10.1186/1471-2180-13-281.
- Schumacher, M. A. (2007). Structural biology of plasmid segregation proteins. *Curr Opin Struct Biol*, 17(1), 103-109. doi: 10.1016/j.sbi.2006.11.005.
- Sherratt, D. J. (2003). Bacterial chromosome dynamics. *Science*, 301(5634), 780-785. doi: 10.1126/science.1084780.
- Soppa, J., Kobayashi, K., Noirot-Gros, M. F., Oesterhelt, D., Ehrlich, S. D., Dervyn, E., Moriya, S. (2002). Discovery of two novel families of proteins that are proposed to interact with prokaryotic SMC proteins, and characterization of the *Bacillus subtilis* family members ScpA and ScpB. *Mol Microbiol*, 45(1), 59-71.
- Suefuji, K., Valluzzi, R., RayChaudhuri, D., (2002). Dynamic assembly of MinD into filament bundles modulated by ATP, phospholipids, and MinE. *Proc Natl Acad Sci USA*, 99, 16776–16781.
- Sullivan, N. L., Marquis, K. A., Rudner, D. Z. (2009). Recruitment of SMC by ParB-*parS* organizes the origin region and promotes efficient chromosome segregation. *Cell*, 137(4), 697-707. doi: 10.1016/j.cell.2009.04.044.
- Thanbichler, M., Shapiro, L. (2006). MipZ, a spatial regulator coordinating chromosome segregation with cell division in *Caulobacter*. *Cell*, 126(1), 147-162. doi: 10.1016/j.cell.2006.05.038.
- Treuner-Lange A, Aguiluz K, van der Does C, Gómez-Santos N, Harms A, Schumacher D, Lenz P, Hoppert M, Kahnt J, Muñoz-Dorado J, Søgaard-Andersen L. (2013). PomZ, a ParA-like protein, regulates Z-ring formation and cell division in *Myxococcus xanthus*. *Mol Microbiol*. 87(2), 235-53. doi: 10.1111/mmi.12094.



Wells, J. A. (1991). Systematic mutational analyses of protein-protein interfaces.

*Methods Enzymol*, 202, 390-411.

Zhou, H., Lutkenhaus, J. (2004). The switch I and II regions of MinD are required for

binding and activating MinC. *J Bacteriol*, 186(5), 1546-1555.

**Table 2.1: *E. coli* strains used in this study**

Strain	Genotype	Reference/Source
BTH101	F <sup>-</sup> <i>cya-99 araD139 galE15 galK16 rpsL1 hsdR2 mcrA1 mcrB1</i>	Euromedex
BW25113	F <sup>-</sup> $\Delta(\textit{araD-araB})567 \Delta\textit{lacZ4787} (::\textit{rrnB-3}) \lambda \textit{rph-1}$ $\Delta(\textit{rhaD-rhaB})568 \textit{hsdR514}$	Datsenko and Wanner 2000
ET12567	F <sup>-</sup> <i>dam-13::Tn9 dcm-6 hsdM hsdR recF143 zjj-201::Tn10 galK2</i> <i>galT22 ara-14 lacY1 xyl-5 leuB6 thi-1 tonA31 rpsL136 hisG4</i> <i>tsx-78 mtl-1 glnV44</i>	MacNeil <i>et al.</i> , 1992
TG1	<i>supE thi-1</i> $\Delta(\textit{lac-proAB}) \Delta(\textit{mcrB-hsdSM})5 (r_K m_K) / F' \textit{traD36}$ <i>proAB lacI<sup>q</sup>ZAM15</i>	Sambrook <i>et al.</i> , 1989
TOP10	F <sup>-</sup> <i>mcrA</i> $\Delta(\textit{mrr-hsdRMS-mcrBC}) \Phi 80\textit{lacZAM15} \Delta\textit{lacX74 deoR}$ <i>recA1 araD139</i> $\Delta(\textit{araA-leu})697 \textit{galU galK}$	Invitrogen

**Table 2.2: *S. coelicolor* A3(2) strains used in this study**

<b>Strain</b>	<b>Genotype</b>	<b>Reference/Source</b>
M145	prototroph SCP1 <sup>-</sup> SCP2 <sup>-</sup>	Hopwood <i>et al.</i> , 1985
MH1	$\Delta parH$ $\phi C31$ <i>att::parH(K99E) aadA parB-egfp</i>	This study
MH2	$\Delta parH$ $\phi C31$ <i>att::parH(R273E) aadA parB-egfp</i>	This study
MH3	<i>parH</i> ( $\Delta 20-80$ ) <i>acc(3)IV</i>	This study
MH4	<i>parH-egfp parB-mCherry acc(3)IV</i>	This study
MH5	$\Delta parH::acc(3)IV$	This study
MH6	$\Delta parA$ $\Delta parH::acc(3)IV$	This study
J3306	$\Delta parA$	Jakimowicz <i>et al.</i> , 2005
J3310	<i>parB-egfp</i>	Jakimowicz <i>et al.</i> , 2005
J3316	<i>parB-mCherry</i>	Jakimowicz Lab
RMD29	$\Delta parH::acc(3)IV$ <i>parB-egfp</i>	Dedrick, PhD Dissertation, 2009
RMD30	<i>parH-egfp acc(3)IV</i>	Dedrick, PhD Dissertation, 2009

# all strains were derived from M145

**Table 2.3: Cosmids and plasmids used in this study**

<b>Cosmid/Plasmid</b>	<b>Description</b>	<b>Reference/Source</b>
H24 <i>parB-egfp</i>	<i>egfp</i> inserted in-frame at 3' of <i>parB</i> in cosmid SCH24, <i>acc(3)IV aphII</i>	Jakimowicz <i>et al.</i> , 2005
I51 <i>parA2-egfp</i>	<i>egfp</i> inserted in-frame at 3' of <i>parH</i> ( <i>parA2</i> ) in cosmid SCI51, <i>acc(3)IV aphII</i>	Dedrick, PhD Dissertation, 2009
pAK67	<i>ftsZ</i> flanked by <i>Acc65I</i> sites cloned into pKT25	Kotun, PhD dissertation, 2013
pAK68	<i>ftsZ</i> flanked by <i>Acc65I</i> sites cloned into pUT18C	Kotun dissertation
pAK78	<i>slzA</i> flanked by <i>Acc65I</i> sites cloned into pKNT25	Kotun dissertation
pAK79	<i>slzA</i> flanked by <i>Acc65I</i> sites cloned into pUT18	Kotun dissertation
pAK80	<i>slzA</i> flanked by <i>Acc65I</i> sites cloned into pUT18C	Kotun dissertation
pAK88	<i>slzA</i> flanked by <i>Acc65I</i> sites cloned into pKT25	Kotun dissertation
ParAT18C	<i>parA</i> flanked by <i>XbaI</i> and <i>KpnI</i> cloned into pUT18C	Jakimowicz <i>et al.</i> , 2007
ParAT25	<i>parA</i> flanked by <i>XbaI</i> and <i>KpnI</i> cloned into pKT25	Jakimowicz <i>et al.</i> , 2007
ParBT18C	<i>parB</i> flanked by <i>XbaI</i> and <i>KpnI</i> cloned into pUT18C	Jakimowicz <i>et al.</i> , 2007
ParBT25	<i>parB</i> flanked by <i>XbaI</i> and <i>KpnI</i> cloned into pKT25	Jakimowicz <i>et al.</i> , 2007
ParJT18C	<i>parJ</i> flanked by <i>XbaI</i> and <i>KpnI</i> cloned into pUT18C	Jakimowicz <i>et al.</i> , 2010
ParJT25	<i>parB</i> flanked by <i>XbaI</i> and <i>KpnI</i> cloned into pKT25	Jakimowicz <i>et al.</i> , 2010
pCR2.1	TA cloning vector	Invitrogen

pIJ773	pBluescript II SK(+) derivative containing <i>aac(3)IV-oriT</i> disruption cassette flanked by <i>frt</i> sites	Gust <i>et al.</i> , 2003
pIJ790	$\lambda$ -RED ( <i>gam, bet, exo</i> ) <i>araC rep101<sup>ts</sup></i>	Gust <i>et al.</i> , 2003
pKNT25	Bacterial two-hybrid vector used to create a fusion to the N-terminus of the CyaA T25 polypeptide	Euromedex
pKT25	Bacterial two-hybrid vector used to create a fusion to the C-terminus of the CyaA T25 polypeptide	Euromedex
pMH1	$P_{lac-gfp-parH}$	This study
pMH2	$P_{lac-gfp-parH(K99E)}$	This study
pMH3	$P_{lac-gfp-parH(R273E)}$	This study
pMH4	<i>parH</i> flanked by <i>KpnI</i> sites cloned into pCR2.1	This study
pMH5	<i>parH</i> flanked by <i>KpnI</i> sites cloned into pUT18	This study
pMH6	<i>parH</i> flanked by <i>KpnI</i> sites cloned into pUT18C	This study
pMH7	<i>parH</i> flanked by <i>KpnI</i> sites cloned into pKT25	This study
pMH8	<i>parH</i> flanked by <i>KpnI</i> sites cloned into pKNT25	This study
pMH9	<i>parH(K99E)</i> flanked by <i>KpnI</i> sites cloned into pCR2.1	This study
pMH10	<i>parH(K99E)</i> flanked by <i>KpnI</i> sites cloned into pUT18	This study
pMH11	<i>parH(K99E)</i> flanked by <i>KpnI</i> sites cloned into pUT18C	This study
pMH12	<i>parH(K99E)</i> flanked by <i>KpnI</i> sites cloned into pKT25	This study
pMH13	<i>parH(K99E)</i> flanked by <i>KpnI</i> sites cloned into pKNT25	This study

pMH14	<i>parH</i> ( $\Delta$ 20-80) flanked by <i>KpnI</i> sites cloned into pCR2.1 TA cloning vector	This study
pMH15	<i>parH</i> ( $\Delta$ 20-80) flanked by <i>KpnI</i> sites cloned into pUT18	This study
pMH16	<i>parH</i> ( $\Delta$ 20-80) flanked by <i>KpnI</i> sites cloned into pUT18C	This study
pMH17	<i>parH</i> ( $\Delta$ 20-80) flanked by <i>KpnI</i> sites cloned into pKT25	This study
pMH18	<i>parH</i> ( $\Delta$ 20-80) flanked by <i>KpnI</i> sites cloned into pKNT25	This study
pMH19	<i>parH</i> (R273E) flanked by <i>KpnI</i> sites cloned into pCR2.1	This study
pMH20	<i>parH</i> (R273E) flanked by <i>KpnI</i> sites cloned into pUT18	This study
pMH21	<i>parH</i> (R273E) flanked by <i>KpnI</i> sites cloned into pUT18C	This study
pMH22	<i>parH</i> (R273E) flanked by <i>KpnI</i> sites cloned into pKT25	This study
pMH23	<i>parH</i> (R273E) flanked by <i>KpnI</i> sites cloned into pKNT25	This study
pMH24	<i>smc</i> flanked by <i>KpnI</i> sites cloned into pCR2.1	This study
pMH25	<i>smc</i> flanked by <i>KpnI</i> sites cloned into pUT18	This study
pMH26	<i>smc</i> flanked by <i>KpnI</i> sites cloned into pUT18C	This study
pMH27	<i>smc</i> flanked by <i>KpnI</i> sites cloned into pKT25	This study
pMH28	<i>smc</i> flanked by <i>KpnI</i> sites cloned into pKNT25	This study
pMH29	<i>scpA</i> flanked by <i>KpnI</i> sites cloned into pCR2.1	This study
pMH30	<i>scpA</i> flanked by <i>KpnI</i> sites cloned into pUT18	This study

pMH31	<i>scpA</i> flanked by <i>KpnI</i> sites cloned into pUT18C	This study
pMH32	<i>scpA</i> flanked by <i>KpnI</i> sites cloned into pKT25	This study
pMH33	<i>scpA</i> flanked by <i>KpnI</i> sites cloned into pKNT25	This study
pMH34	<i>scpB</i> flanked by <i>KpnI</i> sites cloned into pCR2.1	This study
pMH35	<i>scpB</i> flanked by <i>KpnI</i> sites cloned into pUT18	This study
pMH36	<i>scpB</i> flanked by <i>KpnI</i> sites cloned into pUT18C	This study
pMH37	<i>scpB</i> flanked by <i>KpnI</i> sites cloned into pKT25	This study
pMH38	<i>scpB</i> flanked by <i>KpnI</i> sites cloned into pKNT25	This study
pMH39	$\Delta$ 20-80 in-frame deletion of <i>parH</i> in SCI51	This study
pRJ1	<i>parH</i> flanked by <i>KpnI</i> sites cloned into bacterial two-hybrid vector pT18	McCormick Lab
pRJ3	K99E mutation (AAG to GAG) in pRJ1	This study
pRJ4	897 kb <i>MluI</i> - <i>AscI</i> fragment from pRJ3 was ligated to 3.347 kb <i>MluI</i> fragment isolated from pRMD16	This study
pRJ5	K99E mutation (AAG to GAG) in pRMD16	This study
pRMD16	3.6 kb <i>Bgl</i> III fragment of SCI51, contains <i>parH</i> gene, an origin of transfer, and <i>int</i> and <i>attP</i> of $\Phi$ C31, cloned into <i>Bam</i> HI digested pSpc152	Dedrick, PhD Dissertation, 2009
pSEB181	P <sub>lac</sub> - <i>gfp</i>	Zhou and Lutkenhaus, 2004
pSEB200	P <sub>lac</sub> - <i>gfp-soj</i>	Hester <i>et al.</i> , 2007
pTR1	R273E mutation (CGC to GAG) in pRJ1	This study

pTR2	897 kb <i>MluI</i> - <i>AscI</i> fragment from pTR1 was ligated to 3.347 kb <i>MluI</i> fragment isolated from pRMD16	This study
pTR3	R273E mutation in pRDM16	This study
pTR4	XbaI and HindIII recognition sites flanking <i>parH</i> cloned into pCR2.1	This study
pTR5	XbaI and HindIII recognition sites flanking K99E variant of <i>parH</i> cloned into pCR2.1	This study
pTR6	XbaI and HindIII recognition sites flanking R273E variant of <i>parH</i> cloned into pCR2.1	This study
pUT18	Bacterial two-hybrid vector used to create a fusion to the N-terminus of the CyaA T18 polypeptide	Euromedex
pUT18C	Bacterial two-hybrid vector used to create a fusion to the C-terminus of the CyaA T18 polypeptide	Euromedex
SCI51	cosmid source of <i>parH</i> ( <i>SCO1772</i> )	Redenbach <i>et al.</i> , 1996



**Table 2.4: Oligonucleotides used in this study**

Oligonucleotide	Sequence	Application
ParA2KpnIFwd	GGTACCTATGAGTATGGATGGCCAACACGTGA ACGCC	Cloning <i>parH</i> into bacterial two-hybrid plasmids
ParA2KpnIRev	GGTACCTCGGCGTGACACCGGGCGA	Cloning <i>parH</i> into bacterial two-hybrid plasmids
SMCKpnlFwd	GGTACCTGTGCACCTGAAGGCCCTGACCCTCC GCGGG	Cloning <i>smc</i> into bacterial two-hybrid plasmids
SMCKpnlRev	GGTACCGGGCTGACGCAACCGCTGGC	Cloning <i>smc</i> into bacterial two-hybrid plasmids
ScpAKpnlFwd	GGTACCTGTGCGGCTCGCCAACCTTCGAGGGGC CGTTC	Cloning <i>scpA</i> into bacterial two-hybrid plasmids
ScpAKpnlRev	GGTACCCGCCTTCCGCCTCCTCCTCG	Cloning <i>scpA</i> into bacterial two-hybrid plasmids
ScpBKpnlFwd	GGTACCTGTGAGTGAGCGGATCACGGAGGCCG AGGAG	Cloning <i>scpB</i> into bacterial two-hybrid plasmids
ScpBKpnlRev	GGTACCAAATTCCGTCTTGTCGTCT	Cloning <i>scpB</i> into bacterial two-hybrid plasmids
parA2Fwd	AGCACACATGAGTATGGATGGCCAACACGTGA ACGCCATG ATTCCGGGGATCCGTCGACC	Construction of $\Delta parH$
parA2Rev	CTCACTCGGCGTGACACCGGGCGAGCACCTCC CTGGCGAG TGTAGGCTGGAGCTGCTTC	Construction of $\Delta parH$
parA2egfpFwd	CCAGCTCGCCAGGGAGGTGCTCGCCCGGTGTC ACGCCGAG CTGCCGGGCCCGGAGCTG	Construction of ParH-EGFP
parA2egfpRev	CCTGTCGTACGGAAGAGTTCGTCCGCCCCCGG CAGACTCA CATATGTAGGCTGGAGCTGC	Construction of ParH-EGFP
K99EFwd	CAGAAGGGCGGCGTGGGCGAGACCACGTCGA CCATCAAC	Construction of K99E mutation in ParH
K99ERev	GTTGATGGTCGACGTGGTCTCGCCCACGCCG CCTTCTG	Construction of K99E mutation in ParH
R273EFwd	CTGCCACGATGTACGACTCGGAGACCGTGCA CAGCCGTGAG	Construction of R273E mutation in ParH

R273ERev	CTCACGGCTGTGCACGGTCTCCGAGTCGTACA TCGTGGCGAG	Construction of R273E mutation in ParH
ParH60Fdel	GTGAACGCCATGGCCGGCGACGGAAGTGGCGC GCCCCGCAATTTAAATTCCGGGGATCCGTCGA CC	Construction of in-frame deletion in ParH
ParH240Rdel	CTTCTGGTTGCACATCGCGATGATCTTGGCGGG GCCGTGATCATTTAAATTGTAGGCTGGAGCTG CTTC	Construction of in-frame deletion in ParH
XbaI-ParH fwd	CTTGTCTAGAAGTATGGATGGCCAACACGT	Construction of GFP-ParH fusions
HindII-ParH rev	TTGAAGCTTTCACTCGGCGTGACACCGGG	Construction of GFP-ParH fusions

```

ParA      MDDTPIGRAAQLAVEALGRAGEGLPR----- 26
ParH      -----MSMDGQHVNAMAGDGS GAPRNHFADYDELPEGHFYDPDAEYEPDPEYAATLAPD 54
          * *:. *.* **

ParA      -----PEQTRVMVVAHQKGGV GKTTT TVNLAASLALHG 59
ParH      AARQRREIRIGPTGRPLPYFPIPGPLTDHGPAKI IAMCNQKGGV GKTTTSTINLGAALAEYG 114
          :::::*****:*.**:*:* :*

ParA      ARVLVVDLDPQGNASTALGIDHHADVPSIYDVLVESRPLSEVVQVPDVEGLFCAPATID 119
ParH      RRVLVDFDLPQGALS VGLGVNPMELDLTVYNLLMERGMAAEVLLKTAVPNMDLLPSNID 174
          ***:*.**:* *..*:*: :*:*:*: * : * . * .: *:.**

ParA      LAGAEIELVSLVARESRLQRAITAYEQPLDYILIDCPPSLGLLTVNALVAGQEVLIPIQC 179
ParH      LSAAEVQLVSEVARESTLQRALKPLMDDYDYIVIDCQPSLGLLTVNALTAHKVIVPLEC 234
          *:.**:*:* * ** * **:*: : * **:* * ** ** ** * .: :*:*:*:

ParA      EYVALEGLGQLLRNVDLVRGHLNPTLHVSTILLTMYDGRTRLASQVADEVRSHFGEVLR 239
ParH      EFFALRGVALLTETIEKVQERLNPDELDGILATMYDSRTVHSREVLARVVEAFDDHVVH 294
          *:.**:*:. * .: : * : ** *:. ** ** **.* * : :* . * . *:. * :

ParA      TSI PRSVRISEAPSYGQTVLTYDPGSSGALSYLEAAREIALKGVGVTYDATHAHLGAQND 299
ParH      TVIGRTVRFPEPETT VAGEPITTYASNSVGAAYRQLAREVLAR-----CHAE----- 340
          * * *:*:*:.*:. *:.: ** ..* ** :* : ** : : ** .

ParA      PSMVEGTQ 307
ParH      -----

```

**Figure 2.1. Sequence alignment of ParA and ParH for *S. coelicolor*.** Amino acid sequences were aligned using ClustalW2. ParH has 44.8% (111/248) identical residues and 63.3% (157/248) similarity to ParA. In addition, ParH has 61 additional amino acids inserted in the N-terminus (bold and underlined) and ParA has a slight extension at the C-terminus. The ParH residues eliminated for a 5' in-frame deletion in *parH* are underlined. Deviant Walker A box (amino acid change in K99E mutant is shown in bold and underlined) and conserved arginine residue are highlighted in grey. An asterisk (\*) indicates a conserved residue, colon (: ) indicates conservation between groups of strongly similar properties, period (.) indicates conservation between groups of weakly similar

properties.

```

SGR      -MMDGLHVNATAGNESSRDTDRFADF AEVPEGHFYDPDAEYEPDPEYAATLAPDAARQRR
SCLAV    -MMDGLHVNATAGNESGRESTHFAAYEELPEGHFYDPDAEYEPDPEYAATLAPDAARQRR
SVEN     --MDGLHVNATAGNEMGRESTHFAAYDEVPEGHFYDPDAEYEPDPEYAATLAPDAARQRR
SAV      --MDGHHVNAMAGNGSGENRTHFADYDELPEGHFYDPDAEYEPDPEYAATLAPDAARQRR
SCO      MSMDGQHVNAMAGDGS GAPNHFADYDELPEGHFYDPDAEYEPDPEYAATLAPDAARQRR
SCAB     --MDGQHVNAMAGDGS GG VHNHFADYDEL PDGHFYDPDAEYEPDPEYAATLAPDAARQRR
          ***  ****  **:   .       **:  :  *:*:*****

SGR      ERIGPTGRPLPYFP I PGPLTDHGPAK I IAMCNQKGGVGKTTSTINLGAALAEYGRRVLLV
SCLAV    ERIGPTGRPLPYFP I PGPLTDHGPAK I IAMCNQKGGVGKTTSTINLGAALAEYGRRVLLV
SVEN     ERIGPTGRPLPYFP I PGPLTDHGPAK I IAMCNQKGGVGKTTSTINLGAALAEYGRRVLLV
SAV      ERVGPTGRPLPYFP I PGPLTDHGPAK I IAMCNQKGGVGKTTSTINLGAALAEYGRRVLLV
SCO      ERIGPTGRPLPYFP I PGPLTDHGPAK I IAMCNQKGGVGKTTSTINLGAALAEYGRRVLLV
SCAB     ERIGPTGRPLPYFP I PGPLTDHGPAK I IAMCNQKGGVGKTTSTINLGAALAEYGRRVLLV
          **:*****

SGR      DFDPQGALSVGLGVNPMELDLTVYNLLMERGMAADDVLLKTAVPNMDLLPSNIDLSAAEV
SCLAV    DFDPQGALSVGLGVNPMELDLTVYNLLMERGMSADEVLLKTAVPNMDLLPSNIDLSAAEV
SVEN     DFDPQGALSVGLGVNPMELDLTVYNLLMERGMSADEVLLKTAVPNMDLLPSNIDLSAAEV
SAV      DFDPQGALSVGLGVNPMELDLTVYNLLMERGMAADEVLLKTAVPNMDLLPSNIDLSAAEV
SCO      DFDPQGALSVGLGVNPMELDLTVYNLLMERGMAADEVLLKTAVPNMDLLPSNIDLSAAEV
SCAB     DFDPQGALSVGLGVNPMELDLTVYNLLMERGMSADEVLLKTAVPNMDLLPSNIDLSAAEV
          *****:*.*****

SGR      QLVSEVARESTLQRALKPLMADYDYIVIDCQPSLGLLTVNALTAAHKVIVPLECEFFALR
SCLAV    QLVSEVARESTLQRALKPLMSDYDYIVIDCQPSLGLLTVNALTAAHKVIVPLECEFFALR
SVEN     QLVSEVARESTLQRALKPLMNDYDYIVIDCQPSLGLLTVNALTAAHKVIVPLECEFFALR
SAV      QLVSEVARESTLQRALKPLMADYDYIVIDCQPSLGLLTVNALTAAHKVIVPLECEFFALR
SCO      QLVSEVARESTLQRALKPLMDDYDYIVIDCQPSLGLLTVNALTAAHKVIVPLECEFFALR
SCAB     QLVSEVARESTLQRALKPLMADYDYIVIDCQPSLGLLTVNALTAAHKVIVPLECEFFALR
          *****

SGR      GVALLTETIEKVQERLNPELELDGILATMYDSRTVHSREVLARVVEAFDEHVYHTVIGRT
SCLAV    GVALLTETIEKVQERLNPELELDGILATMYDSRTVHSREVLARVVEAFGDHVYHTVIGRT
SVEN     GVALLTETIEKVQERLNPELELDGILATMYDSRTVHSREVLARVVEAFDDHVYHTVIGRT
SAV      GVALLTETIEKVQERLNPELELDGILATMYDSRTVHSREVLARVVEAFDDHVYHTVIGRT
SCO      GVALLTETIEKVQERLNPDLELDGILATMYDSRTVHSREVLARVVEAFDDHVYHTVIGRT
SCAB     GVALLTETIEKVQERLNPDLELDGILATMYDSRTVHSREVLARVVEAFDEHVYHTVIGRT
          *****:*****

SGR      VRFPETTVAGEPITTYASNSVGAAYRQLAREVLARCHAE
SCLAV    VRFPETTVAGEPITTYASNSVGAAYRQLAREVLARCHAE
SVEN     VRFPETTVAGEPITTYASNSVGAAYRQLAREVLARCHAE
SAV      VRFPETTVAGEPITTYASNSVGAAYRQLAREVLARCHAE
SCO      VRFPETTVAGEPITTYASNSVGAAYRQLAREVLARCHAE
SCAB     VRFPETTVAGEPITTYASNSVGAAYRQLAREVLARCHAE
          *****

```

**Figure 2.2. Multiple sequence alignment of ParH homologs among different**

*Streptomyces* species. Amino acid sequences of *Streptomyces* homologs were aligned using ClustalW2. ParH homology have 61 additional amino acids (bold) inserted in the N-terminus when compared to ParA (Figure 2.1.) The sequence of this 61 amino acid

region, including every aromatic residue, is highly conserved as is majority of the protein sequence. An asterisk (\*) indicates a conserved residue, colon (:) indicates conservation between groups of strongly similar properties, period (.) indicates conservation between groups of weakly similar properties. Species abbreviations: SGR, *S. griseus*; SCLAV, *S. clavuligerus*; SVEN, *S. venezuelae*; SAV, *S. avermitilis*; SCO, *S. coelicolor*; SCAB, *S. scabies*.

```

ParASTR      MDDTPIAHTAHLGVHALGRAGEGLRPEQTRVMVAVANQKGGVGKTTTTVNLAASLALHGN
ParASCAB     MDDTPIGRAAQLAVEALGRAGEGLRPEQTRVMVAVANQKGGVGKTTTTVNLAASLALHGA
ParASCO      MDDTPIGRAAQLAVEALGRAGEGLRPEQTRVMVAVANQKGGVGKTTTTVNLAASLALHGA
ParASAV      MDDTPIGRAAQLAVEALGRAGEGLRPEQTRVMVAVANQKGGVGKTTTTVNLAASLALHGG
ParASGR      MDDTPIGRAAQLAVEALGRAGEGLRPRDRTRVMVAVANQKGGVGKTTTTVNLAASLALHGA
ParASCLAV    MDDTPIGRAAQMAMEAMGRSRTLPRPVQKRVAVANQKGGVGKTTTTVNLAASLALHGA
ParASVEN     MDDTPIGRAAQLAVEALGRAGEGLRPAQTRVMVAVANQKGGVGKTTTTVNLAASLALHGA
*****.:*:.:.*:*. * * * * :.*****

ParASTR      RVLVIDLDPQGNASTALGIDHHADEVPSIYDVLVDSRPLSEVVQVPDVEGLFCAPATIDL
ParASCAB     RVLVIDLDPQGNASTALGIDHHADEVPSIYDVLIDSKPLAEVVKPVADVEGLFCAPATIDL
ParASCO      RVLVVDLDPQGNASTALGIDHHADEVPSIYDVLVESRPLSEVVQVPDVEGLFCAPATIDL
ParASAV      RVLVIDLDPQGNASTALGIDHHADEVPSIYDVLIDSKPLSEVVQVPDVEGLFCAPATIDL
ParASGR      RVLVVDLDPQGNASTALGIDHHADEVPSIYDVLVESRPLSEVVQVPDVEGLFCAPATIDL
ParASCLAV    RVLVIDLDPQGNASTALGIDHHADEVPSIYDVLVESKPLAEVVKPVADVEGLFCAPATIDL
ParASVEN     RVLVIDLDPQGNASTALGIDHHADEVPSIYDVLVDSKPLSEVVQVPDVEGLFCAPATIDL
****:*****:*****:.*:*. * * * * * * * * * * * * * * * * * * * * * * * *

ParASTR      AGAEIELVSLVARESRLERAIKSYEQPLDYVLIDCPPSLGLLTVNALVAGAEVLIPIQCE
ParASCAB     AGAEIELVSLVARESRLQRAIQAYEQPLDYILIDCPPSLGLLTVNAMVAGQEVLIPIQCE
ParASCO      AGAEIELVSLVARESRLQRAITAYEQPLDYILIDCPPSLGLLTVNALVAGQEVLIPIQCE
ParASAV      AGAEIELVSLVARESRLERAIQAYEQPLDYILIDCPPSLGLLTVNALVAGAEVLIPIQCE
ParASGR      AGAEIELVSLVARESRLQRAIQAYEQPLDYILIDCPPSLGLLTVNALVAGAEVLIPIQCE
ParASCLAV    AGAEIELVSLVARESRLQRAIQAYEQPLDYILIDCPPSLGLLTVNAMVAGAEVLIPIQCE
ParASVEN     AGAEIELVSLVARESRLQRAIQAYEQPLDYILIDCPPSLGLLTVNAMVAGAEVLIPIQCE
*****:*** :*****:*****:*** * * * * * * * * * * * * * * * * * *

ParASTR      YYALEGLGQLLRNVELVRGHLNPAHVSTILLTMYDGRTRLASQVAEEVRSHFGEVLRT
ParASCAB     YYALEGLGQLLRNVDLVRGHLNPLHVSTILLTMYDGRTRLASQVADEVTRTHFGEEVLRT
ParASCO      YYALEGLGQLLRNVDLVRGHLNPTLHVSTILLTMYDGRTRLASQVADEVRSHFGEVLRT
ParASAV      YYALEGLGQLLRNVDLVRGHLNPTLHVSTILLTMYDGRTRLASQVADEVRSHFGEVLRT
ParASGR      YYALEGLGQLLRNVDLVRGHLNPDHVSTILLTMYDGRTRLASQVAEEVRSHFGEVLRT
ParASCLAV    YYALEGLGQLLRNVDLVRGHLNPTLHVSTILLTMYDGRTRLASQVAEEVRSHFGEVLRT
ParASVEN     YYALEGLGQLLRNVDLVRGHLNPAHVSTILLTMYDGRTRLASQVADEVTRTHFAEVLRT
*****:***** * * * * * * * * * * * * * * * * * * * * * * * *

ParASTR      SIPRSVRRISEAPSYGQTVLTYDPGSSGALSYLEAAREIALRGVGIHYEAHQHQAAPHEQ
ParASCAB     SIPRSVRRISEAPSYGQTVLTYDPGSSGALSYLEAAREIALKGVGVYDPTQAHIGAQNNP
ParASCO      SIPRSVRRISEAPSYGQTVLTYDPGSSGALSYLEAAREIALKGVGVYDATHAHLGAQNDP
ParASAV      SIPRSVRRISEAPSYGQTVLTYDPGSSGALSYLEAAREIALRGVGVAYDAQHAHLGAENEQ
ParASGR      SIPRSVRRISEAPSYGQTVLTYDPGSSGALSYLEAAREIALRGVGVHYEAQHAHTSSQNSQ
ParASCLAV    SIPRSVRRISEAPSYGQTVLTYDPGSSGALSYLEAAREIALRGVGVHYDPQHHAHMGHQNSQ
ParASVEN     SIPRSVRRISEAPSYGQTVLTYDPGSSGALSYLEAAREIALRGVAVHYDPQHHAHVQQNNQ
*****:***:*****:*. : * : : . . .

ParASTR      QNMAEGMQ
ParASCAB     S-VVEGVQ
ParASCO      S-MVEGTQ
ParASAV      S-MVEGIQ
ParASGR      QNVSEGMQ
ParASCLAV    RNISEGIQ
ParASVEN     RNMSEGIQ
: * * * *

```

**Figure 2.3. Multiple sequence alignment of ParA homologs among different**

***Streptomyces* species.** Amino acid sequences of *Streptomyces* ParA homologs were aligned using ClustalW2. ParA has a 22 amino acid extension at the very end of C-terminus compared to ParH. The composition of the additional sequence in ParA is variable amongst other *Streptomyces*, which are shown in bold characters for *S. coelicolor*. An asterisk (\*) indicates a conserved residue, colon (:) indicates conservation between groups of strongly similar properties, period (.) indicates conservation between groups of weakly similar properties. Species abbreviations: SGR, *S. griseus*; SCLAV, *S. clavuligerus*; SVEN, *S. venezuelae*; SAV, *S. avermitilis*; SCO, *S. coelicolor*; SCAB, *S. scabies*; STR, *S. triostinicus*.

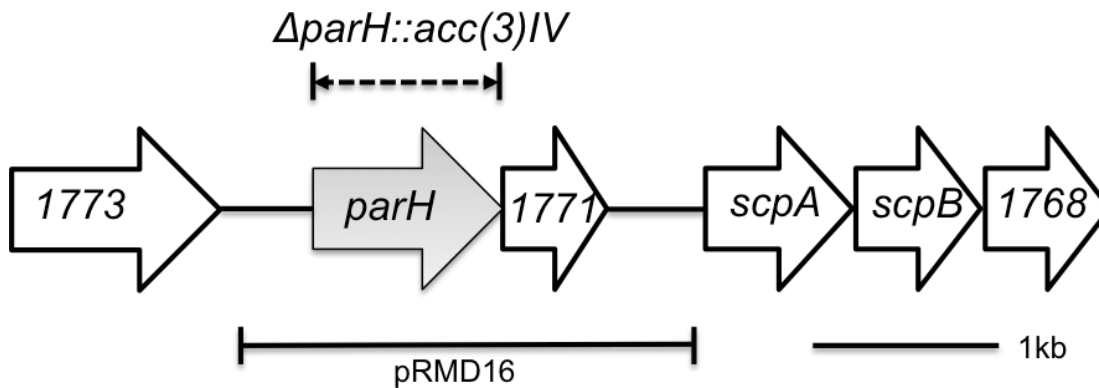


**Figure 2.4. Diagram of the gene organization at the *parH* region of *S. coelicolor* chromosome.** *sco1772* (*parH*) encodes a *parA*-like protein. For mutagenic plasmid pRMD12, the region of *parH* deleted and replaced with an apramycin-resistance gene is shown (dashed arrow). Complementation plasmid pRMD16 is shown in bracketed line. *sco1771* encodes a hypothetical protein, which is conserved in location and sequence among other *Streptomyces*. *scpA* and *scpB* (segregation and condensation proteins) gene products associate with the segregation protein SMC. *sco1768* encodes putative pseudouridine synthase. *sco1773* encodes a developmentally expressed L-alanine dehydrogenase.



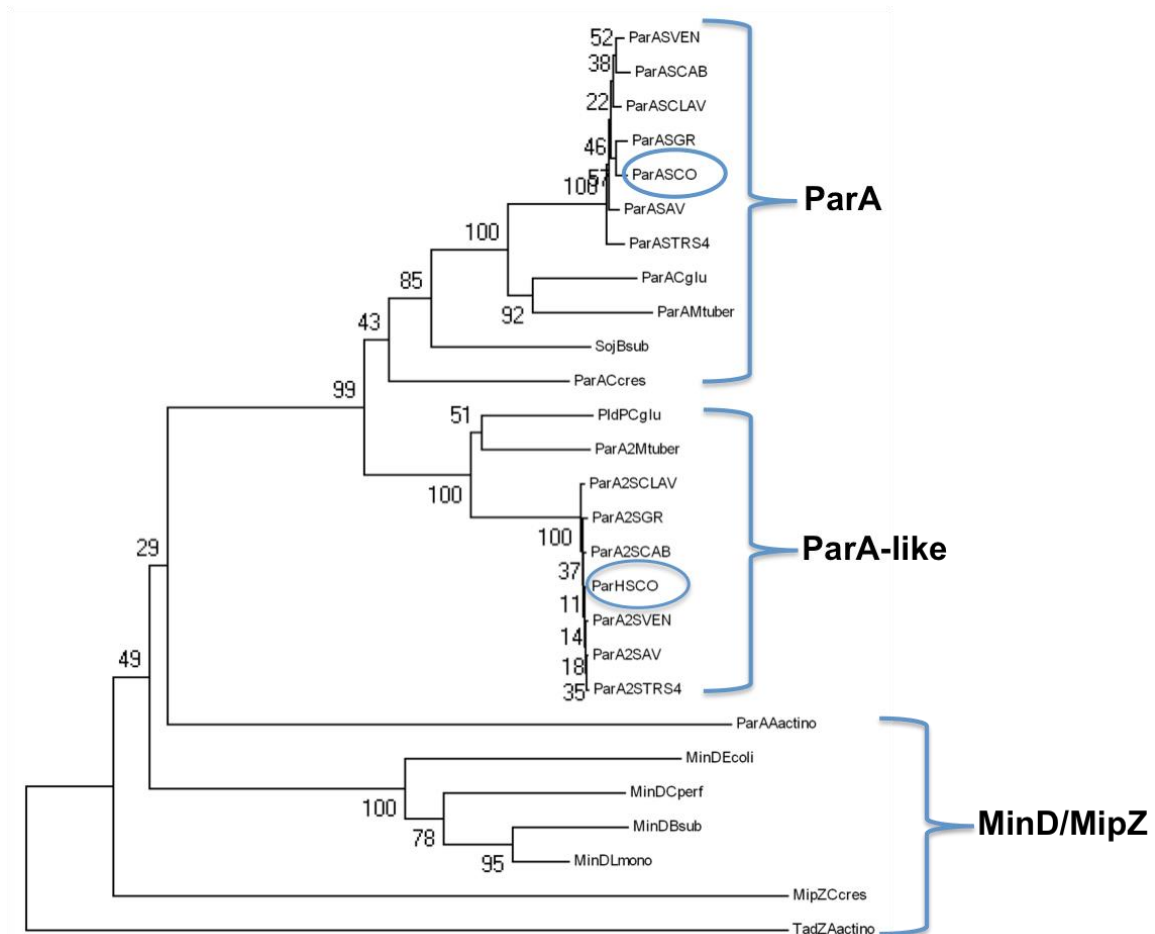


**Figure 2.5. Phylogenetic analysis of ParA and ParA-like protein sequences.**

A phylogenetic neighbor-joining tree based on the ClustalW2 alignment was created using MEGA 5.2.1 phylogeny program for 27 ParA and ParA-like proteins. *S. coelicolor* proteins are denoted as blue circles. MinD proteins (relative deviant Walker A proteins required for cell division) form a separate family according to their sequence similarity and their functions (spatial regulation of cell division) in the cell. Phylogenetic tree reveals a connection between two groups of ParA and ParA-like proteins. The *Actinobacteria*

have two ParA proteins. Strain abbreviations: SCO, *S. coelicolor*; SAV, *S. avermitilis*; SGR, *S. griseus*; SCAB, *S. scabies*; SCLAV, *S. clavuligerus*; STRS4, *S. triostinicus*; SVEN, *S. venezuelae*; Cglu, *C. glutamicum*; Aactino, *A. actinomycetemcomitans*; Bsub, *B. subtilis*; Cperf, *Clostridium perfringens*; Ccres, *Caulobacter crescentus*; *E. coli*, *Escherichia coli*; Lmono, *Listeria monocytogenes*; Mtuber, *Mycobacterium tuberculosis*.

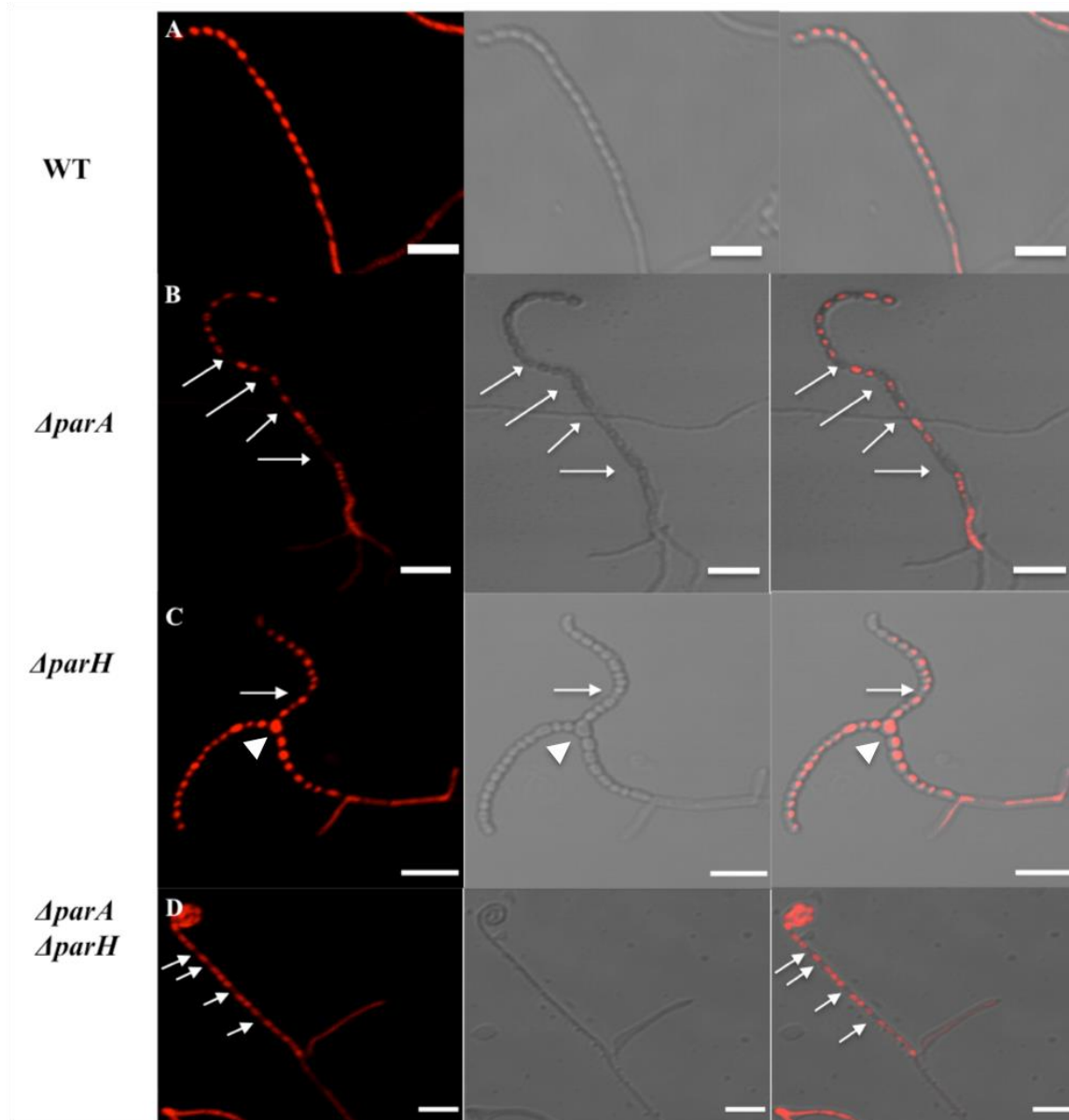


**Figure 2.6. Developmental segregation phenotypes of a WT, *parA*, *parH*, or *parA parH* mutants.** Coverslips, inoculated and hyphae grown for 3-4 days at 30°C on MS agar, were fixed and stained with propidium iodide before image acquisition by confocal microscopy. Left panels are fluorescence, middle panels are DIC, and right panels are merged images. Strains: WT (M145), J3310 ( $\Delta parA$ ), MH5 ( $\Delta parH$ ), MH6 ( $\Delta parA$

$\Delta parH$ ) are shown from top to bottom. Arrows point out anucleate cells. Branching spore chain is occasionally seen in *parH*-null mutant (arrow head). Scale bars are 5  $\mu$ m.

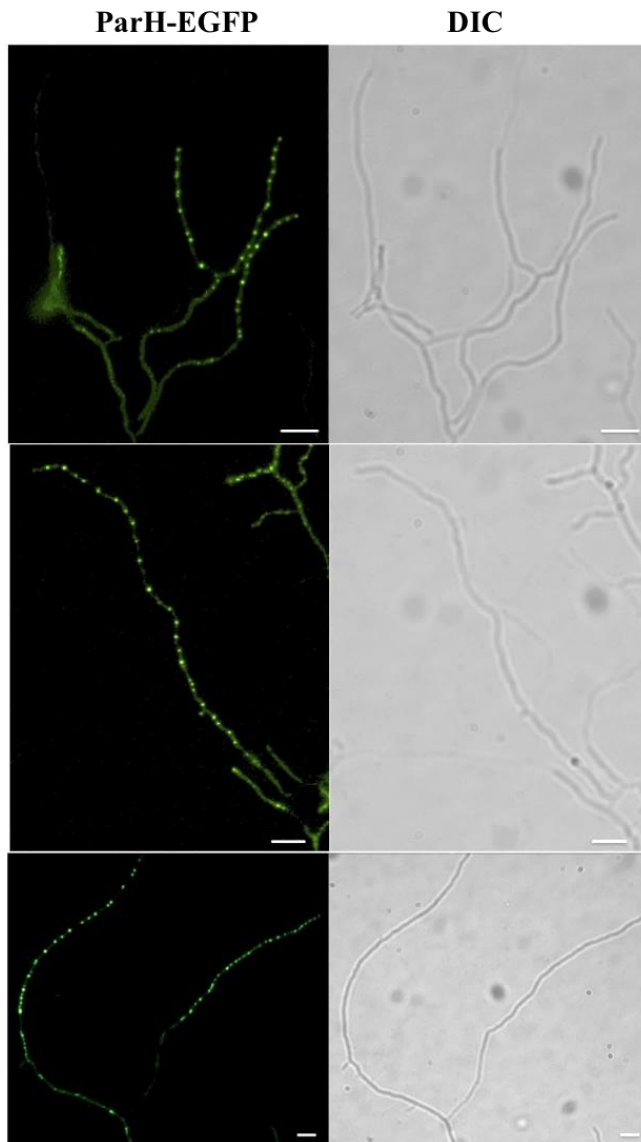


**Figure 2.7. ParH-EGFP localization in predivisive aerial filaments.** Coverslips were inoculated with strain RMD30 (*parH-egfp*) and grown for 3-4 days on MS agar. Images were taken with Nikon Eclipse Ni-U Epi-fluorescent microscope. ParH-EGFP and DIC images are shown in left and right panels, respectively. ParH-EGFP localizes as evenly spaced intervals in predivisive aerial filaments. Scale bar is 5 $\mu$ m.

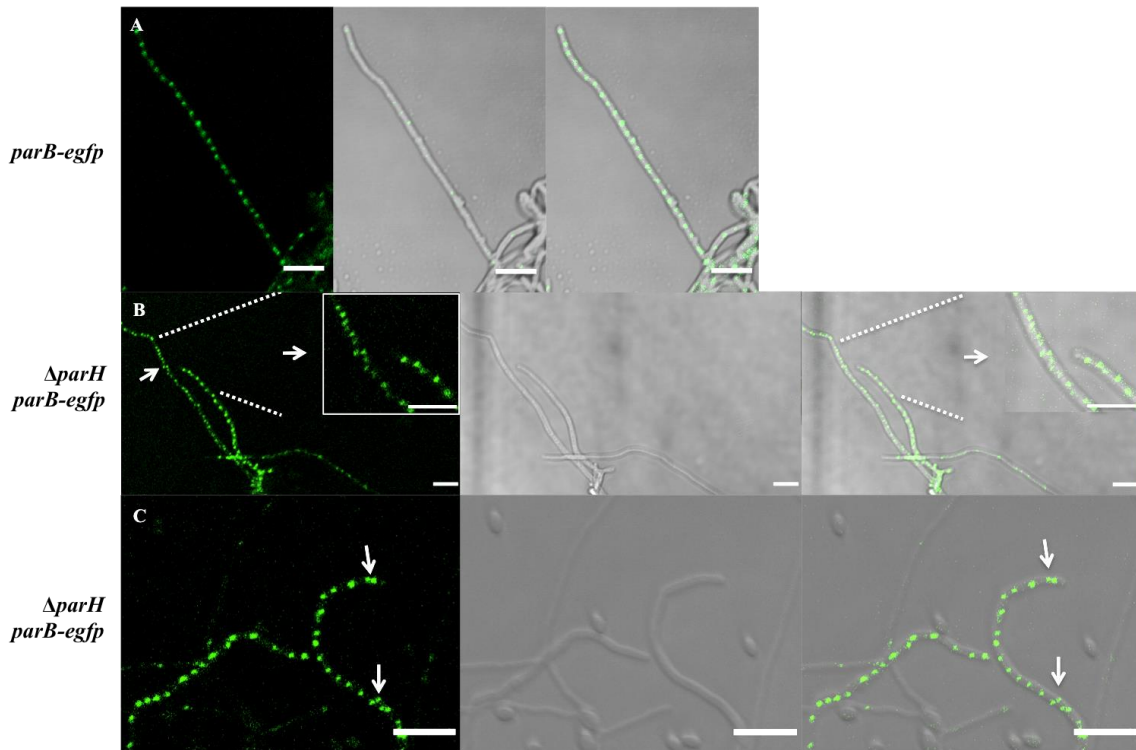
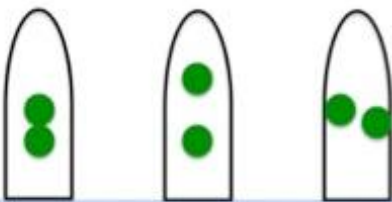
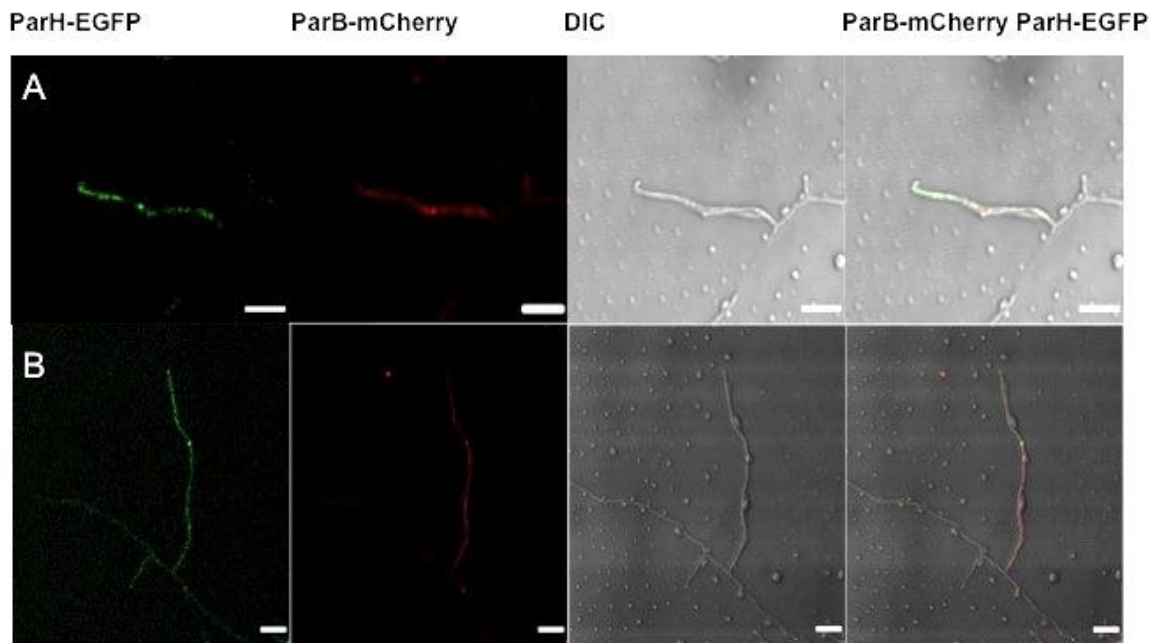


**Figure 2.8. Localization of wildtype ParB-EGFP and *parH*-null strains.** Coverslips were inoculated with strain ParB-EGFP (J3310) or  $\Delta parH::acc(3)IV parB-egfp$  (RMD29) and grown for 3-4 days on MS agar, fixed with 100% methanol and mounted for confocal microscopy. Arrows indicate the disrupted ParB-EGFP localization. The areas indicated with dashed lines in panel B are showing the enlarged part of that aerial filament that has the disrupted ParB-EGFP localization. In each pair, left panels are the fluorescence images, mid panels are DIC picture, and right panels are merged images of the aerial filaments. (A) Images of *parB-egfp* (J3310) showing evenly distributed ParB-EGFP localization. (B-C) Images of  $\Delta parH parB-egfp$  (RMD30) showing disrupted ParB-EGFP localization. Scale bar is 5 $\mu$ m.

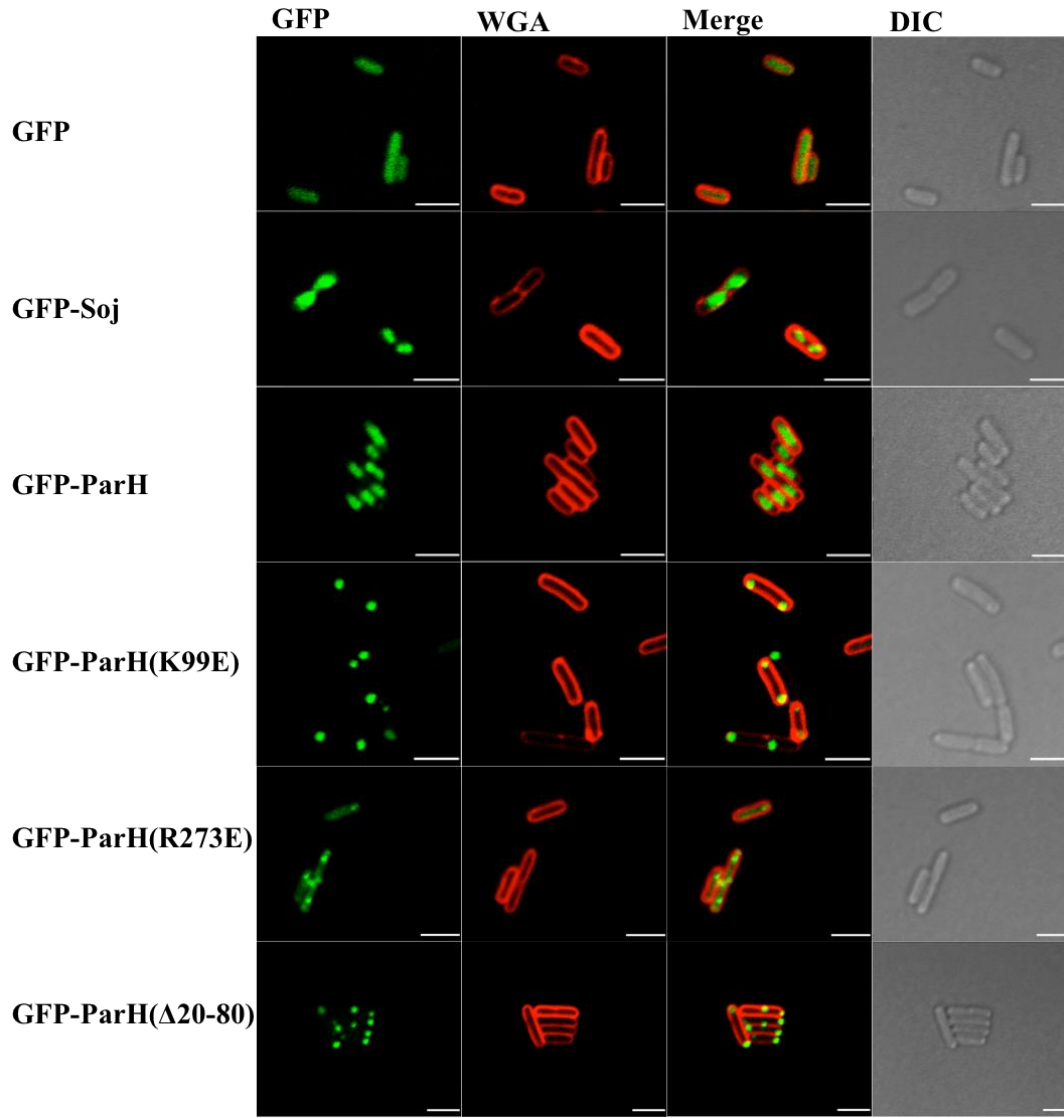


	polar	midcell	lateral	Average foci distance	Total # of foci
WT	3 (1.2%)	247 (98.8%)	0 (0%)	1.13 $\mu\text{m}$	250 (100%)
$\Delta\text{parH}$	7 (2.7%)	245(94.2%)	8 (3.1%)	1.01 $\mu\text{m}$	260 (100%)

**Table 2.5. Analysis of ParB-EGFP localization in wild type and *parH* null mutant strains.** The average ParB-EGFP interfocal distance was found to be approximately 1  $\mu\text{m}$  apart in the wild type strain (J3310) coinciding with the appropriate length of a spore compartment. The total percentage of disrupted ParB-EGFP in *parH* null strain (RMD29) was found to be approximately 6% compared to 1% of the wild type strain (p=0.0052, chi-square test).



**Figure 2.9. Localization of ParB-mCherry and ParH-EGFP fusion proteins in aerial hyphae.** Coverslips were inoculated with a strain expressing both ParB-mCherry and ParH-EGFP (MH4) and hyphae grown for 3-4 days on MS agar, fixed with 100% methanol and observed by confocal microscopy. Two fields are shown (A and B). In panels A and B from left to right: ParH-EGFP, ParB-mCherry, DIC and merged images of the aerial filaments. Scale bar is 5  $\mu$ m.







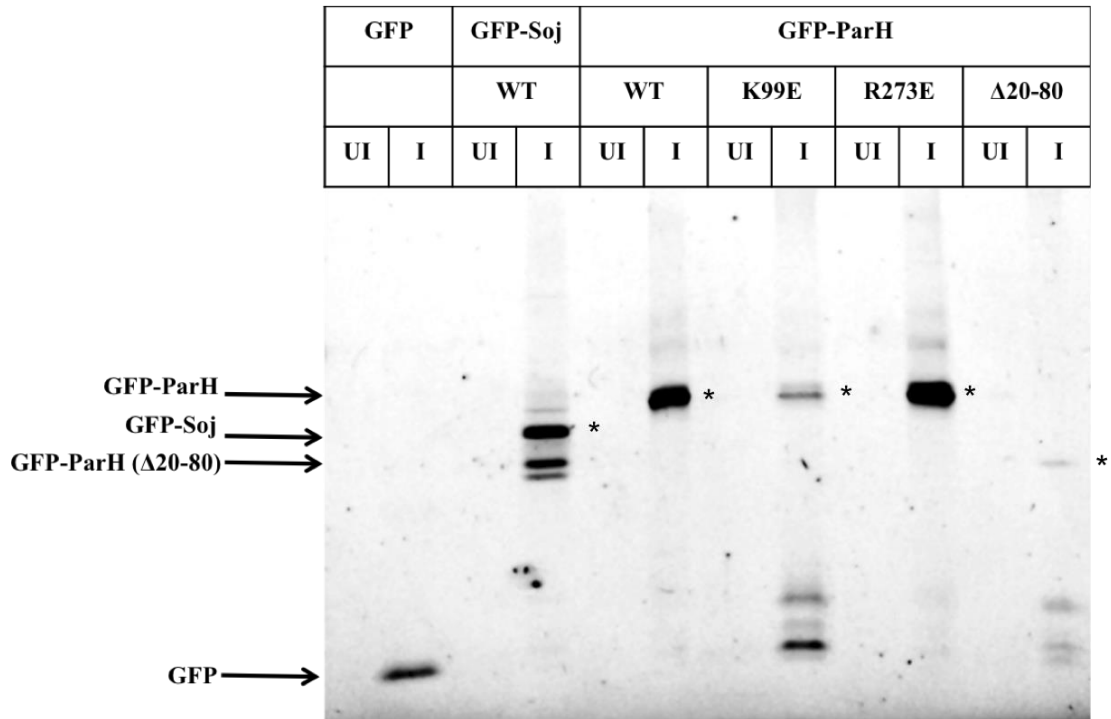






**Figure 2.10. Scanning laser confocal microscope images of *E. coli* strains expressing Soj and ParH fusion proteins.** Expressing GFP fusions after 45 mins of induction with IPTG at 37°C and stained cell wall with WGA Alexa Fluor 647. Derivatives of *E. coli* strain pSEB181 containing plasmids expressing from top to bottom: GFP, GFP-SoJ (*B. subtilis* control), GFP-ParH<sup>+</sup>, GFP-ParH(K99E), GFP-ParH(R273E), and GFP-ParH(Δ20-80). Panels from left to right are GFP, WGA, merge, and DIC images. Punctuate localization of GFP-Soj and GFP-ParH occurs over the nucleoid. Scale bar is 3 μm.











**Figure 2.11. SDS-PAGE analysis of GFP-Soj and GFP-ParH fusion expression in *E. coli*.** Plasmids containing derivatives of *E. coli* strain pSEB181 expressing GFP, GFP-Soj (*B. subtilis* control), GFP-ParH<sup>+</sup>, GFP-ParH(K99E), GFP-ParH(R273E), and GFP-ParH(Δ20-80) were induced with IPTG for 45 minutes. Whole cell protein extracts were fractionated by 12% SDS-PAGE and GFP fluorescence was visualized by Li-cor Odyssey Fc imaging system. Lane 1 (UI), 2 (I) GFP; lane 3 (UI), 4 (I) GFP-Soj; Lane 5 (UI), 6 (I) GFP-ParH<sup>+</sup>; lane 7 (UI), 8 (I) GFP-ParH(K99E); Lane 9 (UI), 10 (I) GFP-ParH(R273E); Lane 11(UI), 12(I) GFP-ParH(Δ20-80). Labelled arrows point to full length proteins (\*). (UI: Uninduced, I: Induced).

T18	ParH	ParA	ParB	ParJ	SMC	ScpA	ScpB	SlzA	(+) control	(-) control
T25 ParH										
interaction	+	-	+	-	-	-	-	+	+	-

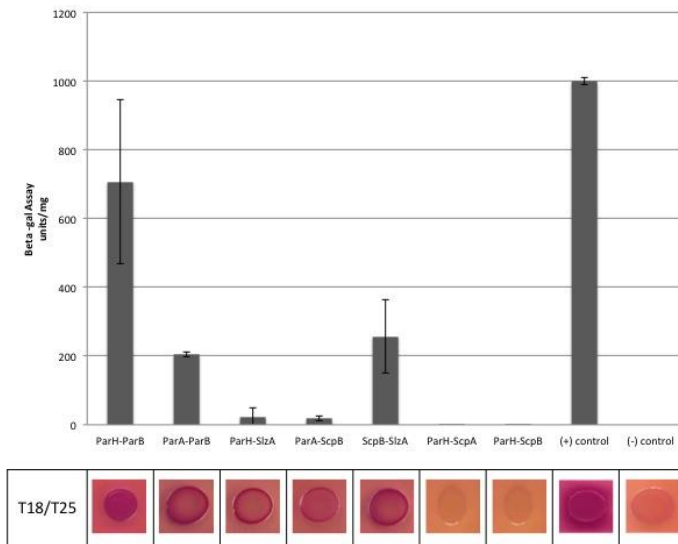
**Figure 2.12. Bacterial two-hybrid analysis of interaction between ParH and known segregation proteins.** Stationary phase *E. coli* cultures containing pairs of two-hybrid vectors were spotted (5  $\mu$ l) on MacConkey maltose or LB-X Gal agar supplemented with 0.5 mM IPTG, ampicillin, and kanamycin and incubated overnight at 30°C. The phenotypes of representative growth spots are pictured. The red/pink (MacConkey) and blue pigment (LB-X Gal) of the spots indicates a positive protein-protein interaction and pale spots indicates no interaction.

T18	ParH	ParH( $\Delta$ 20-80)	ParH(K99E)	ParH(R273E)	(+) control	(-) control
T25 ParB						
interaction	+	-	-	+	+	-

**Figure 2.13. Bacterial two-hybrid analysis of ParH and ParH variants with ParB.**

Stationary phase *E. coli* cultures containing pairs of two-hybrid vectors were spotted (5  $\mu$ l) on MacConkey maltose or LB-X Gal agar supplemented with 0.5 mM IPTG, ampicillin, and kanamycin and incubated overnight at 30°C. The phenotypes of representative growth spots are pictured. The red/pink (MacConkey) and blue pigment (LB-X Gal) of the spots indicates a positive protein-protein interaction and pale spots indicates no interaction.

**A**



**B**

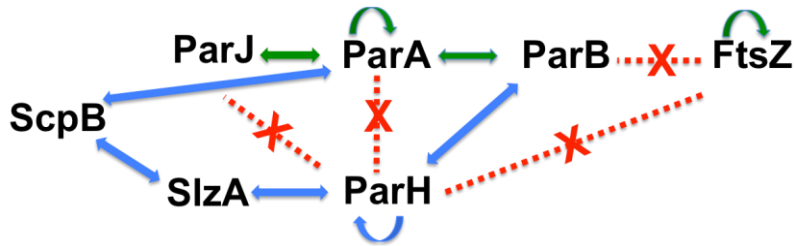


**Figure 2.14 Summary of bacterial two hybrid protein-protein interactions identified**

**for *S. coelicolor* genome segregation proteins.** A) Graph shows the quantitation of beta-

galactosidase enzymatic activity for selected positive interactions. Strains were grown in

LB liquid with 0.5 mM IPTG. Each bar represents the average of the three different

independent liquid culture samples analyzed individually with experimental errors

indicated. B) Blue arrows indicate the interactions that are found using a bacterial-two

hybrid system that were determined in this study. Green arrows indicate interactions that

were previously published (Ditkowski *et al.*, 2010; Jakimowicz *et al.*, 2007). Red dashed

lines indicate no evidence for interactions as determined in this study.

### **CHAPTER 3: *STREPTOMYCES COELICOLOR* HAAA INTERACTS WITH PARA AND PARH AND IS A NOVEL SEGREGATION COMPONENT**

#### **ABSTRACT**

Proper localization and synchronous segregation of the chromosomes during simultaneous cell division within aerial hyphae is a prerequisite for the survival of the next generation in *S. coelicolor*. In this study, I identified a novel partitioning protein that interacts with ParA and ParH. HaaA (ParH and ParA Associated protein A) is required for proper chromosome segregation. As in many other bacterial species, *S. coelicolor* has an active partitioning system. There are four known *trans*-acting proteins (ParA, ParB, ParJ and Scy) and *cis*-acting centromere-like sites (*parS*). In Chapter 2, I showed that ParH, a ParA-like protein and novel interaction partner of ParB, is also part of the partitioning system and appears to play a role in ParB-*parS* nucleoprotein complex positioning. A random chromosomal library was constructed in a bacterial two-hybrid plasmid and screening using ParH as bait revealed a novel interaction partner HaaA. Surprisingly, HaaA is one of the 24 signature proteins of the Actinomycetes that are not found in other bacterial lineages. A bacterial two-hybrid system was used to investigate HaaA protein interactions with known partitioning proteins. I found that HaaA interacts with itself and interaction between ParH and ParA was through the C-terminal unstructured region. Interaction between HaaA and ParA and ParA-like proteins was conserved in other Actinomycetes, such as *S. venezuelae*, *C. glutamicum* (PldP) and *M. smegmatis*. There was no evidence for interaction with other segregation proteins. In addition, a *haaA* insertion-deletion mutant strain revealed that loss of HaaA affected

chromosome segregation and HaaA-EGFP localizes within spores of the mature spore chains.

## INTRODUCTION

The proper distribution of chromosomes into daughter cells during cell division is an important part of the bacterial cell cycle. Chromosome organization and segregation after DNA replication and before cell division is mediated by an active partitioning mechanism, which is still quite elusive. *S. coelicolor* is an advantageous organism for studying chromosome segregation since all of the tested segregation mutants are viable and double or triple mutants are not synthetic lethal or synthetic sick (Dedrick *et al.*, 2009).

As in many other bacterial species, *S. coelicolor* has an active partitioning system. There are 5 known components of developmental chromosome segregation: the *cis*-acting centromere-like sites (*parS*) and 4 characterized *trans*-acting proteins. ParA and ParB are conserved among other species, and Actinobacterial signature protein ParJ and intermediate filament protein Scy are unique for *Streptomyces*. *parA* encodes a Walker-type ATPase that is required for efficient DNA segregation and proper placement of the ParB-*parS* nucleoprotein complexes. A paralog of ParA is encoded by the *S. coelicolor* genome, SCO1772 (named ParH). *parH* encodes a ParA-like ATPase protein that has 45% identical residues to ParA. Compared to ParA, ParH contains an N-terminal extension with unusual amino acid composition. In Chapter 2, I identified ParH as a novel interaction partner of *S. coelicolor* ParB. However, the Walker A motif K99E substitution in ParH and N-terminal extension deletion in ParH impaired interaction between them, as judged by the bacterial two-hybrid analyses. Also, no evidence has been found that ParA and ParH can form a heterodimer. Coinciding with the localization of ParB, ParH localizes as evenly-spaced foci in the aerial filaments of *S. coelicolor*. In

aerial hyphae of the  $\Delta parH$  mutant, anucleate spores are approximately 4% more than in wild type. In addition, the *parH* mutant appears to be unable to properly organize the *oriC* regions, because the loss of ParH appears to result in abnormal positioning of a fraction of ParB-EGFP foci in aerial hyphae.

The goal of this study was to search for novel ParH interacting proteins and to better understand how the partitioning system works in development-associated chromosome segregation in a filamentous bacterium. Here, by screening a bacterial two-hybrid library, I identified HaaA (ParH and ParA Associated protein A) as a novel interaction partner of both ParH and ParA. Remarkably, HaaA is one of the 24 signature proteins of the Actinomycetes, whose members include many species of medical and biotechnological importance (Gao *et al.*, 2009). In addition, a bacterial two-hybrid system was used to investigate HaaA protein-protein interactions with known segregation and condensation proteins. No other interactions were identified for tested proteins. However, I found that HaaA interaction between ParA and ParA-like paralogs was conserved in other Actinomycetes: *S. venezuelae*, *C. glutamicum* and *M. smegmatis*. In addition, a *haaA* insertion-deletion mutation mildly affected chromosome segregation (6% anucleate spores) and showed delayed aerial mycelium formation and HaaA-EGFP translational fusion localizes within the spores of the mature spore chains.



## **MATERIALS AND METHODS**

### **Bacterial strains, media, and growth conditions**

*E. coli* and *S. coelicolor* strains used in this study are listed in Table 3.1 and Table 3.2, respectively. *E. coli* strains were grown in either LB, SOB, or SOC media (Sambrook *et al.*, 1989) and were supplemented with final concentrations of ampicillin (100 µg ml<sup>-1</sup>), apramycin (50 µg ml<sup>-1</sup>), carbenicillin (100 µg ml<sup>-1</sup>), chloramphenicol (25 µg ml<sup>-1</sup>), or kanamycin (50 µg ml<sup>-1</sup>), when appropriate. TG1 and TOP10 were used for basic plasmid propagation. *E. coli* strains were grown at 37°C, except BW25113/pIJ790, which were grown at 30°C to ensure propagation of the temperature sensitive plasmid.

*S. coelicolor* strains were grown at 30°C in ISP2 or YEME liquid medium or on glucose (1%) minimal medium (MM), mannitol (0.5%) minimal medium (MM), R2YE, or soy flour mannitol (SFM) agar (Hopwood *et al.*, 1985; Kieser *et al.*, 2000) and were supplemented with the final concentration of the following antibiotics when appropriate: apramycin (25 µg ml<sup>-1</sup>), kanamycin (50 µg ml<sup>-1</sup>), nalidixic acid (20 µg ml<sup>-1</sup>), or spectinomycin (50 µg ml<sup>-1</sup>).

### **Plasmids and general DNA techniques**

Cosmids and plasmids used in this study are listed in Table 3.3. Wizard Genomic DNA Purification Kit (Promega) was used for *S. coelicolor* total DNA preparations. Redirect technology (Gust *et al.*, 2004) was used for λ RED-mediated recombination using mutagenic linear DNA cassettes in *E. coli*. Standard techniques were used for plasmid purification, creation of electrocompetent cells, and transformation (Sambrook *et al.*, 1989). DNA restriction and modification enzymes (New England Biolabs); *Taq* (New England Biolabs) and *Pfx* (Invitrogen) DNA polymerases; plasmid purification and DNA

cleanup kits (Qiagen and Zymo Research Corporation) were used according to the manufacturers' instructions.

### **Creating plasmids containing *haaA*, *parA*, *parB*, and *parH* for use in a bacterial two-hybrid assay**

Plasmids were created according to the previously described protocol (Karimova *et al.*, 2000). Primers listed in Table 3.4 for the genes of interest were used to amplify and add flanking *KpnI* restriction sites to the complete coding regions of *haaA*, *parH*, *parA*, and *parB* of *S. coelicolor* and *S. venezuelae*. Cosmid St9B10 was used as a template to amplify *S. coelicolor haaA* (<http://strepdb.streptomyces.org.uk>). Cosmids Sv-3-B02, P12-H20, and 2H19 were used as templates to amplify *S. venezuelae haaA*, *parA*, *parB*, and *parH*, respectively (<http://strepdb.streptomyces.org.uk>). Genomic DNA of *M. smegmatis* and *C. glutamicum* was kindly provided from Dr. D. Jakimovicz (University of Wroclaw, Wroclaw, Poland) and Dr. M. Brahmkamp (Ludwig-Maximilians University, Munich, Germany) and used as template for amplifying and adding *KpnI* restriction sites to *haaA*, *parH*, and *parA*.

The PCR products were cloned into vector pCR2.1 (Invitrogen), sequenced to verify integrity of the gene, digested with *KpnI* and ligated into *KpnI*-digested and dephosphorylated bacterial-two hybrid vectors pUT18, pUT18C, pKT25, and pKNT25. Restriction enzyme digestion and sequence analysis were used to verify the insert, orientation, and the reading frame of each construct before co-transforming test pairs into the *E. coli* strain BTH101. The visualization of possible protein-protein interactions was performed following manufacturer's protocol with the following modifications. Co-transformants were grown on LB agar containing ampicillin (100 µg ml<sup>-1</sup>), and

kanamycin ( $50 \mu\text{g ml}^{-1}$ ) and incubated overnight at  $37^\circ\text{C}$ . Individual colonies from these plates were picked and patched on MacConkey agar containing 1% maltose, 0.5 mM IPTG, ampicillin ( $100 \mu\text{g ml}^{-1}$ ), and kanamycin ( $50 \mu\text{g ml}^{-1}$ ) and incubated overnight at  $30^\circ\text{C}$ .

The  $\beta$ -galactosidase assays were averaged from single determinations of three independent isolates of each strain (Euromedex).

### **Constructing a genomic library of M145**

To construct a genomic library of M145 chromosome, total DNA was processed according to the protocol of Nybo *et al.* (2010). Eight  $\mu\text{l}$  of genomic DNA ( $150 \text{ ng}/\mu\text{l}$ ) was partially digested with 2  $\mu\text{l}$  of 1:200 dilution of 4  $\text{u}/\mu\text{l}$  of *Bfu*CI for 35-40 minutes at  $37^\circ\text{C}$  and 2.5 to 3.5 kb fragments were size-selected from a 0.9% agarose gel. In the gene fusion library, if the genomic DNA fragment is in the right orientation, there are 3 possible reading frames. To improve chances to find interacting partners of ParH, pKT25 was modified to make both +1 and -1 frameshifts. Using *Xba*I and DNA PolII, or *Pst*I and T4 DNA Pol treated and ligated DNA were called pMH97 (TCTAGCTAGA) and pMH98 (GGGCGGGT), respectively. For the library construction, 2  $\mu\text{l}$  of 2.5 to 3.5 kb size-selected DNA fragments ( $40 \text{ ng}/\mu\text{l}$ ) and 4  $\mu\text{l}$  from the mixture of equal amounts of (2  $\text{ng}/\mu\text{l}$  from each) pKT25 and each modified pKT25 were used for ligation in a 20  $\mu\text{l}$  reaction volume. Ligations were transformed into NEB chemically competent cells by using the high efficiency transformation protocol and plated into LB-Kan plates. Total colony number from the transformation was approximately 29,000. Three ml of LB liquid medium was added into each plate and all colonies were pooled into a 15 ml screw top tube. Cells were harvested and resuspended in 7 ml 50% glycerol and stored at  $-80^\circ\text{C}$  until

needed. A plasmid expressing either ParH-T18 (pMH5) or ParH-T18C (pMH6) was used as a bait (50 ng/μl of each) and library DNA (50 ng/μl) was used as a prey to screen for novel interacting proteins. Approximately 70,000 colonies were screened on LB X-Gal plates and 1,400 suspected colonies were rescreened on McConkey plates to identify 3 positive clones (pMH106, pMH107, pMH108).

### **Isolation of *haaA*-null strain**

An insertion-deletion mutation for *haaA* (*sco5855*) of *S. coelicolor* was created in cosmid St9B10 resulting in pMH101 by using *in vivo E. coli* λ Red-mediated recombination (Gust *et al.*, 2004). Oligonucleotides *haaA*delFwd and *haaA*delRev were used to amplify and add *haaA* homology to an *aac(3)IV* disruption cassette isolated from pIJ733. The mutagenic PCR product was transformed into the *E. coli* strain BW25113/pIJ790/St9B10 to create pMH101. Then pMH101 was introduced into the chromosome of *S. coelicolor* strain M145 via homologous recombination after conjugation from *E. coli*, selecting for apramycin and screening for kanamycin sensitivity. One representative strain was named as MH7 ( $\Delta$ *haaA::aac(3)IV*).

### **Creation of a *haaA* in-frame deletion expressing a $\Delta$ 338-345 variant of HaaA**

A 24 nucleotide in-frame deletion in *haaA* (nucleotide sequence: AGCTGGGACGAGATCGTCTTCGGC), for the codons of 8 amino acids (SWDEIVFG) near the very C-terminus of the HaaA, was constructed [HaaA( $\Delta$ 338-345)]. Oligos HaaAinframedelFwd and HaaAinframedelRev were used to amplify and add *haaA* homology to an *aac(3)IV* disruption cassette isolated from pIJ733. In addition, *Xba*II and *Spe*I recognition sites were included in the primers and inserted flanking the apramycin cassette. The mutagenic PCR product was transformed into the *E. coli* strain

BW25113/pIJ790/St9B10, creating cosmid pMH102. Then, pMH102 was digested with *SpeI* and partially digested with *XbaI* (because there are two *XbaI* restriction cut sites in the backbone of the cosmid) restriction enzymes to remove the disruption cassette and ligated to generate pMH103 containing *haaA*( $\Delta$ 338-345) with a 6 base scar sequence from ligating *SpeI* to *XbaI* (ACTAGA) restriction sites. Then, pMH103 was transformed into TG1 electro competent cells and screened for kanamycin resistant and apramycin sensitive candidates. PCR and sequencing were used to verify the candidate. The amino acid sequence encoded at the deletion junction is RRAAVP|TRRKKQ.

### **Creation of the HaaA-EGFP expressing strain**

A *haaA-egfp* fusion was constructed by using *in vivo E. coli*  $\lambda$  Red-mediated recombination (Gust *et al.*, 2004). Oligonucleotides *haaAegfpFwd* and *haaAegfpRev* were used to amplify and add *haaA* homology to the *egfp-aac(3)IV-oriT* cassette of the cosmid H24-ParB-EGFP (Jakimowicz *et al.*, 2005). The mutagenic PCR product was transformed into the *E. coli* strain BW25113/pIJ790/St9B10 to create, pMH104 (9B10*haaA-egfp*) and fusion junction was verified by sequencing. Cosmid pMH104 was introduced into the native location of the chromosome of *S. coelicolor* strain M145 via homologous recombination after conjugation, selecting for apramycin resistance and screening for kanamycin sensitivity and one representative strain was named as MH8. *haaA-egfp* was verified by PCR and is the only source of HaaA in strain MH8.

### **Construction of a *haaA* genetic complementation plasmid**

To facilitate genetic complementation, the complete intergenic region upstream of *haaA* and *haaA* was amplified as a ~2.5 kb by oligonucleotides *HaaAcompPvuIIFwd* and *HaaAcompPvuIIRRev* and cloned into site-specific integrating plasmid pMS82. The

resulting plasmid, pMH105, was confirmed with both restriction enzyme digestion and sequencing. pMH105 allowed *haaA* and the complete intergenic region of *haaA* to be delivered to *attB*<sub>ΦBT1</sub> for complementation of *haaA* null mutant. *E. coli* donor containing pMH105 was mated with MH7 ( $\Delta$ *haaA::aac(3)IV*) selecting for hygromycin resistance and one representative strain was named MH9.

### **Fluorescence Microscopy**

*S. coelicolor* strains were prepared for microscopy using cover slips that were embedded at a 45° angle in the agar medium and incubated for the indicated lengths of time and fixed with 100% methanol, mounted in 50% glycerol or 50% glycerol containing 0.01% propidium iodide and analyzed using a TCS SP2 Spectral Confocal Microscope System (Leica) with 63X immersion lens and 488- and 543-nm lasers. Volocity Demo program (Perkin Elmer Inc, Version 6.1.1) was used to crop images, optimize contrast, and add scale bars.

## RESULTS

### ParH and ParA interacts with a highly conserved signature protein for

#### Actinomycetes

Characterization of *S. coelicolor* ParH, a ParA homolog, was described in Chapter 2. An identified protein-protein interaction between ParH and ParB, evenly-spaced localization of ParH-EGFP in predivisional aerial filaments and slight segregation defect of a *parH* mutant suggested that ParH was a component of the segregation apparatus. These facts prompted me to search for novel ParH-interacting partners by using a bacterial two-hybrid system to possibly identify a new protein(s) that might be involved in chromosome segregation. Previously, a random library screening was used to identify two novel ParA-interacting proteins, ParJ and Scy (Ditkowski *et al.*, 2013; Ditkowski *et al.*, 2010). To find novel ParH interacting proteins, I followed a protocol by Nybo *et al.* (2010) to construct a genomic library of M145 DNA. Genomic DNA was partially digested with *BfuCI* (GATC) and 2.5 to 3.5 kb fragments were size-selected (see Materials and Methods). In the library, if a genomic DNA fragment is in the right orientation, there are 3 possible reading frames. To improve chances to find interacting partners of ParH, pKT25 was modified and derivatives were made with +1 and -1 frameshifts (pMH97 and pMH98, respectively). For the library construction, 2.5 to 3.5 kb size-selected DNA fragments were ligated with equal amounts of *BamHI*-digested pKT25, pMH97, and pMH98. ParH-T18 (pMH5) and ParH-T18C were used as a bait and library DNA was used as a prey to screen for interacting proteins. Approximately 70,000 colonies were screened for blue colonies on LB X-Gal plates. Because the X-Gal plates had high background, 1,400 suspected colonies were rescreened by patching on

McConkey maltose plates. Two candidates were found potentially expressing T25 fusions interacting with ParH-T18. The plasmids were isolated, retransformed, and rescreened (Figure 3.1). One of the candidates for a potential ParH interacting protein was named pMH106. It contained the entire gene for *sco4928* (adenylate cyclase) cloned in reverse orientation relative to T25 coding region. *sco4928* was not fused to T25 and must be complementing the *cya* mutation in *E. coli*. However, 2 isolated plasmids, pMH107 and pMH108, contained the 3' end of *sco5855* (an ~3.2 kb insert containing 237 bp of the 3' end of *sco5855* at the fusion junction) had the same restriction patterns, fused at the same point and were possible siblings (Figure 3.1). Subsequently, the complete gene of the *sco5855* was amplified and cloned into pKT25 and it was independently confirmed that SCO5855 interacts with ParH, as judged by bacterial two-hybrid system (Figure 3.5).

SCO5855 is a putative DNA binding protein of 352 amino acids and is one of the 24 signature proteins of actinobacterial species (high G+C Gram<sup>+</sup> lineage) that are not found in other bacteria (Gao and Gupta, 2012). Its function is unknown for *S. coelicolor* and its homologs are potential DNA-binding proteins in *Mycobacterium leprae* and *Mycobacterium tuberculosis* and the homolog is listed as an essential gene in *M. tuberculosis* (*Rv0883c*; <http://tuberculist.epfl.ch>). Although the amino acid sequence is not as highly conserved among divergent Actinomycetes, HaaA amino acid sequence is highly conserved among *Streptomyces* species (Figure 3.2 and 3.3, respectively). After finding an interaction between ParH and SCO5855, other partitioning proteins (ParA, ParB, and ParJ) were tested for interaction with SCO5855 in a bacterial two-hybrid system. Interestingly, ParA was found to be another interacting partner of



SCO5855. Since SCO5855 interacted with both ParA and ParH, it was named HaaA (ParH and ParA Associated Protein A). ParA and ParH are paralogs that presumably interact with HaaA by conserved residues. The results showed that HaaA interacts strongly with ParH and ParA, as well as with itself, showing that HaaA forms homodimers in the bacterial two-hybrid system. Possible interactions between HaaA and other known segregation and condensation (ParB, ParJ, SMC, ScpA, ScpB, FtsK) and division proteins (FtsZ) were also tested, but no evidence was found (data not shown).

HaaA is annotated as a putative DNA-binding protein, which has a conserved N-terminal domain (1-169; DUF3071) that encodes a weakly predicted HTH motif (PSIPRED protein structure prediction server) and a disordered C-terminal domain (169-352) (Figure 3.4). Interestingly, the homolog of *haaA* in *S. venezuelae*, Sven5529, was identified as a highly significant WhiA (Bush *et al.*, 2013) and WhiB target gene (M. Bush and M. Buttner, personal communication), which are involved in the regulation of key steps in aerial growth, initiation of cell division, and chromosome segregation (Bush *et al.*, 2013). This developmental control would be consistent with the possible role of HaaA in developmentally-regulated chromosome segregation in *S. coelicolor*.

While the entire amino acid sequence is not highly conserved among the homologs of other Actinomycetes, HaaA homologs have a short highly conserved 8 amino acid sequence near the very end of the disordered C-terminal domain (Figure 3.2). In addition, the original clone from the library screening included only the final 273 nucleotides of the 3' end of the *haaA* gene, which identified this coding sequence as a potential site for protein-protein interaction. To investigate the importance of these 8 conserved residues, recombineering was used to make a *haaA* in-frame deletion that was

expressing  $\Delta 338-345$  variant of HaaA (shown in bold and underlined in Figure 3.2) and cloned into the bacterial two hybrid plasmids (Gust *et al.*, 2004). Even though HaaA( $\Delta 338-345$ ) still interacted with both ParH and ParA in *E. coli*, the intensity of the interactions was reduced significantly compared to wild type HaaA, as judged by the beta-galactosidase activity assays (Figure 3.5). This may suggest that these residues are not the only ParA/ParH interacting region in HaaA. Alternatively, these amino acid residues could be important for HaaA protein stability and formation of HaaA homodimers in *E. coli*.

### **HaaA interactions with ParA and ParA-like proteins are also conserved in other Actinomycetes**

*Streptomyces*, *Corynebacterium*, and *Mycobacterium* represent divergent but well known species of the Actinobacteria for their importance in biotechnology and model organisms for pathogenic bacteria. They share similar chromosome segregation systems and most of the partitioning proteins have homologs in these species (Donovan *et al.*, 2010; Ginda *et al.*, 2013; Maloney *et al.*, 2009; Thanbichler and Shapiro, 2006). HaaA is one of the conserved proteins (a signature protein in Actinomycetes) that has homologs in these organisms. The positive interaction between *S. coelicolor* HaaA with ParH and ParA in bacterial two-hybrid system prompted me to investigate if the interactions between these proteins are also conserved in other Actinomycetes, such as *S. venezuelae*, *C. glutamicum*, and *M. smegmatis*.

Homologs for HaaA, ParH, ParA, and ParB protein interactions were tested in an independent Streptomyce, *S. venezuelae*, which showed similar results with *S. coelicolor*. HaaA interacts with ParA and ParH but interaction between ParA with

ParB was weaker than *S. coelicolor* (Figure 3.6, A). *M. smegmatis* and *C. glutamicum* were tested for HaaA, ParA, and ParH (PldP in *C. glutamicum*) interactions, which also showed similar results with *S. coelicolor*. HaaA interacts with ParA and ParH in both *M. smegmatis* and *C. glutamicum* (Figure 3.6 B-C). In addition to HaaA being an essential protein in *M. tuberculosis*, conserved protein-protein interactions in bacterial two-hybrid system also indicated the conserved potential participation of HaaA in the Actinomycetes genome partitioning mechanism.

### **Deletion of *haaA* affects the formation of aerial hyphae formation and chromosome segregation into spores**

To analyze the function of the putative partitioning protein HaaA in *S. coelicolor*, a deletion-insertion mutation of *haaA* was isolated for *S. coelicolor*. A representative *haaA*-null strain grew normally but had a slight white developmental phenotype on SFM agar as judged by the macroscopic analyses (Figure 3.7). Phase-contrast microscopy revealed that the mutant strain was able to sporulate and there was no significant difference in spore size or shape compared to wild type strain when grown on SFM agar (average spore lengths of 1.03  $\mu\text{m}$  and 1.02  $\mu\text{m}$ , respectively; n=500). However, the *haaA* mutant did not form a robust aerial mycelium when grown on rich solid medium R2YE, which generally slows development and showed delayed aerial mycelium formation on minimal medium containing mannitol as the carbon source (Figure 3.7).

Even though no obvious developmental phenotype was observed with respect to spore size and length, in the white pigmented aerial mycelium on SFM agar, when the nucleic acid was stained with propidium iodide to visualize DNA segregation, the *haaA* mutant revealed a slight segregation defect with a frequency of approximately 6% of

anucleate spores (n=1911). Infrequent branched spore chains were observed as well (Figure 3.8). For comparison, 1.5% anucleate spores (n=1304) and 1.7% anucleate spores (n=1593) were observed for wild type and *haaA* complementation strain (MH9), and no branched spore chains were observed.

### **HaaA-EGFP is located in spore chains, but not in vegetative hyphae**

To determine the *in vivo* localization pattern of HaaA, a HaaA-EGFP translational fusion was created and expressed by replacing *haaA* with *haaA-egfp* at the native location in the chromosome of the wild type strain as the only source of HaaA. The HaaA-EGFP fusion protein appears to be fully functional; the fusion strain was able to sporulate and the spores were similar to wildtype strain M145 in regards to shape and size. Although HaaA interacts with ParA and ParH in bacterial two-hybrid system, the localization pattern of HaaA resembled neither helical filaments as in ParA (Jakimowicz *et al.*, 2007) nor evenly-spaced foci as in ParH (Figure 2.7). Localization of HaaA-EGFP signal was observed notably in mature spores but not in vegetative hyphae or undifferentiated aerial filaments (Figure 3.9). This may indicate that the expression of HaaA-EGFP is developmentally regulated and is consisted with its expression being dependent on WhiA and WhiB.

## DISCUSSION

The proper distribution of chromosomes into daughter cells before cell septation is mediated by an active partitioning mechanism. While recent studies on partitioning proteins and their roles in chromosome segregation provide considerable information, the whole segregation mechanism is still quite elusive. In our previous studies (Chapter 2 and Dedrick, 2009), interaction between ParH and ParB, evenly-spaced localization in predivisive aerial filaments, and slight segregation defects of ParH have encouraged me to think that ParH might have a role in the chromosome segregation of *S. coelicolor*. In this study, I identified a completely novel ParA and ParH interaction partner, SCO5855, which was named HaaA (ParH and ParA Associated Protein A) that is required for efficient sporulation and chromosome segregation in *S. coelicolor*.

Upon screening a random genomic library prepared from wild type strain M145, I found that ParH interacted strongly with the C-terminal end of HaaA, which is one of the 24 signature proteins of actinobacterial species that are not found in other bacteria. Full length HaaA was also screened for possible interactions with other known segregation proteins. Interestingly, bacterial two-hybrid results revealed another novel interaction between HaaA and ParA. Since HaaA interacted strongly with ParH and ParA of *S. coelicolor* in a bacterial two-hybrid system, proteins of several other Actinobacteria were also tested in this system. *S. venezuelae* was tested for HaaA, ParH, ParA, and ParB interactions and showed similar results with *S. coelicolor*. HaaA interacted with ParA and ParH in *S. venezuelae*. Other more distantly related Actinomycete species were also tested. Results were the same for *M. smegmatis* and *C. glutamicum* as in the two tested *Streptomyces* species. In addition, the HaaA homolog in *M. tuberculosis* is annotated as

being essential, which is also another indicator of the importance of this protein for a major pathogen.

It is quite remarkable that HaaA is one of the 24 signature proteins of Actinobacterial species that are not found in other bacterial divisions. Even though HaaA is annotated as a putative DNA-binding protein in *Streptomyces* genome web site, the predicted HTH motif in the conserved N-terminal domain is a weak prediction. On the other hand, HaaA has a predicted disordered C-terminal domain. This disordered domain is also a feature of several cell division proteins such as membrane protein ZipA of *E. coli*, which anchors FtsZ to the cytoplasmic membrane (Pazos *et al.*, 2013). Even though HaaA is unstructured, it is possible that it may transition into a more ordered state or fold into a secondary or tertiary structure when it binds to its targets. In this disordered C-terminus, there are only 8 conserved amino acid residues that are highly conserved among Actinomycetes. A 3' in-frame deletion mutation removing codons for these 8 residues was constructed in *S. coelicolor* to investigate if they were important in ParA and ParH protein-protein interactions. As judged by the bacterial two-hybrid system and  $\beta$ -galactosidase assays, HaaA( $\Delta$ 338-345) still formed dimers and interacted with ParA and ParH, but the intensity of their interaction was significantly reduced. These results indicated that these residues might play a role in other protein-protein interactions or protein folding and stability.

*haaA*-null mutant phenotypic results revealed that it produces 6% anucleate spores (similar to 7% anucleate cells in *smc*-null mutant, Dedrick *et al.*, 2009), and has a slight white macroscopic phenotype on SFM agar. However, it does not form a robust aerial hyphae when grown on rich medium R2YE and shows delayed sporulation on soy

flour mannitol and minimal medium. To see the localization pattern of HaaA during development, *haaA* was replaced by *haaA-egfp* in the native location on the chromosome of the wild type strain. Interestingly, the localization of HaaA-EGFP was observed in mature spores and not in vegetative hyphae or prespore compartments. It was surprising that HaaA-EGFP localization resembled neither filamentous localization of ParA nor evenly-spaced foci ParH-EGFP foci. Remarkably, the homolog of HaaA in *S. venezuelae*, Sven5529, was identified as a highly significant WhiA (Bush *et al.*, 2013) and WhiB target (Bush and Buttner, personal communication) which are involved in the regulation of key steps in aerial growth, initiation of cell division, and chromosome segregation (Bush *et al.*, 2013). My results are consistent and suggest that the expression of HaaA-EGFP is developmentally regulated.

To understand the role of HaaA in chromosome segregation, the localization of ParA and/or ParB foci in a *haaA*-null strain in the aerial filaments could help to understand the role of HaaA of *S. coelicolor*. In addition, constructing double or triple mutants with ParA and ParH could reveal whether the phenotypes are additive. Investigation of when HaaA is expressed in the cells and when it interacts with ParA and ParH could also help to identify its role in chromosome segregation in *S. coelicolor*. It is also worthy to investigate if HaaA binds to DNA by a direct assay. To do this, HaaA could easily be tested in a DNA binding assay in *E. coli* (see Chapter 2 materials and methods). If it is not a non-specific DNA-binding protein, it would also be worthy to investigate the sequence of the HTH motif to see if it is important for HaaA protein-protein interactions.

## REFERENCES

- Ainsa, J. A., Ryding, N. J., Hartley, N., Findlay, K. C., Bruton, C. J., Chater, K. F. (2000). WhiA, a protein of unknown function conserved among gram-positive bacteria, is essential for sporulation in *Streptomyces coelicolor* A3(2). *J Bacteriol*, 182(19), 5470-5478.
- Bentley, S. D., Chater, K. F., Cerdeno-Tarraga, A. M., Challis, G. L., Thomson, N. R., James, K. D., Hopwood, D. A. (2002). Complete genome sequence of the model actinomycete *Streptomyces coelicolor* A3(2). *Nature*, 417(6885), 141-147. doi: 10.1038/417141a.
- Bush, M. J., Bibb, M. J., Chandra, G., Findlay, K. C., Buttner, M. J. (2013). Genes required for aerial growth, cell division, and chromosome segregation are targets of WhiA before sporulation in *Streptomyces venezuelae*. *mBio*, 4(5), e00684-00613. doi: 10.1128/mBio.00684-13.
- Ditkowski, B., Holmes, N., Rydzak, J., Donczew, M., Bezulska, M., Ginda, K., Jakimowicz, D. (2013). Dynamic interplay of ParA with the polarity protein, Scy, coordinates the growth with chromosome segregation in *Streptomyces coelicolor*. *Open Biol*, 3(3), 130006. doi: 10.1098/rsob.130006.
- Ditkowski, B., Troc, P., Ginda, K., Donczew, M., Chater, K. F., Zakrzewska-Czerwinska, J., Jakimowicz, D. (2010). The actinobacterial signature protein ParJ (SCO1662) regulates ParA polymerization and affects chromosome segregation and cell division during *Streptomyces* sporulation. *Mol Microbiol*, 78(6), 1403-1415. doi: 10.1111/j.1365-2958.2010.07409.x.



- Donovan, C., Schwaiger, A., Kramer, R., Bramkamp, M. (2010). Subcellular localization and characterization of the ParAB system from *Corynebacterium glutamicum*. *J Bacteriol*, 192(13), 3441-3451. doi: 10.1128/JB.00214-10.
- Gao, B., Gupta, R. S. (2012). Phylogenetic framework and molecular signatures for the main clades of the phylum Actinobacteria. *Microbiol Mol Biol Rev*, 76(1), 66-112. doi: 10.1128/MMBR.05011-11.
- Ginda, K., Bezulska, M., Ziolkiewicz, M., Dziadek, J., Zakrzewska-Czerwinska, J., Jakimowicz, D. (2013). ParA of *Mycobacterium smegmatis* co-ordinates chromosome segregation with the cell cycle and interacts with the polar growth determinant DivIVA. *Mol Microbiol*, 87(5), 998-1012. doi: 10.1111/mmi.12146.
- Gregory, M.A., Till, R., and Smith, M.C.M. (2003). Integration site for *Streptomyces* phage phiBT1 and development of site-specific integrating vectors. *J Bacteriol*, 185, 5320–5323.
- Gust, B., Chandra, G., Jakimowicz, D., Yuqing, T., Bruton, C. J., Chater, K. F. (2004). Lambda red-mediated genetic manipulation of antibiotic-producing *Streptomyces*. *Adv Appl Microbiol*, 54, 107-128. doi: 10.1016/S0065-2164(04)54004-2.
- Jakimowicz, D., Gust, B., Zakrzewska-Czerwinska, J., Chater, K. F. (2005). Developmental-stage-specific assembly of ParB complexes in *Streptomyces coelicolor* hyphae. *J Bacteriol*, 187(10), 3572-3580. doi:10.1128/JB.187.10.3572-3580.2005.
- Karimova, G., Ullmann, A., Ladant, D. (2000). Bordetella pertussis adenylate cyclase toxin as a tool to analyze molecular interactions in a bacterial two-hybrid system. *Int J Med Microbiol*, 290(4-5), 441-445. doi: 10.1016/S1438-4221(00)80060-0.

- Maloney, E., Madiraju, M., Rajagopalan, M. (2009). Overproduction and localization of *Mycobacterium tuberculosis* ParA and ParB proteins. *Tuberculosis (Edinb)*, 89, Suppl 1, S65-69. doi: 10.1016/S1472-9792(09)70015-0.
- Nybo, S. E., Shepherd, M. D., Bosserman, M. A., Rohr, J. (2010). Unit 10E.3: Genetic manipulation of *Streptomyces* species. *Current Protocols in Microbiology*. doi: 10.1002/9780471729259.mc10e03s19.
- Pazos, M., Natale, P., Vicente, M. (2013). A specific role for the ZipA protein in cell division: stabilization of the FtsZ protein. *J Biol Chem*, 288(5), 3219-26. doi: 10.1074/jbc.M112.434944
- Thanbichler, M., Shapiro, L. (2006). MipZ, a spatial regulator coordinating chromosome segregation with cell division in *Caulobacter*. *Cell*, 126(1), 147-162. doi: 10.1016/j.cell.2006.05.038.

**Table 3.1: *E. coli* strains used in this study**

<b>Strain</b>	<b>Genotype</b>	<b>Reference/Source</b>
BTH101	F <sup>-</sup> <i>cya-99 araD139 galE15 galK16 rpsL1 hsdR2 mcrA1 mcrB1</i>	Euromedex
BW25113	F <sup>-</sup> $\Delta(\textit{araD-araB})567 \Delta\textit{lac Z4787 (::rrnB-3) rph-1}$ $\Delta(\textit{rhaD-rhaB})568 \textit{hsdR514}$	Datsenko and Wanner, 2000
ET12567	F <sup>-</sup> <i>dam-13::Tn9 dcm-6 hsdM hsdR recF143 zjj-201::Tn10 galK2 galT22 ara-14 lacY1 xyl-5 leuB6 thi-1 tonA31 rpsL136 hisG4 tsx-78 mtl-1 glnV44</i>	MacNeil <i>et al.</i> , 1992
TG1	<i>supE thi-1 <math>\Delta(\textit{lac-proAB}) \Delta(\textit{mcrB-hsdSM})5 (rK-mK) / F' \textit{traD36 proAB lacIqZ}\Delta M15</math></i>	Sambrook <i>et al.</i> , 1989
TOP10	F <sup>-</sup> <i>mcrA <math>\Delta(\textit{mrr-hsdRMS-mcrBC}) \Phi 80\textit{lacZ}\Delta M15/\Delta\textit{lacX74 deoR recA1 araD139 \Delta(\textit{araA-leu})697 galU galK}</math></i>	Invitrogen

**Table 3.2: *S. coelicolor* strains used in this study**

<b>Strain</b>	<b>Genotype</b>	<b>Reference/Source</b>
M145	prototroph SCP1 <sup>-</sup> SCP2 <sup>-</sup>	Hopwood <i>et al.</i> , 1985
MH7	$\Delta haaA::aac(3)IV$	This study
MH8	<i>haaA-egfp aac(3)IV</i>	This study
MH9	$\Delta haaA::aac(3)IV / attP_{\Phi BT1}::haaA^{+}hyg$ (MH8/pMH105)	This study

**Table 3.3: Cosmids and plasmids used in this study**

Strain	Description	Reference/Source
St9B10	cosmid source of <i>haaA</i> ( <i>sco5855</i> )	<a href="http://strepdb.streptomyces.org.uk">http://strepdb.streptomyces.org.uk</a>
Sv-3-B02	cosmid source of <i>haaA</i> ( <i>sven5529</i> )	<a href="http://strepdb.streptomyces.org.uk">http://strepdb.streptomyces.org.uk</a>
P12-H20	cosmid source of <i>parAB</i> ( <i>sven3662</i> )	<a href="http://strepdb.streptomyces.org.uk">http://strepdb.streptomyces.org.uk</a>
2H19	cosmid source of <i>parH</i> ( <i>sven1406</i> )	<a href="http://strepdb.streptomyces.org.uk">http://strepdb.streptomyces.org.uk</a>
ParAT18C	<i>parA</i> flanked by <i>XbaI</i> and <i>KpnI</i> cloned into pUT18C	Jakimowicz <i>et al.</i> , 2007
ParAT25	<i>parA</i> flanked by <i>XbaI</i> and <i>KpnI</i> cloned into pKT25	Jakimowicz <i>et al.</i> , 2007
ParBT18C	<i>parB</i> flanked by <i>XbaI</i> and <i>KpnI</i> cloned into pUT18C	Jakimowicz <i>et al.</i> , 2007
ParBT25	<i>parB</i> flanked by <i>XbaI</i> and <i>KpnI</i> cloned into pKT25	Jakimowicz <i>et al.</i> , 2007
ParJT18C	<i>parJ</i> flanked by <i>XbaI</i> and <i>KpnI</i> cloned into pUT18C	Jakimowicz <i>et al.</i> , 2010
ParJT25	<i>parB</i> flanked by <i>XbaI</i> and <i>KpnI</i> cloned into pKT25	Jakimowicz <i>et al.</i> , 2010
pKNT25	Bacterial two-hybrid vector used to create a fusion to the N-terminus of the CyaA T25 polypeptide	Euromedex
pKT25	Bacterial two-hybrid vector used to create a fusion to the C-terminus of the CyaA T25 polypeptide	Euromedex
pMH40	<i>S. coelicolor haaA</i> flanked by <i>KpnI</i> sites cloned into pKT25	This study
pMH41	<i>S. coelicolor haaA</i> flanked by <i>KpnI</i> sites cloned into pKNT25	This study
pMH42	<i>S. coelicolor haaA</i> ( $\Delta$ 338-345) flanked by <i>KpnI</i> sites cloned into pCR2.1 TA cloning vector	This study

pMH43	<i>S. coelicolor haaA</i> ( $\Delta$ 338-345) flanked by <i>KpnI</i> sites cloned into pUT18	This study
pMH44	<i>S. coelicolor haaA</i> ( $\Delta$ 338-345) flanked by <i>KpnI</i> sites cloned into pUT18C	This study
pMH45	<i>S. coelicolor haaA</i> ( $\Delta$ 338-345) flanked by <i>KpnI</i> sites cloned into pKT25	This study
pMH46	<i>S. coelicolor haaA</i> ( $\Delta$ 338-345) flanked by <i>KpnI</i> sites cloned into pKNT25	This study
pMH47	<i>C. glutamicum haaA</i> flanked by <i>KpnI</i> sites cloned into pCR2.1 TA cloning vector	This study
pMH48	<i>C. glutamicum haaA</i> flanked by <i>KpnI</i> sites cloned into pUT18	This study
pMH49	<i>C. glutamicum haaA</i> flanked by <i>KpnI</i> sites cloned into pUT18C	This study
pMH50	<i>C. glutamicum haaA</i> flanked by <i>KpnI</i> sites cloned into pKT25	This study
pMH51	<i>C. glutamicum haaA</i> flanked by <i>KpnI</i> sites cloned into pKNT25	This study
pMH52	<i>C. glutamicum parA</i> flanked by <i>KpnI</i> sites cloned into pCR2.1 TA cloning vector	This study
pMH53	<i>C. glutamicum parA</i> flanked by <i>KpnI</i> sites cloned into pUT18	This study
pMH54	<i>C. glutamicum parA</i> flanked by <i>KpnI</i> sites cloned into pUT18C	This study
pMH55	<i>C. glutamicum parA</i> flanked by <i>KpnI</i> sites cloned into pKT25	This study
pMH56	<i>C. glutamicum parA</i> flanked by <i>KpnI</i> sites cloned into pKNT25	This study
pMH57	<i>C. glutamicum parH</i> flanked by <i>KpnI</i> sites cloned into pCR2.1 TA cloning vector	This study
pMH58	<i>C. glutamicum parH</i> flanked by <i>KpnI</i> sites cloned into pUT18	This study
pMH59	<i>C. glutamicum parH</i> flanked by <i>KpnI</i> sites cloned into pUT18C	This study

pMH60	<i>C. glutamicum parH</i> flanked by <i>KpnI</i> sites cloned into pKT25	This study
pMH61	<i>C. glutamicum parH</i> flanked by <i>KpnI</i> sites cloned into pKNT25	This study
pMH62	<i>M. smegmatis haaA</i> flanked by <i>KpnI</i> sites cloned into pCR2.1 TA cloning vector	This study
pMH63	<i>M. smegmatis haaA</i> flanked by <i>KpnI</i> sites cloned into pUT18	This study
pMH64	<i>M. smegmatis haaA</i> flanked by <i>KpnI</i> sites cloned into pUT18C	This study
pMH65	<i>M. smegmatis haaA</i> flanked by <i>KpnI</i> sites cloned into pKT25	This study
pMH66	<i>M. smegmatis haaA</i> flanked by <i>KpnI</i> sites cloned into pKNT25	This study
pMH67	<i>M. smegmatis parA</i> flanked by <i>KpnI</i> sites cloned into pCR2.1 TA cloning vector	This study
pMH68	<i>M. smegmatis parA</i> flanked by <i>KpnI</i> sites cloned into pUT18	This study
pMH69	<i>M. smegmatis parA</i> flanked by <i>KpnI</i> sites cloned into pUT18C	This study
pMH70	<i>M. smegmatis parA</i> flanked by <i>KpnI</i> sites cloned into pKT25	This study
pMH71	<i>M. smegmatis parA</i> flanked by <i>KpnI</i> sites cloned into pKNT25	This study
pMH72	<i>M. smegmatis parH</i> flanked by <i>KpnI</i> sites cloned into pCR2.1 TA cloning vector	This study
pMH73	<i>M. smegmatis parH</i> flanked by <i>KpnI</i> sites cloned into pUT18	This study
pMH74	<i>M. smegmatis parH</i> flanked by <i>KpnI</i> sites cloned into pUT18C	This study
pMH75	<i>M. smegmatis parH</i> flanked by <i>KpnI</i> sites cloned into pKT25	This study
pMH76	<i>M. smegmatis parH</i> flanked by <i>KpnI</i> sites cloned into pKNT25	This study

pMH77	<i>S. venezuelae haaA</i> flanked by <i>KpnI</i> sites cloned into pCR2.1 TA cloning vector	This study
pMH78	<i>S. venezuelae haaA</i> flanked by <i>KpnI</i> sites cloned into pUT18	This study
pMH79	<i>S. venezuelae haaA</i> flanked by <i>KpnI</i> sites cloned into pUT18C	This study
pMH80	<i>S. venezuelae haaA</i> flanked by <i>KpnI</i> sites cloned into pKT25	This study
pMH81	<i>S. venezuelae haaA</i> flanked by <i>KpnI</i> sites cloned into pKNT25	This study
pMH82	<i>S. venezuelae parA</i> flanked by <i>KpnI</i> sites cloned into pCR2.1 TA cloning vector	This study
pMH83	<i>S. venezuelae parA</i> flanked by <i>KpnI</i> sites cloned into pUT18	This study
pMH84	<i>S. venezuelae parA</i> flanked by <i>KpnI</i> sites cloned into pUT18C	This study
pMH85	<i>S. venezuelae parA</i> flanked by <i>KpnI</i> sites cloned into pKT25	This study
pMH86	<i>S. venezuelae parA</i> flanked by <i>KpnI</i> sites cloned into pKNT25	This study
pMH87	<i>S. venezuelae parB</i> flanked by <i>KpnI</i> sites cloned into pCR2.1 TA cloning vector	This study
pMH88	<i>S. venezuelae parB</i> flanked by <i>KpnI</i> sites cloned into pUT18	This study
pMH89	<i>S. venezuelae parB</i> flanked by <i>KpnI</i> sites cloned into pUT18C	This study
pMH90	<i>S. venezuelae parB</i> flanked by <i>KpnI</i> sites cloned into pKT25	This study
pMH91	<i>S. venezuelae parB</i> flanked by <i>KpnI</i> sites cloned into pKNT25	This study
pMH92	<i>S. venezuelae parH</i> flanked by <i>KpnI</i> sites cloned into pCR2.1 TA cloning vector	This study
pMH93	<i>S. venezuelae parH</i> flanked by <i>KpnI</i> sites cloned into pUT18	This study



pMH94	<i>S. venezuelae parH</i> flanked by <i>KpnI</i> sites cloned into pUT18C	This study
pMH95	<i>S. venezuelae parH</i> flanked by <i>KpnI</i> sites cloned into pKT25	This study
pMH96	<i>S. venezuelae parH</i> flanked by <i>KpnI</i> sites cloned into pKNT25	This study
pMH97	pKT25+1 in-frame shift, <i>XbaI</i> digestion and DNA Pol I were used to create +1frame shift in pKT25	This study
pMH98	pKT25-1 in-frame shift <i>PstI</i> digestion and T4 DNA Pol I were used to create -1frame shift in pKT25	This study
pMH101	St9B10 <i>haaA ΔhaaA::aac(3)IV</i>	This study
pMH102	St9B10 <i>haaA(Δ338-345)</i>	This study
pMH103	<i>XbaI</i> and <i>SpeI</i> digested and ligated St9B10 <i>haaA(Δ338-345)</i>	This study
pMH104	9B10 <i>haaA-egfp</i>	This study
pMH105	<i>haaA/haaA<sup>+</sup></i> (2339 bp fragment of complete intergenic region of <i>haaA</i> and <i>haaA</i> was cloned into <i>PvuII</i> site of pMS82)	This study
pMH106	<i>cyaA</i> gene <i>sco4928</i> cloned into pKT25 in reverse orientation	This study
pMH107	original clone from library screening (candidate 2), partial <i>sco5855</i> (encodes last 66 amino acids of HaaA) cloned into pKT25	This study
pMH108	original clone from library screening (candidate 3), partial <i>sco5855</i> (encodes last 66 amino acids of HaaA) cloned into pKT25	This study
pMS82	Integrative vector for <i>Streptomyces</i> ; <i>oriT<sub>RK2int</sub></i> <i>attP<sub>ΦBT1</sub></i> ; <i>hyg</i>	Gregory <i>et al.</i> , 2003
pUT18	Bacterial two-hybrid vector used to create a fusion to the N-terminus of the CyaA T18 polypeptide	Euromedex
pUT18C	Bacterial two-hybrid vector used to create a fusion to the C-terminus of the CyaA T18 polypeptide	Euromedex

### 3.4: Oligonucleotides used in this study

Oligonucleotide	Sequence	Application
Sven HaaA KpnI Fwd	GGT ACC TAT GCC CGA ACT GCG TGT CGT GGC CGT CTC CAA CG	Cloning <i>S. venezuelae haaA</i> into bacterial two-hybrid plasmids
Sven HaaA KpnI Rev	GGT ACC GTC CTG CTT CTT CCG CCG CGT GCC GAA GAC G	Cloning <i>S. venezuelae haaA</i> into bacterial two-hybrid plasmids
Sven ParA KpnI Fwd	GGT ACC TGT GGG CAA GAC GAC CAC GAC GGT CAA CCT TG	Cloning <i>S. venezuelae parA</i> into bacterial two-hybrid plasmids
Sven ParA KpnI Rev	GGT ACC CTG GAT CCC CTC CGA CAT GTT GCG CTG G	Cloning <i>S. venezuelae parA</i> into bacterial two-hybrid plasmids
Sven ParB KpnI Fwd	GGT ACC TAT GGC CCC GGA TCG GGG AGT GGC TG	Cloning <i>S. venezuelae parB</i> into bacterial two-hybrid plasmids
Sven ParB KpnI Rev	GGT ACC GCC CTC GGC GTC CTC GGC GTT CTC GTT GG	Cloning <i>S. venezuelae parB</i> into bacterial two-hybrid plasmids
Sven ParH KpnI Fwd	GGT ACC TGT GAA TGA GTC GAC AAT TAC TCC CGG GAG CGG	Cloning <i>S. venezuelae parH</i> into bacterial two-hybrid plasmids
Sven ParH KpnI Rev	GGT ACC CTC GGC GTG ACA CCG GGC GAG CAC CTC CCT GG	Cloning <i>S. venezuelae parH</i> into bacterial two-hybrid plasmids
Msme HaaA KpnI Fwd	GGT ACC TAT GCG AGA ACT CAG GGT CGT CGG ACT G	Cloning <i>M. smegmatis haaA</i> into bacterial two-hybrid plasmids
Msme HaaA KpnI Rev	GGT ACC GCG CTG CGT ACC CGA CGA GCG CAC GCC CAG	Cloning <i>M. smegmatis haaA</i> into bacterial two-hybrid plasmids
Msme ParA KpnI Fwd	GGT ACC TAT GGG TTC GGG TCA GAA CAA AGG ACA G	Cloning <i>M. smegmatis parA</i> into bacterial two-hybrid plasmids
Msme ParA KpnI Rev	GGT ACC CTG CTG GCG CGG CGG CGC CCC ACG CTC GGC G	Cloning <i>M. smegmatis parA</i> into bacterial two-hybrid plasmids
Msme ParH KpnI Fwd	GGT ACC TGT GGG CCT GAC GGG CCG GCC TCC CCG CGA G	Cloning <i>M. smegmatis parH</i> into bacterial two-hybrid plasmids
Msme ParH KpnI Rev	GGT ACC CAC GCC GAA CCG GTG GAT GAC TTC CCG	Cloning <i>M. smegmatis parH</i> into bacterial two-hybrid plasmids
Cglu HaaA KpnI Fwd	GGT ACC TAT GCG GGA AAT ATT CCT GAT CAG CGG	Cloning <i>C. glutamicum haaA</i> into bacterial two-hybrid plasmids
Cglu HaaA KpnI Rev	GGT ACC TTT CTT CGG GCG CTT TGT GTT TGC G	Cloning <i>C. glutamicum haaA</i> into bacterial two-hybrid plasmids
Cglu ParA KpnI Fwd	GGT ACC TAT GGA AGA CAC TAC TTG GGA AGA CAC AC	Cloning <i>C. glutamicum parA</i> into bacterial two-hybrid plasmids
Cglu ParA KpnI Rev	GGT ACC TTT CGC AGG TTT TAG	Cloning <i>C. glutamicum parA</i>

	GCC GAT CGG AC	into bacterial two-hybrid plasmids
Cglu PldP KpnI Fwd	GGT ACC TGT GAG TGA TGC AGG GAA GAA GGA CTC	Cloning <i>C. glutamicum pldP</i> into bacterial two-hybrid plasmids
Cglu PldP KpnI Rev	GGT ACC GTC GTT GAC GCG GCT GAT AAC TTC ACG	Cloning <i>C. glutamicum pldP</i> into bacterial two-hybrid plasmids
HaaA C-ter in-frame del Fwd	GGC CGA CGG CGT CCG GCC GGG TCG CCG CGC GGC GGT GCC GAC TAG TAT TCC GGG GAT CCG TCG ACC	Creating ( $\Delta$ 338-345) in <i>S. coelicolor</i> HaaA
HaaA C-ter in-frame del Rev	ACG TCA TCC GGC GAA GAC CGG ACT ACT CCT GCT TCT TGC GTC TAG ATG TAG GCT GGA GCT GCT TC	Creating ( $\Delta$ 338-345) in <i>S. coelicolor</i> HaaA
haaAegfpFwd	ATGCCCGAACTGCGTGTCGTGGCC GTCTCGAATGACGGCACTGCCGG GCCCCGAGCTG	Creating HaaA-EGFP in <i>S. coelicolor</i>
haaAegfpRev	GCCCCGACCTCGGTCACGTCATCC GGCGAAGACCGGACTACATATGT AGGCTGGAGCTGC	Creating HaaA-EGFP in <i>S. coelicolor</i>
haaAdelFwd	GCACGTGACGTCGGCAGGCACCA CCCCGGAGGTCCCC ATG ATT CCG GGG ATC CGT CGA CC	Creating <i>haaA</i> null mutant in <i>S. coelicolor</i>
haaAdelRev	GCCCCGACCTCGGTCACGTCATCC GGCGAAGACCGGACTA TGT AGG CTG GAG CTG CTT C	Creating <i>haaA</i> null mutant in <i>S. coelicolor</i>
haaAKpnIFwd	GGT ACC TAT GCC CGA ACT GCG TGT CGT GGC CG	Cloning <i>S. coelicolor haaA</i> into BTH plasmids
haaAKpnIRev	GGT AC CTC CTG CTT CTT GCG CCG CGT GC	Cloning <i>S. coelicolor haaA</i> into BTH plasmids
HaaAcompPvuIIFwd	ACTGCAGCTGCCGAGGCGTCCGG GTCGGGGGCTCCG	Creating <i>haaA</i> complementation strain
HaaAcompPvuIIRev	GTCCAGCTGCTACTCCTGCTTCTT GCGCCGCGTGCCG	Creating <i>haaA</i> complementation strain

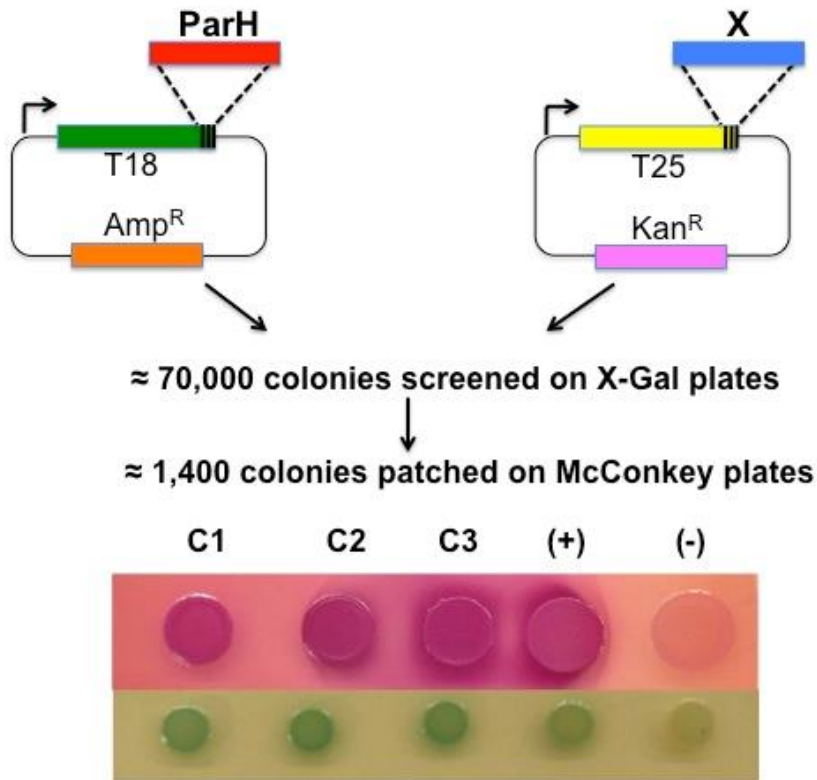


**Figure 3.1. Representation of genomic library screening for ParH interacting proteins.** Plasmids expressing ParH-T18 or ParHT18C were used as bait and library DNA was used as a prey to screen for novel interacting proteins. Approximately 70,000 colonies were screened on LB X-Gal plates and 1,400 suspected colonies were rescreened on McConkey plates. The phenotypes of the final 3 candidates with the most intense phenotypes are shown spotted on McConkey maltose and X-gal IPTG plates. One of the candidates (C1) for a potential ParH interacting protein contained the entire gene for SCO4928 (adenylate cyclase) cloned in reverse orientation. However, 2 candidates (C2 and C3) contained plasmids with the 3' end of *sco5855* fused at the same point and were possible siblings. The negative control was strain BTH101 expressing pKT25 and pT18C, and the positive control with strain BTH101 expressing pT25-zip and pT18-zip.

RHA1_ro04984	MRELRVIGLEPDGSHVVCADAST--GEKFRLPADDKLRAASRGDIAR-----	45
nfa6540	MRELRVIGLTPDSTHIVCVDTES--GQKFRLPADDKLRAAARGDLAR-----	45
SACE_0629	MRALRVVGLDEDGETVICEDPEN--GDRFSVPADERLRAAARGDLTR-----	45
Rv0883c	MRELKVVGLDADGKNIICQGAIP--SEQFKLPVDDRRLRAALRDDSVQP-----	46
NCg10793	MREIFLISGDSTESSLVFKTSEEDGAEFFIAVTDLHAILAGHSEIKSAPEPEEHKEVP	60
SCO5855	MPRELRVAVSNDGTRLVVLKAADS---TEYTLPIDERLRAAVRGDR-----	42
SVEN_5529	MPRELRVAVSNDGTRLVVLKAADS---TEYTLPIDERLRAAVRNR-----	42
KSE_54260	MPRELRVAVSNDGTRLVVLKAADS---TEYTLPIDERLRAAVRGDR-----	42
Tfu_1947	MQELRLVAVSEGDGYLVLASAGRG--TRFMPLVDDRRLRAAVRGQF-----	43
Micau_0513	MRPVRFVALSEGGQALVLADEVG---RLRALPIDERIASALHAEPGAPP-----	46
	* : . . . : : : . : : : .	

RHA1_ro04984	-----LGQIEIEMDSQLRPREIQARIRAGASVEQVADEAGIPLAKVER	88
nfa6540	-----FGQIEIETEASMRPRDIQARIRAGASVEQVTAESGMPAARVER	88
SACE_0629	-----LGQVQIEEQAQMRPREIQARIRAGASVEQVAEAAAGIPEQRVER	88
Rv0883c	-----EQAQLDIEVTNVLSPKEIQARIRAGASVEQVAASGSDIARIRR	90
NCg10793	PPVLEPVAAVEEPREEKEIDPRISAPLTMSPREIQIRVRSRGATIEELAEIEGVTEARVEP	120
SCO5855	-----PRLGQIEIEVESHRLPRDIQARIRAGATAEEVAQMAGIPVDRVRR	87
SVEN_5529	-----ARLQIEIEVESHRLPRDIQARIRAGASAEVEVAQMAGIPVDRVRR	87
KSE_54260	-----PRLGQIEIEVESHRLPRDIQARIRAGASAEVEVAQAAGISVERVRR	87
Tfu_1947	-----SRLGQYIEIENPLRPEIQARIRAGETAESIAQAAGIPVERVRW	88
Micau_0513	-----LAVVPSATDPTPLSPRDIQARIRSGESAEDVARIAGVPVDRVLR	91
	. : * : * * * : * : : * : :	

RHA1_ro04984	FAYPVLLERSRAAEMAQGGHPVRDNGPA-VPTLAEIVTQAFRARGHNIIDDATWDARDED	147
nfa6540	FAYPVLLERARAAELAQAHPVRADGPA-VETLIEVVTAAFTERGHTELENAEWDANKDEK	147
SACE_0629	YAYPVLLERAQVAEMAQRAHPVREDGPD-VQTLGCVVAHTFGMRGHDYNETSVDWARDED	147
Rv0883c	FAHPVLLERSRAAELATAAHFVLADGPA-VLTMQETVAAALVARGLNPDLSLTDWARDED	149
NCg10793	YAHPVLLERARIADLAKQSHPIRENGPA-KLTLWEILATAFATRGHDLTTARWDAYKDAT	179
SCO5855	FEGPVLAERAFMAERARKTPVRRPGENS-GPPLGAVQERLLLRLGADKDTVQWDSWRD	146
SVEN_5529	FEGPVLAERAFMAERARKTPVRRPGENS-GPQLGAVQERLLLRLGAEKDTVQWDSWRD	146
KSE_54260	FEGPVLAERAFMAERARKTAIRRHGEST-GPQLGAVAERLALRGAEKDSEERWDSWRD	146
Tfu_1947	FESPVLQEREYMARQAQLALVRRPGETAPGPTLGLDVAERIGVAQLESGEATWDSWKRED	148
Micau_0513	YAGPVLQERAMLAQHARRTRLKGAEKPT---PLAEVNGRLAQHGIDTEKISWDAYRRD	148
	: * * * * * : : : : * * * * :	

RHA1_ro04984	NHWVAQLQWQAGRTTNAAHWRYQPDAHGG-TIVALDDTAFDLIDPDFG-----	194
nfa6540	GFWIAQLQWQNGRSEIAAHWRYQPDAHGG-TVAPLDDPADLIDPDFG-----	194
SACE_0629	GKVVVQLQWQNGRSEIAAHWVFPAGHGG-TVAALDDHAADLLDPSFN-----	194
Rv0883c	SRWTVQLAWKAGRS DNLAHFRTPGAHGG-TATAIDDTAHELINPTFN-----	196
NCg10793	NQWIVRVDWKAGLS DNYAEWTLNLHNTSNPTADPRTPVAADLIDPEFI-----	227
SCO5855	GTWEVLLVYLVAGEPHSASWTYDP---PRRLVQAVDDEARALIGESDD---LAAPEPSFPF	201
SVEN_5529	GTWEVLLVYRVAGEVHTASWTYDP---PRRLVQAVDDEARALIGETDDTIAAEPSPFPF	203
KSE_54260	GTWEVLLWYRAEGEHRRAGWSDYDP---PRRLVQPNDDDEARALIGENVE---REEDSVFPF	200
Tfu_1947	NTWQVKLSFRVMGEEHVAHWIYEP---RRRSVTPYDEEAVRLLSADDR-----EVSVPF	199
Micau_0513	GTWRIIATWPWGKATAQAVWDLDK---TRQNVAPHDDMAQYLCASERPTPIILGQEPAPERG	205
	. * : * : * * *	

RHA1_ro04984	-----RPLRGLAPVASDEPEQ----LLEAEPTEVEVPTIEPEEIEADVTTEE-	238
nfa6540	-----RALRGLATI LPTEPEPEPAGPAEPVVEPRESAAAAPVPAQPVVVEEYFEKR	244
SACE_0629	-----RPLRTVRPVTTELAREA----LELDQQSGAERAEAPPHPRAEFPASVPPL	239
Rv0883c	-----RPLRPLAPVAHLDFDE-----PEPAQPT-----	219
NCg10793	-----QPVRTLTSVNSTQEQYD---DETDVFDTVSPDDAPDSSEDAVAEITN-	272
SCO5855	VPRIARLPDRPLDRDRLDREQRERPSLPPPPSEPADDTAATAASAER-ERDSLTSLEAVP	260
SVEN_5529	VPRIARLPDRPLDRALDRQLDHR-----QLERASAPAEPEE-ERDSLTSLEAVP	253
KSE_54260	IPRIARLPDRPARPMIERPSADRIMQVREAREATAAAAATAAVPERDSLTSLLDVVP	260
Tfu_1947	AP-----PEATVTPFTPRRSPAR-----EAAPPQAPAAATPQ-ETDASTTPRSPIT	244
Micau_0513	GHALPGPSRGEPSRGGHGLPAASEHARPGRDIIRACRDALLASLDRPLGGTSGRGLDTRS	265

RHA1_ro04984	-----PED-----EPAPSEEPAAKPIAPHQTNN--	261
nfa6540	AVAAGGGAAA-----IPAAPVAGSAGAVEPAASADAAPADATPEPAE	290
SACE_0629	DLDGAAAPAAK-----APEAPAAEPDDEPEAPADDAEPGEAPAEAAATAEDE	285
Rv0883c	-----LTVPSAQPV-----	229
NCg10793	-----DNEPEVDAEGP-----	283
SCO5855	SFRGDVVPERAPDPVEEPVEEPE-VEEPPAPAASAGS--AYADVLMPRSVASHDRDLTG	317

```

SVEN_5529      SFRGDMVVPE-QPD--SEPAAEAE-AEPPAPAASAGAGAYADVLMPRVSGHRDRLTG 309
KSE_54260     SYRGDLTPVG--PSVETTIAEEPEEVEETAAPAASVAGSAYADILMPRSVAPHRDRLVG 318
Tfu_1947      T---ELVRPTTEDTVFTATVPERH---HRPGPAPTTPGPGSPTQRGASQQRASRPEASVPA 298
Micau_0513    PAALAGQEAPRQRAVAGGAAALLGGGQGSADFDDSDAPKEIPAVPSLAVLRPRRTGPAAA 325

RHA1_ro04984  -----KDKRGKPALPSWDDVLLGVRSSGR---- 285
nfa6540       KEQKAPAKPARAKRGKAPMPSWEDVLLGVRSSGH---- 324
SACE_0629     AGQRKAEPQRRGRKNHPIVPSWEDVLLGVRSHR----- 318
Rv0883c      -----NRRGKPAIPAWEDVLLGVRSGGRR--- 253
NCgl0793     -----RNRRRKAVTPHWEDVLLGVRANTKRPKK 311
SCO5855      STDRQAEADGVRPGRRAAVPSWDEIVFGTRRKKQE--- 352
SVEN_5529    TTDRQAEADGVRPGRRAAVPSWDEIVFGTRRKKQD--- 344
KSE_54260    TTDRQAEADGVRPGRRAATVPSWDEIVFGSRKKPE--- 353
Tfu_1947     ATGASQQPRRKR-GRRTSVPSWDEIMFGSKRSD----- 330
Micau_0513   TGGAAAESTDAGGKPRKRLPSWDDVLFGTGPAARESS- 362
              : * * * : : : *

```

### Figure 3.2 ClustalW2 alignment of HaaA homologs from several divergent

**Actinomycetes species.** HaaA homologs from diverse Actinomycetes were aligned using ClustalW2. Network Protein Sequence Analysis ([https://npsa-prabi.ibcp.fr/cgi-bin/npsa\\_automat.pl?page=/NPSA/npsa\\_hth.html](https://npsa-prabi.ibcp.fr/cgi-bin/npsa_automat.pl?page=/NPSA/npsa_hth.html)) suggests that HaaA contains a helix-turn-helix motif with an approximately 50% probability at the position which is shown in bold and highlighted in grey. The amino acids removed by a 3' in-frame deletion constructed for this study is shown in bold and underlined. An asterisk (\*) indicates a conserved residue, colon (: ) indicates conservation between groups of strongly similar properties, period (.) indicates conservation between groups of weakly similar properties. Strain abbreviations: RHA1\_ro04984, *Rhodococcus jostii*; nfa6540, *Nocardia farcinica*; SACE\_0629, *Saccharopolyspora erythraea*; Rv0883c, *Mycobacterium tuberculosis*; NCgl0793, *Corynebacterium glutamicum*; SCO5855, *S. coelicolor*; SVEN\_5529, *S. venezuelae*; KSE\_54260, *Kitasatospora setae*; Tfu\_1947, *Thermobifida fusca*; Micau\_0513, *Micromonospora aurantiaca*.

```

STRS4_03849      MPELRVVAVSNDGTRLVLKAAADSTEYTLPI DERLRAAVRGDRPRLGQIEIEVESHRLRPRD      60
SVEN_5529        MPELRVVAVSNDGTRLVLKAAADSTEYTLPI DERLRAAVRNRDRARLGQIEIEVESHRLRPRD      60
SGR_1677         MPELRVVAVSNDGTRLVLKAAADSTEYTLPI DERLRAAVRNRDRARLGQIEIEVESHRLRPRD      60
SCAB24141        MPELRVVAVSNDGTRLVLKAAADSTEYTLPI DERLRAAVRGDRPRLGQIEIEVESHRLRPRD      60
SCO5855          MPELRVVAVSNDGTRLVLKAAADSTEYTLPI DERLRAAVRGDRPRLGQIEIEVESHRLRPRD      60
SLI_6127         MPELRVVAVSNDGTRLVLKAAADSTEYTLPI DERLRAAVRGDRPRLGQIEIEVESHRLRPRD      60
SAV_2411         MPELRVVAVSNDGTRLVLKAAADSTEYTLPI DERLRAAVRGDRPRLGQIEIEVESHRLRPRD      60
*****

STRS4_03849      IQARI RAGASAE EVA SLAGI PVDRVRRFEGP VLAERAFMAERARKTPVRRPGEN-TGFPQL      119
SVEN_5529        IQARI RAGASAE EVA QMAGI PVDRVRRFEGP VLAERAFMAERARKTPVRRPGEN-SGFPQL      119
SGR_1677         IQARI RAGASAE EVA QFAGI PVDRVRRFEGP VLAERAFMAERARKTPVRRPGEN-TGFPQL      119
SCAB24141        IQARI RAGATAE EVA QLAGI PVDRVRRFEGP VLAERAFMAERARKTPVRRPGENAAGFPQL      120
SCO5855          IQARI RAGATAE EVA QMAGI PVDRVRRFEGP VLAERAFMAERARKTPVRRPGEN-SGFPQL      119
SLI_6127         IQARI RAGATAE EVA QMAGI PVDRVRRFEGP VLAERAFMAERARKTPVRRPGEN-SGFPQL      119
SAV_2411         IQARI RAGASAE EVA QLAGI PVDRVRRFEGP VLAERAFMAERARKTPVRRPGEN-AGFPQL      119
*****:*****.:*****:*****:*****:*****:*****:*****:*****

STRS4_03849      GEAVRERLLLRGADRD TVQWDSWRRDDGTWEVLLVYGVAGERHSASWSYDPPRRLVQAVD      179
SVEN_5529        GEAVQERLLLRGAEKD TVQWDSWRRDDGTWEVLLVYRVAGEVHTASWTYDPPRRLVQAVD      179
SGR_1677         GEAVQERLLMRGADKETVQWDSWRRDDGTWEVLLVYRVAGEPHSASWTYDPPRRLVQAVD      179
SCAB24141        GEAVQERLLLRGAEKD TVQWDSWRRDDGTWEVLLVYCVAGEPHSASWTYDPPRRLVQAVD      180
SCO5855          GEAVQERLLLRGADKDTVQWDSWRRDDGTWEVLLVYLVAGEPHSASWTYDPPRRLVQAVD      179
SLI_6127         GEAVQERLLLRGADKDTVQWDSWRRDDGTWEVLLVYLVAGEPHSASWTYDPPRRLVQAVD      179
SAV_2411         GEAVQERLLLRGADKDTVQWDSWRRDDGTWEVLLVYLVAGEPHSASWTYDPPRRLVQAVD      179
****:****:***:.:*****:*****:*****:*****:*****:*****:*****

STRS4_03849      DEARSLIGESDDV--SAPEPSFFV PRIARLPRERPERPERGPHA-----VE---      224
SVEN_5529        DEARALIGETDDTIAAAPEPSFFV PRIARLPRDRPLDRALDRQLDHRQL-----E      230
SGR_1677         DEARSLIGETDDV--AAPEPSFFV PRIARLPRDRPLDRSLDRQIDRDRPLDRALDRQIE      237
SCAB24141        DEARSLIGESDDL--GTPEPSFFV PRIARLPRDRPLDRQA-----DRPALPGPPPE--      231
SCO5855          AEARALIGESDDL--AAPEPSFFV PRIARLPRDRPLDRTLDRERPSLPPPPSEF--      235
SLI_6127         AEARALIGESDDL--AAPEPSFFV PRIARLPRDRPLDRTLDRERPSLPPPPSEF--      235
SAV_2411         DEARSLIGESDDL--AAPEPSFFV PRIARLPRDRPLDRALDRQT-ERPALPSQAPEF--      234
***:***:*** .:*****:*****:*****:*****:*****:*****

STRS4_03849      -----PETEE-LPATAEQGG RDSLTSLLEAVPSFRGDMVVPERPAER-PLLEEPEQEQA      277
SVEN_5529        RA-SAP-----AEPEEERDSLTSLLEAVPSFRGDMVVP EQPD-----SEPAAEEAEA      275
SGR_1677         RPAPAAAEPEEYVSSASAGERDSLTSLLEAVPSFRGDMVVP ERPSQPEPPALEPAEEAEA      297
SCAB24141        -----DED-----LVSERDSLTSILEAVPSYRGDLVVP ELPSLEPQEEESASVEEVAE      278
SCO5855          -----ADDTAATASAERERDSLTSLLEAVPSFRGDLVVP ERA---PDPVEEPVVEEPEV      285
SLI_6127         -----ADDTAATASAERERDSLTSLLEAVPSFRGDLVVP ERA---PDPVEEPVVEEPEV      285
SAV_2411         -----AEE-----STAERDSLTSLLEAVPSFRGDMVVP ERPAEIPAGQDEPAPEPEA      281
*****:*****:***:*****

STRS4_03849      EEPAPAAS--AGSAYADVLM PRAVAHRDRLIGSTDRQAEADGVRPGRRAAVPSWDEIV      335
SVEN_5529        EEPAPAASAGAGAA YADVLM PRAVSGHRDRLTGTTDRQAEADGVRPGRRAAVPSWDEIV      335
SGR_1677         DEPPA-AASAGAGSAYADVLM PRAVAGHRDRLTGTTDRQAEADGVRPGRRAAVPSWDEIV      356
SCAB24141        EESAAPAAS--AGSAYADVLM PRSVNGHRDRLIGATDRQAEADGVRPGRRAAVPSWDEIV      336
SCO5855          EEPAPAAS--AGSAYADVLM PRSVASHRDRLTGTTDRQAEADGVRPGRRAAVPSWDEIV      343
SLI_6127         EEPAPAAS--AGSAYADVLM PRSVASHRDRLTGTTDRQAEADGVRPGRRAAVPSWDEIV      343
SAV_2411         EEPAPAAS--AGSAYADVLM PRSVGHRDRLVGATDRQAEADGVRPGRRAAVPSWDEIV      339
:* * :** **:******:* .***** *:*****:*****:*****:*****

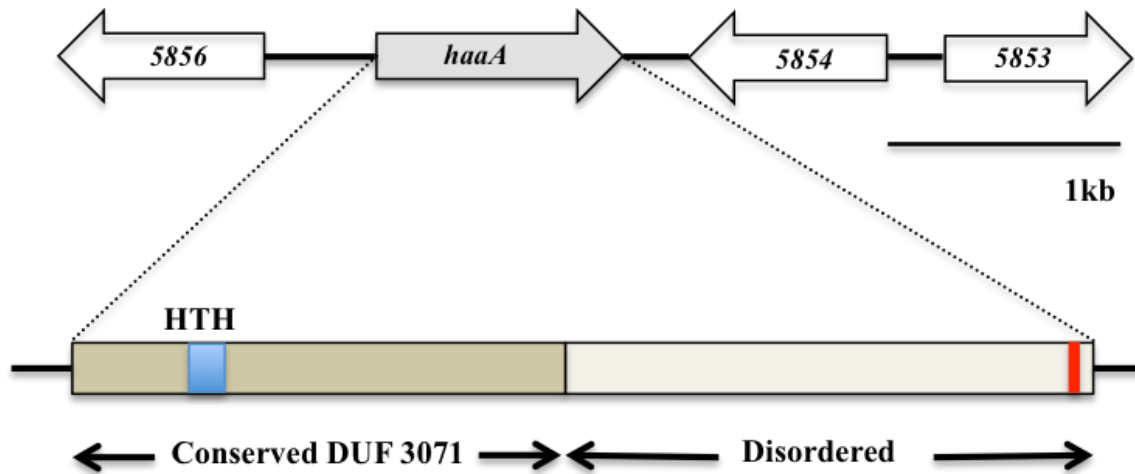
STRS4_03849      FGTRRNKE      344
SVEN_5529        FGTRRKQD      344
SGR_1677         FGTRRKQD      365
SCAB24141        FGTRRKQE      345
SCO5855          FGTRRKQE      352
SLI_6127         FGTRRKQE      352
SAV_2411         FGTRRKQE      348
*****:.:

```

**Figure 3.3 ClustalW2 multiple sequence alignment of HaaA from different**

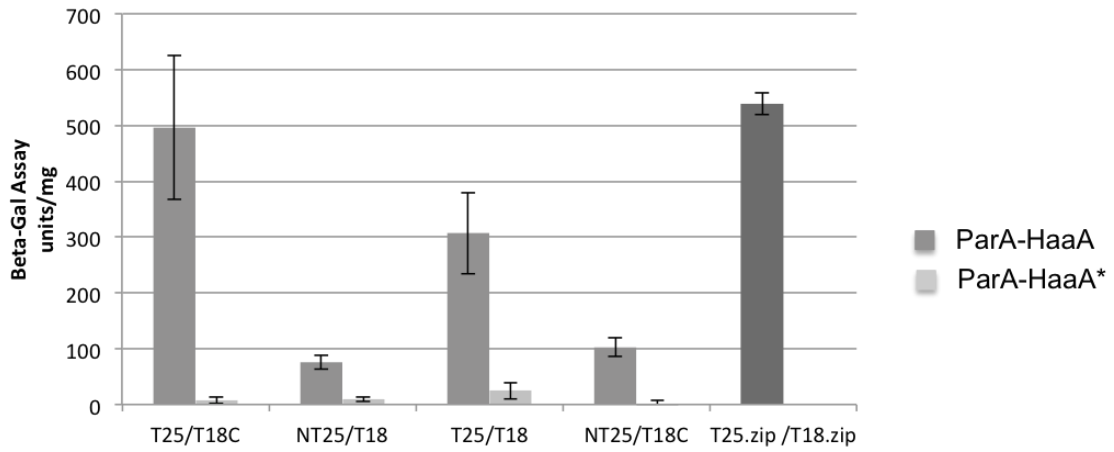
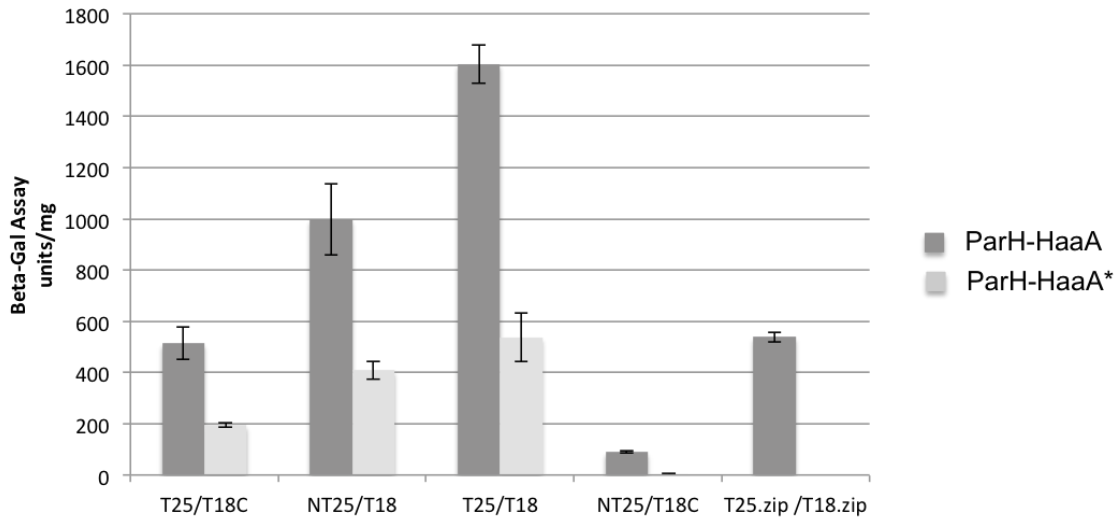
***Streptomyces* species.** HaaA homologs from different Streptomyces were aligned by ClustalW2. HaaA amino acid sequence is highly conserved among *Streptomyces* species. An asterisk (\*) indicates a conserved residue, colon (:) indicates conservation between groups of strongly similar properties, period (.) indicates conservation between groups of weakly similar properties. Species abbreviations: SGR, *S. griseus*; SCLAV, *S. clavuligerus*; SVEN, *S. venezuelae*; SAV, *S. avermitilis*; SCO, *S. coelicolor*; SCAB, *S. scabies*; STR, *S. triostinicus*; SLI, *S. lividans*.





**Figure 3.4 Diagram of the gene organization at the *haaA* region of *S. coelicolor* chromosome and predicted structure of HaaA.** (Top) *sco5855* (*haaA*) encodes a putative DNA binding protein of 352 amino acids. *sco5856* encodes an unknown ATP/GTP binding protein. *sco5854* encodes a possible thiosulfate sulfurtransferase (also conserved in other *Streptomyces* species) and *sco5853* encodes a conserved hypothetical protein with unknown function. (Bottom) A predicted HTH motif in the N terminal region of HaaA is shown in blue color. A predicted disordered C terminal domain is shown in light beige color and 8 aminoacids conserved among Actinomycetes is shown in red color.



**A****B**

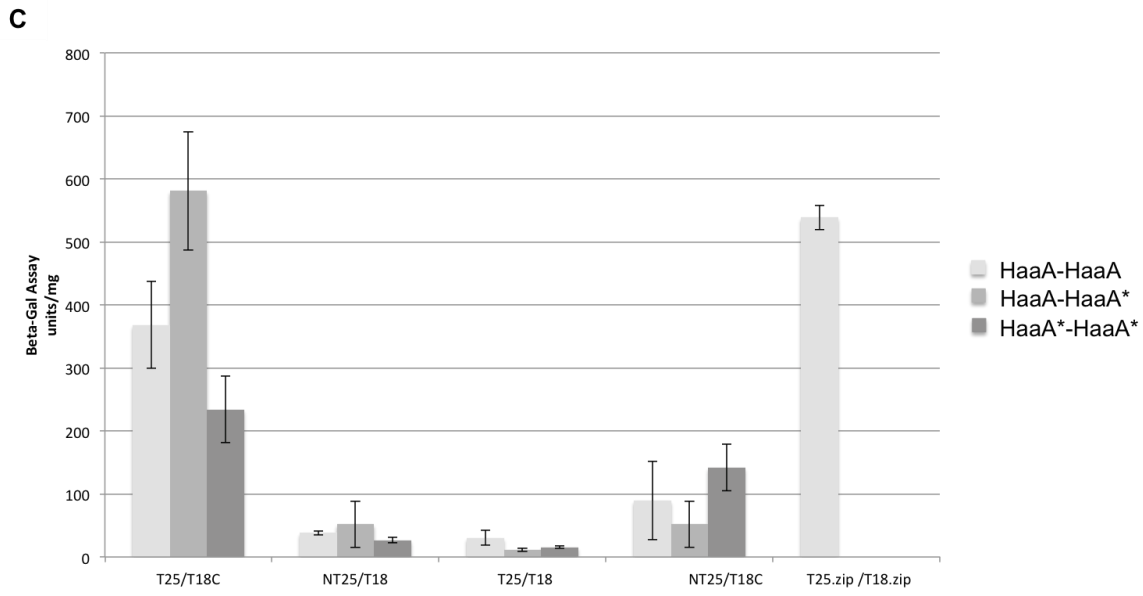
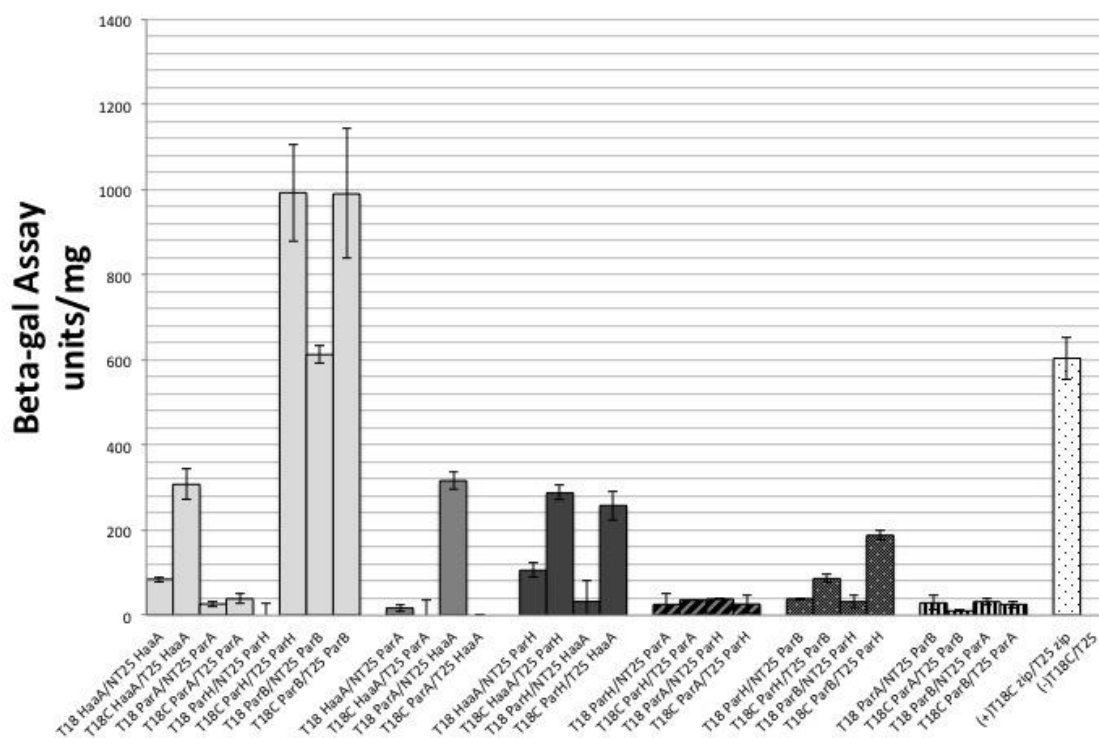
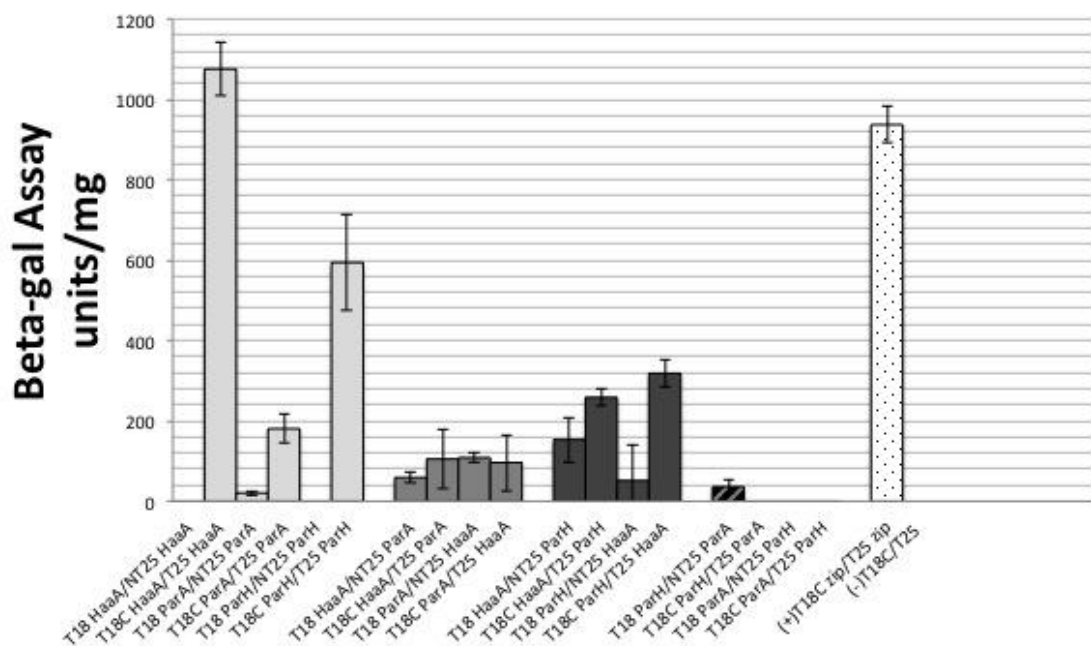


**Figure 3.5 Quantification of beta-galactosidase activity for selected positive interactions for plasmids expressing *S. coelicolor* fusion proteins.** Strains were grown in LB liquid with 0.5 mM IPTG. HaaA\* is HaaA( $\Delta$ 338-345). (a) ParA-HaaA and ParA-HaaA\*, (b) ParH-HaaA and ParH-HaaA\*, (c) HaaA-HaaA and HaaA-HaaA\*. Each bar represents the average of the three different independent liquid culture samples analyzed individually with experimental errors indicated.. T25.zip/T18 zip was the positive control with strain BTH101 expressing pT25-zip and pT18-zip.

**A**



**B**



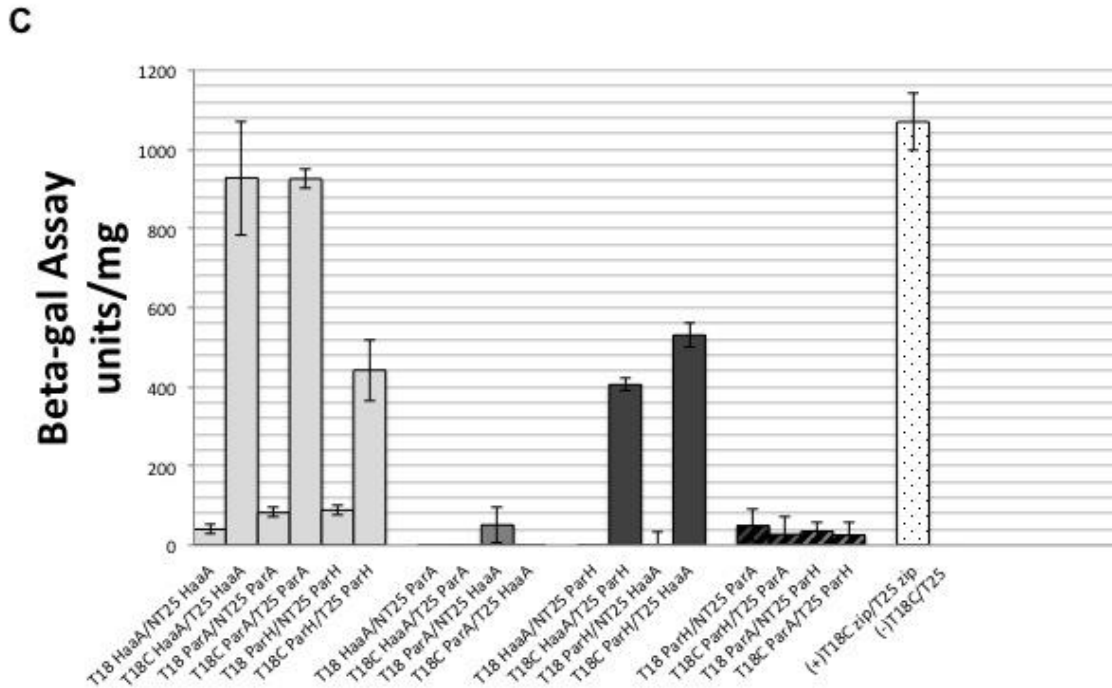


**Figure 3.6 Quantification of beta-galactosidase activity for HaaA, ParA, ParB, and ParH interactions in other Actinomycetes.** All strains were grown in LB liquid with 0.5 mM IPTG. Each bar represents the average of the three different independent liquid culture samples analyzed individually with experimental errors indicated.

**A-** Quantification of beta-galactosidase activity for *S. venezuelae* HaaA, ParA, ParB, and ParH interactions. **B-**Quantification of beta-galactosidase activity for *M. smegmatis* HaaA, ParA, and ParH interactions. Interactions with ParB were not tested. **C-** Quantification of beta-galactosidase activity for *C. glutamicum* HaaA, ParA, and PldP (labeled as ParH in the figure for consistency) interactions. Interactions with ParB were not tested. T25.zip/T18 zip was the positive control with strain BTH101 expressing pT25-zip and pT18-zip. T18C/T25 was the negative control with strain expressing pKT25 and pUT18C.

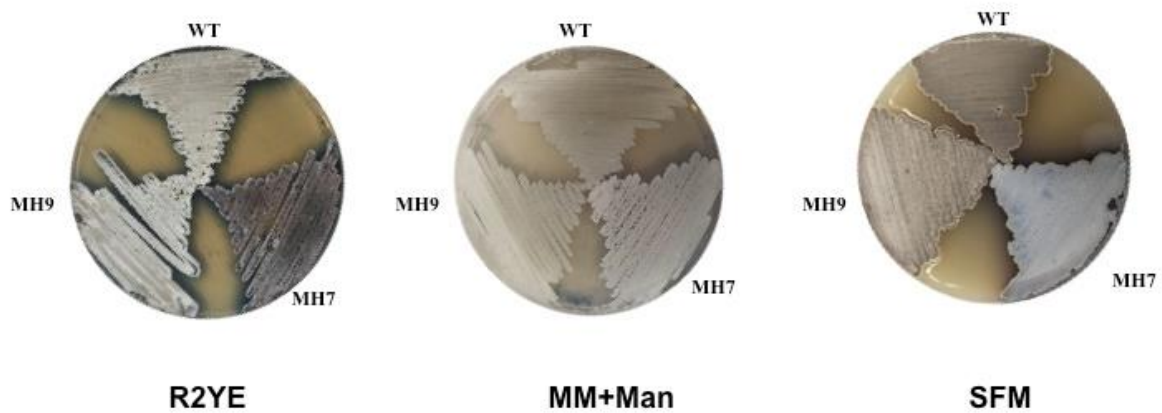


**Figure 3.7 Macroscopic phenotype of *haaA*.** Macroscopic phenotypes of the wildtype strain (M145),  $\Delta haaA$  strain (MH7),  $\Delta haaA/haaA^+$  complementation strain (MH9; MH7/pMH105) are shown in R2YE, MM and SFM media. Strains were grown at 30°C for 5 days. Little and delayed aerial filament formation occurred for MH7 on R2YE and minimal medium (MM) with mannitol, respectively. Slight white developmental phenotype in aerial filaments of mutant MH7 was observed on SFM agar.

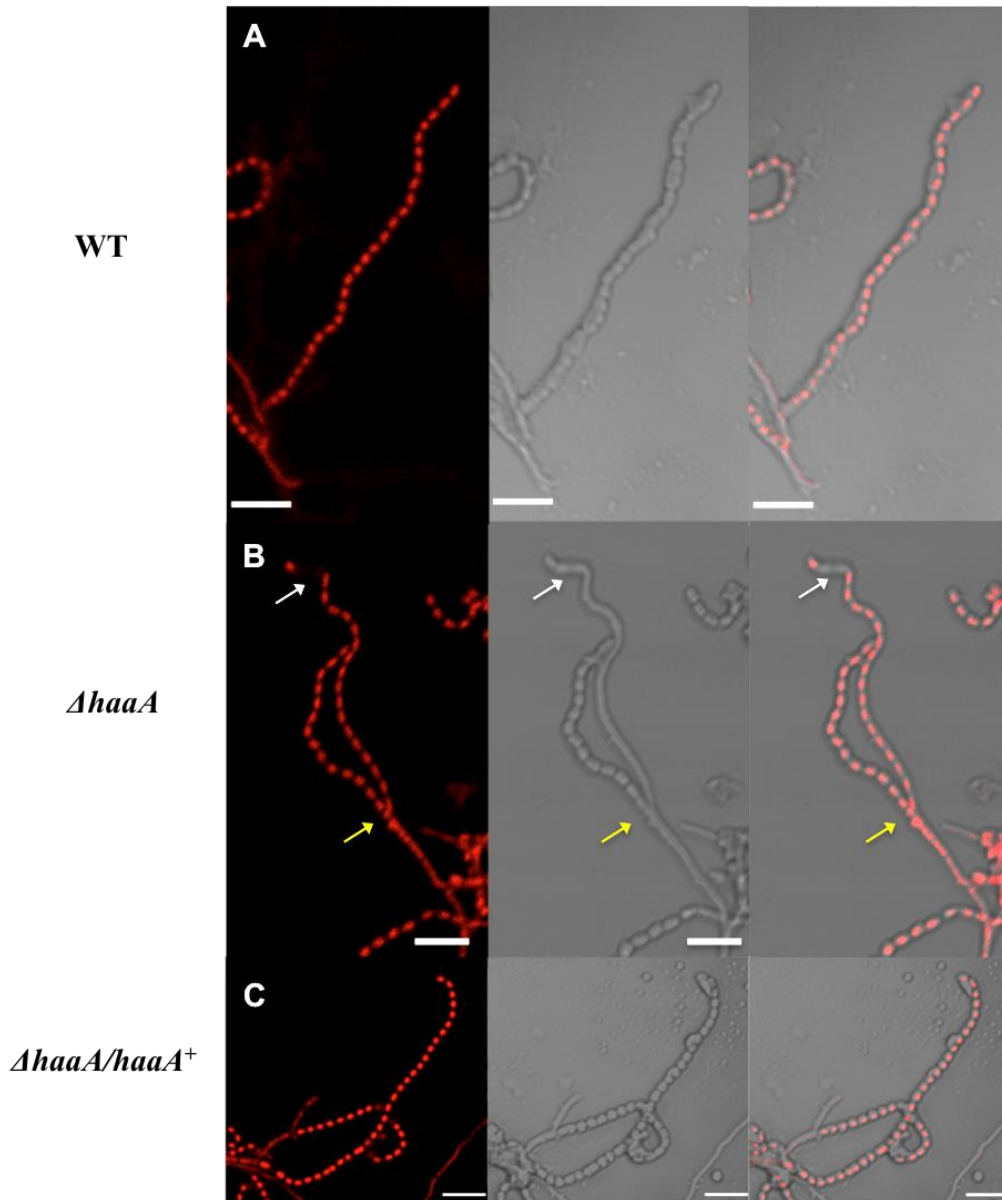


**Figure 3.8 Developmental segregation phenotype of a *haaA* null mutant.** Coverslips were inoculated and hyphae grown for 4 days on MS agar, fixed and stained with propidium iodide. Left panel shows a propidium iodide image, mid panel shows a DIC image, and right panel shows a merged image of a single aerial hypha. Strains WT (M145), MH7 ( $\Delta ha a A$ ), and MH9 ( $\Delta ha a A / \Delta ha a A^+$ ) are shown from top to bottom. Arrows show occasional branched spore chains and white arrows show anucleate cells in the spore chain. Scale bar is 5  $\mu$ m.



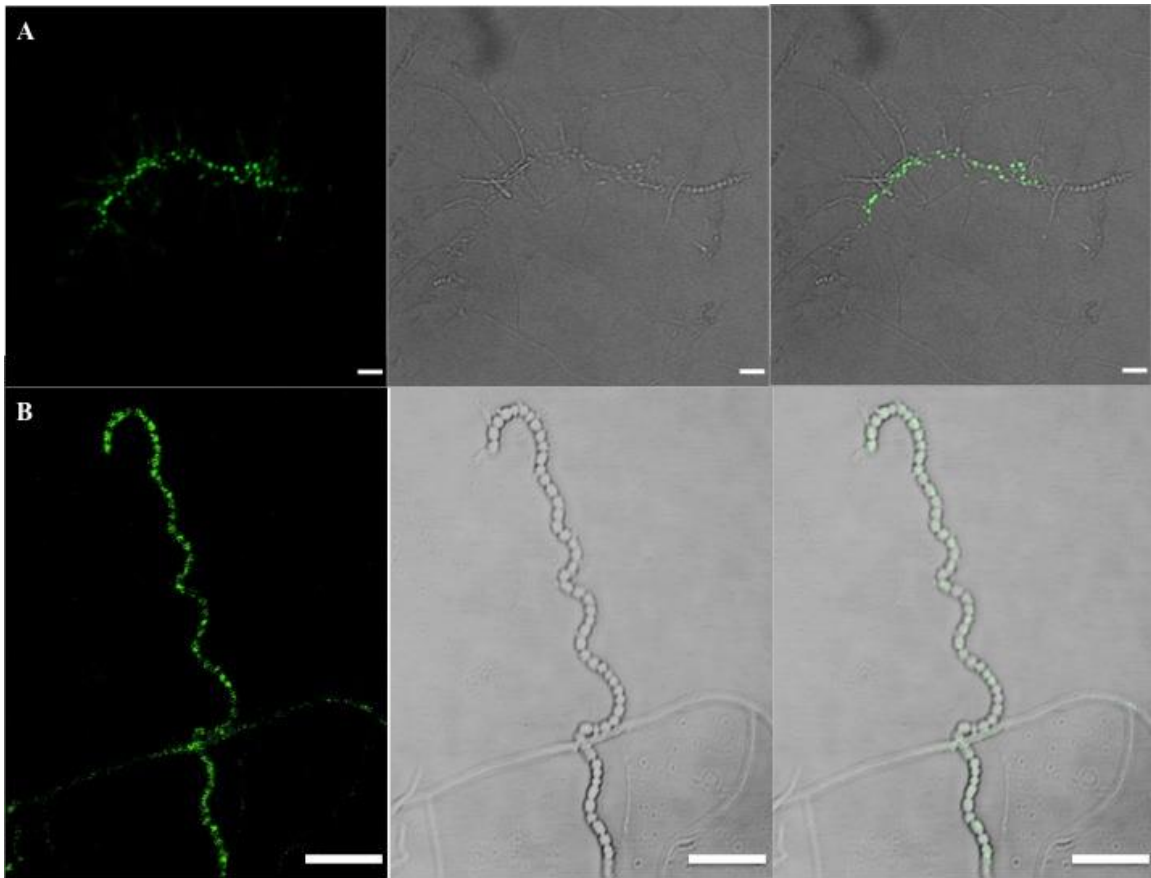


**Figure 3.9 Localization of HaaA-EGFP fusion protein in aerial hyphae.** HaaA-EGFP appears to localize in mature spore chains. Coverslips were inoculated and hyphae grown for 4 days on MS agar. Left panel shows fluorescence images, mid panel shows DIC images, and left panel shows merged images. Scale bar is 5  $\mu\text{m}$ .

## CHAPTER 4: SUMMARY AND FUTURE DIRECTIONS

### Characterization of ParH, a new partitioning protein

For *S. coelicolor* chromosome segregation, ParAB proteins are mainly responsible for organizing the proper even distribution of ParB-*oriC* complexes along the aerial hyphae (Jakimowicz *et al.*, 2007). My study revealed that a ParA-like protein, ParH, is an additional part of the partitioning system in *S. coelicolor* and appears to play a role in proper nucleoprotein complex positioning.

Similar to the other segregation/condensation gene mutants in *S. coelicolor*, a *parH* deletion mutant has also a slight chromosome segregation defect (5% anucleate spores) as well as infrequent branching spore chains. This defect is comparable to that for *smc* (8% anucleate), *ftsK* (0.8% anucleate), and *parJ* (8% anucleate) mutants (Dedrick *et al.*, 2009; Ditekowski *et al.*, 2010). Furthermore, a *parA parH* double null mutant has 17% anucleate spores as compared to 20% for *parA* mutant strain in the aerial filaments of *S. coelicolor*, which suggests that the genes function in the same pathway and are not additive (Chapter 2, Figure 2.6). In addition, the average ParB-EGFP interfocal distance in a wild type strain was found to be altered in a *parH* null strain (approximately 6% of the foci). These results suggested that ParH might play a direct or indirect role in positioning of ParB foci and, therefore, a direct or indirect role of ParH in the chromosome segregation of *S. coelicolor*.

WhiA and WhiB are involved in the regulation of key steps in aerial growth, initiation of cell division, and chromosome segregation in *S. coelicolor* and *S. venezuelae* (Ainsa *et al.*, 2000; Bush *et al.*, 2013). In *S. coelicolor*, *parAB* is a target of WhiA and WhiB and the *parH* homolog in *S. venezuelae* (*sven1405*) is a direct WhiA target and its

expression depends on *whiA* (Jakimowicz *et al.*, 2006, Bush *et al.*, 2013). It is not known if ParH is a target of WhiA and/or WhiB target in *S. coelicolor*. *whiA* and *whiB*-null mutants could be used in an S1 nuclease protection assay to investigate whether ParH is under the control of WhiA and/or WhiB. The ParH localization pattern could also be observed in *whiA* and *whiB*-null mutants to show if these two regulatory proteins affect the ParH expression and evenly-distributed ParH-EGFP foci.

Interestingly, ParH-EGFP localizes as evenly-spaced focal intervals within predivisional aerial filaments, reminiscent of the pattern observed for ParB-EGFP of *S. coelicolor*. This data suggested that ParH might co-localize with the evenly-spaced ParB-*parS* complexes in aerial filaments. ParH might assist ParA directly or indirectly for proper localization of ParB/*parS* complexes and help ParB-*oriC* to stay evenly distributed along the aerial hyphae until septation begins. To further explore chromosome segregation in *S. coelicolor* in the future, it would also be important to investigate the localization or behavior of ParH-EGFP in a strain unable to produce ParB. If the loss of ParH disrupts ParB-EGFP localization, and given the fact that ParH and ParB interact (Chapter 2, Figure 2.12), it is also possible that ParB might also have an effect on ParH-EGFP positioning. Isolating and characterizing double (*parH parB*) or triple (*parH parB parA*) mutants could also help to further elucidate the roles of these genes in chromosome segregation in *S. coelicolor*. Since, expression of ParH-EGFP is not as strong as ParB-EGFP in the aerial filaments, immunostaining of ParH could be worthwhile to try to visualize co-localization of ParH and ParB as in immunostaining of ParA with ParB-EGFP colocalization (Jakimowicz *et al.*, 2007).

Most chromosomally encoded ParA and ParA-like proteins bind to DNA in a nonspecific manner, as for ParA of *C. crescentus*, and Soj of *Thermus thermophilus* and *B. subtilis* (Easter and Gober, 2002; Hester and Lutkenhaus, 2007; Leonard *et al.*, 2005), and ParA-like PomZ from *Myxococcus xanthus* (Treuner-Lange *et al.*, 2012). Similar to GFP-Soj (Hester and Lutkenhaus, 2007), GFP-ParH localizes over the nucleoid of the cells in *E. coli* in a heterologous *in vivo* assay (Chapter 2, Figure 2.10). In addition, localization of GFP-ParH was affected for its variants (K99E, R273E, and  $\Delta$ 20-80), which either localized at the poles or diffused in the cytoplasm, as in the strain expressing only GFP (Figure 2.10). Alteration in localization of the variant due to the impaired DNA association of GFP-ParH variant R273E was expected due to the importance of this surface residue in DNA-binding in *B. subtilis* (Hester *et al.*, 2007). For variants K99E and  $\Delta$ 20-80, this alteration in localization might have been caused by a partially degraded or unstable protein (Figure 2.11), it is also possible that the ATPase activity might be important for DNA-binding of the protein. To further investigate the ability of dimerization for ParH and its ATPase mutant derivative in more detail, surface plasmon resonance (SPR), size exclusion chromatography, or native polyacrylamide gel electrophoresis analyses could be useful to confirm that ParH dimerizes and ATPase activity is required for dimerization. It is possible that, depending on nucleotide binding and hydrolysis, ParH might function as a molecular switch that cycles between an ATP-bound and ADP-bound state. By doing so, ParH might help ParB-*oriC* to stay evenly distributed along the aerial hyphae until septation begins. It is also possible that ParB might stimulate ParH binding to DNA in aerial filaments and could be investigated by DNA electrophoretic mobility shift assay (EMSA). Exploring the DNA-binding property

of ParA would also be helpful to understand the segregation mechanism of *S. coelicolor*, as this has not been investigated.

Similar to ParB-EGFP, ParH has an evenly-spaced localization pattern, which suggests possible colocalization and/or protein interaction between ParH and ParB. In support of potential direct interaction in the native situation, these two proteins were found to be interacting partners in a heterologous bacterial two-hybrid system. Interestingly, the ATPase active site and N-terminal extension of ParH were not only found to be required for ParH-ParH dimerization since these two variants impaired ParH-ParH interaction, and also impaired ParH-ParB interaction, as judged by the bacterial two-hybrid system. These outcomes could have been the result of an unstable or improper folding of the protein as in the heterologous *in vivo E. coli* DNA binding assay. An independent assay, such as co-immunoprecipitation could be used to retest these interactions by epitope tagging or isolating polyclonal antibody.

Interactions between ParH and other known segregation/condensation proteins (i.e., ParA, ParJ, SMC, ScpA, ScpB, and FtsK) and division protein FtsZ were also tested and no evidence for interaction was found. Again these results should not be discarded because of the potential false-negative outcomes of the *cya* bacterial two-hybrid system.

An organization model summarizing interactions of segregation and condensation proteins during development-associated genome segregation is shown in Figure 4.1. Evidence for new interactions was found between ScpB-ParA, ScpB-SlzA, and SlzA-ParH protein pairs (Chapter 2, Figures 2.12 and 2.14). Interaction between ScpB and ParA is important since it suggests a link between the SMC condensation complex and segregation of the chromosomes in *S. coelicolor*. This interaction may be analogous to

the fact that Spo0J/ParB recruits SMC to *oriC* regions and promotes chromosome segregation in *B. subtilis* and *S. pneumoniae* (Minnen *et al.*, 2011, Gruber and Errington, 2009). ParA, on the other hand, might help coordinate the activity rather than the localization of condensins. Therefore, ParA might have a role in addition to the proper localization of ParB-EGFP in the aerial filaments of *S. coelicolor*. Since *scpAB* and *scpA*-null mutants produce bilobed nucleoids within spores and 26% and 15% anucleate cells, respectively (Dedrick *et al.*, 2009), making double and triple mutants with *parA*, *parB*, and *scpAB* might reveal more information about the possible additional roles of ParA and ParB in nucleoid condensation. On the other hand, even though *slzA* has no obvious segregation and condensation defects, close proximity of *slzA* to *smc*, interaction of the gene product with ScpB and ParH, and *slzA* being a direct target of WhiA in *S. venezuelae* make SlzA a possible segregation/condensation protein and a link between chromosome partitioning and condensation in *S. coelicolor*.

In conclusion, this summary model for segregation protein interactions, which is represented in Figure 4.1, does not suggest that these proteins interact synchronously during development-associated genome segregation in *S. coelicolor*. To be able to make a proper temporal and spatial model, expression profiles of these proteins need to be investigated. Unfortunately, only the developmental regulation of ParAB is known (Jakimowicz *et al.*, 2006), but the expression profiles of other proteins, which are represented in the model, are still not identified. In addition, ParB and ParH are the only proteins in the model in Figure 4.1 that are known for their DNA-binding properties (Jakimowicz *et al.*, 2002). Since all of these proteins are involved in chromosome

segregation, it might also necessary to investigate their association of at least ParA with DNA to be able to complete a proper proposed model.

### **Identification of a novel ParA and ParH interacting protein**

In a search for novel ParH interacting proteins by screening a random bacterial two-hybrid library, a novel interaction partner of ParH and ParA was identified. Remarkably, HaaA (ParH ParA Associated protein A) is one of the 24 signature proteins of Actinomycetes (Gao *et al.*, 2009). Interestingly, ParJ was also discovered by screening a random bacterial two-hybrid library (Ditkowski *et al.*, 2010). As for HaaA, ParJ and ParJ paralog (SCO1997) are both signature proteins for the Actinobacteria phylum. ParJ is an interaction partner of *S. coelicolor* ParA and it is believed to regulate ParA depolymerization *in vitro* (Ditkowski *et al.*, 2010). The *parJ*-null mutant also has a slight segregation phenotype of 8% anucleate cells which is similar to *haaA*-null mutant (Ditkowski *et al.*, 2010). Similarly, the phenotype for a *haaA*-null mutant was 6% anucleate spores and colonies had a slight white macroscopic phenotype on SFM agar. This segregation phenotype was similar to 5% anucleate cells in *parH* (Figure 2.6) and 8% anucleate cells in *smc* mutants (Dedrick *et al.*, 2009 and Kois *et al.*, 2009), which showed that the loss of one component resulted in a similar phenotype. The delayed aerial mycelium phenotype of a *haaA* mutant suggests that HaaA might have another role earlier in development, in addition to chromosome segregation defect in aerial hyphae. Inconsistent with expectation, the localization of HaaA-EGFP was observed later in mature spores and not in vegetative hyphae or prespore compartments. Surprisingly, that HaaA-EGFP localization resembled neither filamentous localization of ParA nor evenly-spaced foci ParH-EGFP foci, which also suggests the inconsistency in macroscopic and

microscopic results for HaaA. Unexpected localization of HaaA-EGFP might imply that the fusion is not functional. The homolog of *haaA* in *S. venezuelae*, *sven5529*, was identified as a highly significant WhiA (Bush *et al.*, 2013) and WhiB target (Bush and Buttner, personal communication), which are involved in the regulation of key steps in aerial growth, initiation of cell division, and chromosome segregation (Bush *et al.*, 2013). The fusion results reported here are consistent and suggest that the expression of HaaA is developmentally regulated. One of the ways to show that HaaA is also under the regulation of WhiA or WhiB in *S. coelicolor* is to investigate HaaA-EGFP localization in a *whiA* or *whiB*-null mutant. If the HaaA-EGFP localization in the mature spores is affected in *whiA* or *whiB*-null mutants, then it shows that HaaA is a WhiA and/or WhiB target in *S. coelicolor* as in *S. venezuelae*.

Several other Actinobacteria (*S. venezuelae*, *C. glutamicum*, *M. smegmatis*) were also investigated to see if interaction between HaaA and ParA and ParH homologs was conserved. Homologs of ParA and ParH interacted with the cognate homolog of HaaA in the bacterial two-hybrid assay for each tested bacterium. Conservation of the interaction results with *S. coelicolor* were interpreted as an indicator of the importance of this novel protein.

There are only eight amino acid residues in the predicted disordered C-terminus region of HaaA that are highly conserved among the homologs of widely divergent Actinomycetes. A variant protein lacking these eight amino acid residues (Figure 3.2), HaaA( $\Delta$ 338-345) still formed dimers and interacted with ParA and ParH as judged by the bacterial two-hybrid system. However, the intensity of their interaction was significantly reduced. These results indicated that these residues might play a role in other protein-



protein interactions or protein folding and stability.

It will be necessary to investigate the expression time points of HaaA to be able to understand the role of HaaA in chromosome segregation as well as to propose a more accurate model that represents the segregation protein interactions during development-associated genome segregation in *S. coelicolor*. S1 nuclease protection assay, RT-PCR, northern blot are some of the assays that could be done to investigate HaaA expression for the future studies.

Even though recent studies on partitioning proteins provided considerable information, a complete understanding of the whole segregation mechanism is still elusive. Identification of a novel interaction partner of ParA and ParH also confirmed that there are still additional unknown proteins that are involved in chromosome segregation of *S. coelicolor*.

## REFERENCES

- Bush, M. J., Bibb, M. J., Chandra, G., Findlay, K. C., Buttner, M. J., (2013). Genes required for aerial growth, cell division, and chromosome segregation are targets of WhiA before sporulation in *Streptomyces venezuelae*. *mBio*, 4(5), e00684-00613. doi: 10.1128/mBio.00684-13.
- Dedrick, R. M., Wildschutte, H., McCormick, J. R., (2009). Genetic interactions of *smc*, *ftsK*, and *parB* genes in *Streptomyces coelicolor* and their developmental genome segregation phenotypes. *J Bacteriol*, 191(1), 320-332. doi: 10.1128/JB.00858-08.
- Ditkowski, B., Troc, P., Ginda, K., Donczew, M., Chater, K. F., Zakrzewska-Czerwinska, J., Jakimowicz, D. (2010). The actinobacterial signature protein ParJ (SCO1662) regulates ParA polymerization and affects chromosome segregation and cell division during *Streptomyces* sporulation. *Mol Microbiol.*, 78(6), 1403-1415. doi: 10.1111/j.1365-2958.2010.07409.x.
- Easter, J., Jr., Gober, J. W., (2002). ParB-stimulated nucleotide exchange regulates a switch in functionally distinct ParA activities. *Mol Cell*, 10(2), 427-434.
- Gruber, S., Errington, J. (2009). Recruitment of condensin to replication origin regions by ParB/SpoOJ promotes chromosome segregation in *B. subtilis*. *Cell*, 137(4), 685-696. doi: 10.1016/j.cell.2009.02.035.
- Hester, C. M., Lutkenhaus, J., (2007). Soj (ParA) DNA binding is mediated by conserved arginines and is essential for plasmid segregation. *Proc Natl Acad Sci U S A*, 104(51), 20326-20331. doi: 10.1073/pnas.0705196105.
- Jakimowicz, D., Zydek, P., Kojs, A., Zakrzewska-Czerwinska, J., Chater, K. F., (2007). Alignment of multiple chromosomes along helical ParA scaffolding in sporulating

- Streptomyces* hyphae. *Mol Microbiol.*, 65(3), 625-641. doi: 10.1111/j.1365-2958.2007.05815.x.
- Jones, S., Barker, J. A., Nobeli, I., Thornton, J. M., (2003). Using structural motif templates to identify proteins with DNA binding function. *Nucleic Acids Res*, 31(11), 2811-2823.
- Leonard, T. A., Butler, P. J., Lowe, J., (2005). Bacterial chromosome segregation: structure and DNA binding of the Soj dimer-a conserved biological switch. *EMBO J*, 24(2), 270-282. doi: 10.1038/sj.emboj.7600530.
- Minnen A., Attaiech L., Thon M., Gruber S., Veening J.W., (2011). SMC is recruited to *oriC* by ParB and promotes chromosome segregation in *Streptococcus pneumoniae*. *Mol Microbiol*, 81(3), 676-88.
- Pazos, M., Natale, P., Vicente, M., (2013). A specific role for the ZipA protein in cell division: stabilization of the FtsZ protein. *J Biol Chem*, 288(5), 3219-26. doi: 10.1074/jbc.M112.434944
- Treuner-Lange A, Aguiluz K, van der Does C, Gómez-Santos N, Harms A, Schumacher D, Lenz P, Hoppert M, Kahnt J, Muñoz-Dorado J, Søggaard-Andersen L., (2013). PomZ, a ParA-like protein, regulates Z-ring formation and cell division in *Myxococcus xanthus*. *Mol Microbiol.* 87(2), 235-53. doi: 10.1111/mmi.12094.

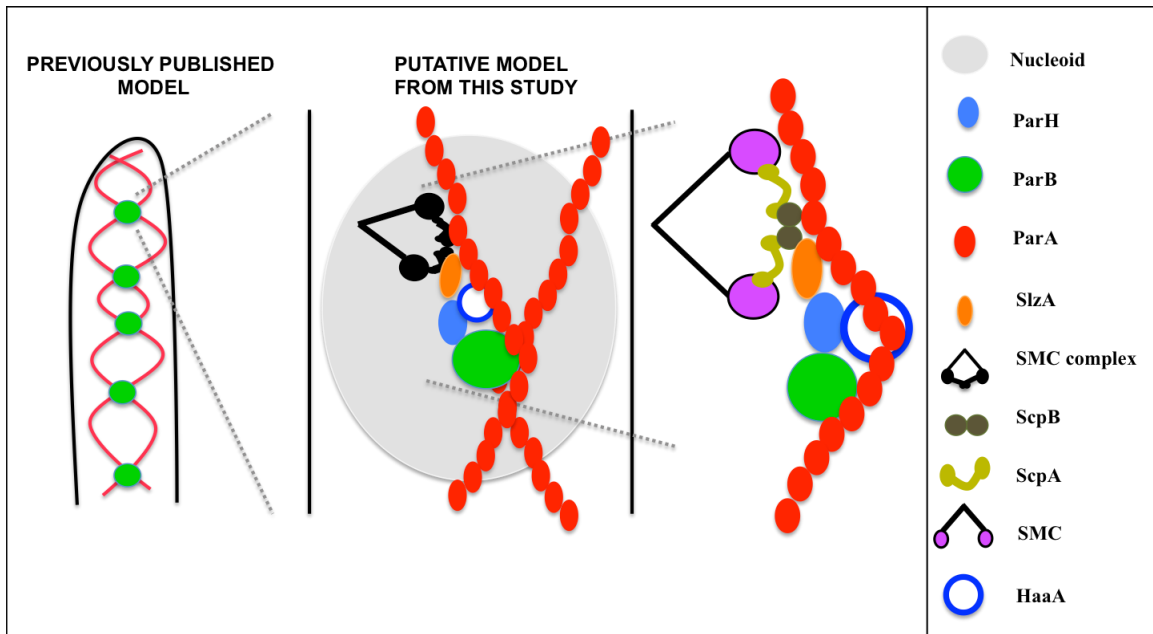


**Figure 4.1. Putative model for segregation protein interactions during development-associated genome segregation of aerial hyphae in *S. coelicolor*.** Chromosomal DNA is not shown on the left part of the figure, but ParB organizes the *oriC* region of the copies of the chromosome. Left side of the figure shows previously known information, which is the evenly distributed ParB-EGFP foci and helical filaments of ParA in the aerial filaments of *S. coelicolor* (Jakimowicz et al., 2007). Right side of the figure shows the model of segregation proteins with the contribution of this study as determined by bacterial two-hybrid assays. ParH interacts with ParB and SlzA, ScpB interacts with SlzA and ParA, and HaaA interacts with ParH and ParA in a bacterial two-hybrid assay.